Automotive Events Detection using MEMS Accelerometers

Authoress: Lorena San Vicente Foronda

PildoLabs

Advisor: Ivan Fernàndez i Corbaton

Universitat Politècnica de Catalunya

Escola Tècnica Superior d'Enginyeria de Telecomunicacions de Barcelona

Co-Advisor: Josep Vidal Manzano

ABSTRACT (English version)

Imagine a mobile telephone capable of detecting a traffic accident and notifying it to a call centre. But not only that, but also informing of the position where you are situated. The emergency systems will arrive to the place of the accident earlier, reducing the number of deaths in the roads. It is possible.

The European Commission is developing a project called "eCall", through which a black box inserted in the car for detecting and notifying automatically accidents, is being developed. Focusing on this idea, this thesis presents a study of the viability of the implementation of an Automatic Crash Notification System(ACNS) in a mobile phone provided with two accelerometers and a GPS chip.

A first study of the evolution of the mobiles, demonstrates that the cell phones will be provided with the necessary devices for the implementation of the ACDN in them. Basing on this fact, the design of an algorithm for developing the system have been carried out.

For verifying if the implementation of the system in the cell phone is viable several accident data and different models of normal driving have been used. After having analysed this data, with it different synthetic models have been developed, for obtaining several parameters as the probabilities of false alarm and detection, and the time to the first detection, for the study of the quality of the system.

After analysing the results it is deduced that the implementation of an ACNS in cell phones is possible. The obtained probabilities of detection are of the order of 93%. Although not being a legislation which determinates the required characteristics of the system, this results are acceptable for implementing an ACNS in a mobile phone.

ABSTRACT (Spanish version)

Imagine un teléfono móvil, que sea capaz de detectar un accidente de tráfico y notificarlo a una central. Pero no solo eso si no que además, envíe la posición donde está situado. Los sistemas de emergencia tendrían toda la información antes, lo que disminuiría el número de fallecidos en las carreteras. Todo ello es posible.

La Comisión Europea está llevando a cabo un proyecto denominado "eCall", mediante el cual se está desarrollando una caja negra que irá integrada en el coche para detectar y notificar accidentes. Basándose en esta idea, ésta tesis presenta el estudio de viabilidad para la implementación de un sistema de detección y notificación automático de accidentes (ACNS) integrado en un teléfono móvil,con acelerómetros y un chip GPS.

Un primer estudio sobre la evolución de los móviles, demuestra que los teléfonos móviles serán una posibilidad real para la implementación del sistema. Basándose en este hecho, se ha diseñado un algoritmo para el desarrollo del sistema.

Para comprobar si la implementación del sistema en el teléfono móvil es viable, se han utilizado datos de distintos accidentes, y dos modelos de conducción. Después de haber analizado los datos se han generado distintos modelos sintéitcos, para obtener distintos parámetros, como las probabilidades de detección y de falsa alarma así como el tiempo transcurrido hasta la primera detección, para el estudio de la calidad del sistema.

Tras analizar los resultados se deduce que la implementación del ACNS en los teléfonos móviles es viable obteniendo probabilidades de detección del orden de 93 % en algunos casos. Aunque hoy en día no exista una legislación que determine las características de los sistemas de detección de accidentes, los resultados obtenidos son aceptables par una implementación de un ACNS en los teléfonos móviles.

Index of Contents

1 INTRODUCTION

1.1 Motivation

Each day 9 people in Spain die because of traffic accident. More than 1,2 millions of people around the world die each year due to traffic accidents[1][2]. The implementation of an Automatic Crash Notification System could reduce in Europe the number of road deaths in between a 5% and 15%. In Spain this system could save the life to between 150 and 460 people, but not only that, the seriousness of the injuries could be reduced in between a %10 and %15. Regarding the European Union, up to 2500 lives could be saved.

Different researches, conclude that one of the most important factors which contributes to the gravity of the traffic accident injuries is the response time of the emergency services, the time that takes place between accident occurs and the services arrive to the accident placement. In that response time a combination of circumstances influence as, the organization and the coordination of the team, the time spent searching the accident localisation, and the time between the accident occurs and the emergency call is made. All these circumstances could be more complicated in inter-cities areas, where people have less references for indicating the exact place,and in less busy zones, where the probability of being an accident witness who could alert the services is very low.

Because of that, the reduction of time of response in the assistance services plays a very important role for avoiding deaths in traffic accidents, reducing the number of injuries and their seriousness.

A research made by the “Real Automovil Club de Cataluña” (RACC), about the state of the medical emergencies in Spain shows that the 66% of the traffic accident deaths is produced in the first 20 minutes after the accident, so a correct emergency attention could reduce the death people on a 11% [3].

The European Commission is developing a project called “eCall”, which intended to bring rapid assistance to motorist involved in a collision. The projects aims to employ a hardware black box installed in vehicles that will wirelessly send airbag deployment and impact sensor information as well as GPS coordinates to local emergency agencies.

Nowadays early everybody has a mobile phone. Taking into account the evolution of the technologies, concretely of the mobiles phones, almost all of them will be equipped with a GPS receptor. In the 2008 the 20 % of the sold cell phones, had a GPS incorporated. In the 2012 GPS in consumer mobile phones will rise to a 65 % [4], so the warning system could take advantage of this fact.

As far as mechanism for detecting accident is concern, the accelerometers gives a good information for detecting it. These measure the acceleration in the different coordinates,

through these measurements an accident could be detected. According to iSuppli Corporation, accelerometers are expected to appear in one-third of mobile phones shipped next year [5].

In the following graphic, there is the evolution of the penetration of accelerometers in all types of Mobile Phones.

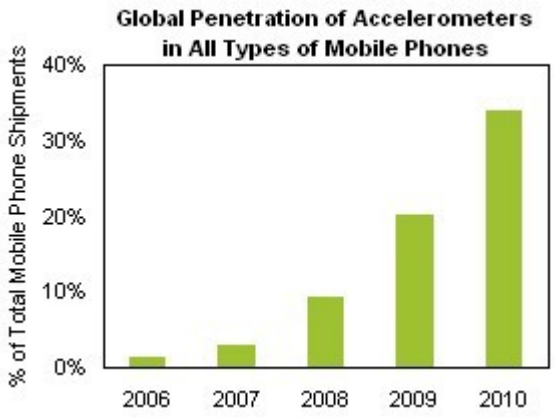

Figure 1: Global Penetration of Accelerometers in mobile phones

As it can be seen in the graphic, the increased of the accelerometers in the mobile phones is considerable, and if the penetration continues in 2013 year, almost all of the new mobiles phones will have incorporated, one or two accelerometers.

Joining all the information,the subtracted conclusion is that nowadays there are a lot of mobiles which give connectivity, the position through the GPS, and also have the tools for detecting accidents. So, they would be a good device for implementing the automatic crash detection and notification system.

1.2 Global view of the project

The final idea of this project is to take advantage of all of the circumstances previously commented and to develop a platform of detection and notification of automotive accidents. This platform will be integrated in a mobile, and taking advantage of the different devices, will be able to detect traffic accidents and to report to a centrality the detection of the accident and the coordinates where the car is situated.

The scheme of the functional model is represented in Figure 2:

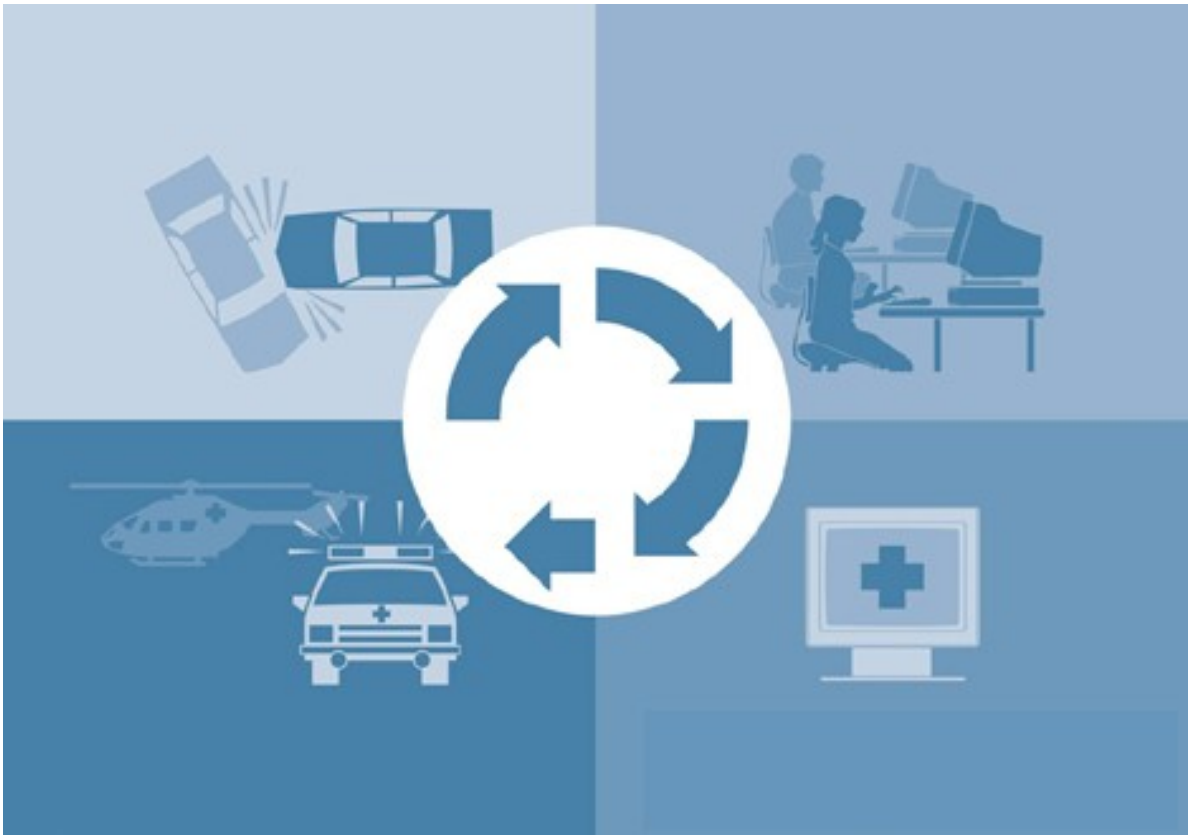

Figure 2: Scheme of the functional model

The process till the accident is detected to the emergency services arrives is the following one:

- The accident is produced

- The system detects the accident and it activates the protocol. This is composed of transmission of a SMS message which contains the Minimum Set of Data (MSD), this transmission is made through GSM/GPRS/UMTS technology. The MSD contains the exact localization of the accident using the GPS system.

- The switchboard, receives the emergency message, and send the emergency services where the accident have had place, for giving assistance to the injured people and for solving the problems which would have came up.

The next project is going to be focused on the study of the accelerometers and their application for detecting automotive accidents. For developing the project, an open mobile called *"Neo FreeRunner"* has been used, because of its characteristics.

1.3 Methodology

For detecting the accidents the following methodology has been followed:

First of all with the data of the accelerometers of the "*Neo FreeRunner"* the noise have been studied, analysing the different correlations. After a coherent probability of false alarm has been chosen, and with this the needed threshold has been calculated. Then two different algorithms have been developed, using one and two accelerometers.

Once having these algorithms, they have been evaluated with matlab, using different syntethic models. For the evaluation different parameters have been studied as the probabilities of detection and of false alarm.As it has been previouly commented different type of data have been used, first of all the accident data itself has been used. Then a model consisting of a normal driving followed by an accident has been analysed, because this model is the one which would happen in the real life. After an analyse of the time to the first detection has been made. This is an important point because, the lower the time is, the more probabilities would be for carrying out all the process before a possible destruction of the mobile phone. Then the decision of the accident is taken, this means what it is going to consider an accident. For it two different methods have been studied, the first one considering an accident when an accident sample is detected, and the second one considering an accident, when 2 of 3 accident samples are detected. Finally an analysis of the influence of the possible vibrations occurred in a car has been studied.

1.4 Project outline

The remainder of this project is outlined as follows:

Chapter 2 is a state of the art of the situation. First of all Openmoko project is going to be introduced, focussing in the *"Neo Freerunner"* the hardware part of the project. An study of the market is also made, analysing the different similar devices.

Chapter 3 is dedicated to the explanation of the previous work made on this project, describing the different applications for sending SMS and for acquitting the GPS data.

Chapter 4 describes all the development of the project. First of all, there is a comprehensive review of accelerometers, including an explanation of the data acquisition and an exhaustive study of the noise. After an exposition of driving models and accident data is given. Next step explained is the election of the threshold, meeting specified requirements. Continuing the used algorithm and the obtained results using one and two accelerometers is shown. Following, an analysis of the Time to the first detection has been made. After the decision of

accident is explained. Next an analyse of the influence of the possibly vibrations occurred in a car is made. Continuing it is going to be explained the study of the development of an algorithm knowing every time where the floor is. Finally an algorithm capably of detecting free-fall with spin is presented.

Chapter 5 summarizes the conclusions and the findings and provides some suggestions for further research.

2 STATE OF THE ART

2.1 Market research

2.1.1 Opportunities for the final project

The first step given that allows the ACNS (Automatic Crash Notification Systems) to work in a bigger area and in an easier way is the European emergency number 112 in all the member States of EU. This was introduced in 1991 to provide a single emergency call number in all EU Member States to make emergency services more accessible. Since 1998, EU rules have required Member States to ensure that all fixed and mobile phone users can call 112 free of charge. But it is not since December 2008, that all the EU citizens can contact emergency services from anywhere in the European Union by dialling 112, free of charge from both fixes and mobile phones [8]. This fact is considered a big important opportunity for all ACNS, due to the facilities that gives to the notification section and the possibility of its proper performance in all the EU without any changes.

The other significant factor that is make an opportunity for the market of ACNS is the *"eCall Project"* [9] . Through this ,all the Member States of the European Union are solving the remaining legal, technical and socio-economic issues and proceeding with the necessary for the ACNS. Preparing phone networks and emergency services for the roll out of the ACNS across Europe has the full support of the European Parliament and 15 EU countries.

Through this project all the Member States are making progress in three important areas. First of all they are integrating emergency centres, bringing together all services (ambulance, fire brigade, police). They are also bringing additional language capabilities of emergency centres and finally they are upgrading their electronic infrastructure to enable the emergency services to receive and process the car's location[10-13].

2.1.2 Similar devices

Around the world some similar systems have been successfully developed, specially in the United States and in Japan. In the following lines there is a summarize of the level of presence of this technology in the international market.

USA

"Mayday": In the United Stated the devices called "Mayday" were commercialized in the 1996. They are based in two different communication technologies. In one hand there is "Mayday by mobile telephone", consisting of a device collocated into the car, that in case of accident transmits an emergency signal to a central call reception. In the other hand there is the "Mayday via satellite", it is very similar to the previous system, but in this case the signal instead of transmitting by a mobile telephone, it is transmitted by a satellite communication called LEO (Low Earth Orbit) [14].

" *On·Guard®Tracker*": ATX Technologies emerged in 1998 as the leader in the mayday industry with the largest dedicated Response Centre serving North America. ATX Technologies is the developer and manufacturer of the On·Guard®Tracker that uses satellite and wireless technologies to pinpoint a vehicle's location, speed and direction and to provide emergency and convenience services [15].

Rescu system: Motorola has joined forced with Ford and Protection One and have developed the Lincoln RESCU system, which it said is the first original equipment manufacturer emergency messaging system launched in the United States. The Lincoln RESCU provides roadside assistance and emergency response services [16].

On Star: OnStar services are only available currently on vehicles manufactured by General Motors. The OnStar service relies on CDMA mobile phone voice and data communication, as well as location information using GPS technology. Drivers and passengers can use its audio interface to contact OnStar representatives for emergency services, vehicle diagnostics and directions. OnStar equipped vehicles with an active subscription will also contact representatives, in the event of a collision where the airbags are deployed [17].

JAPAN

"HELPNET": The HELPNET service was begun by Japan Mayday Service Co., Ltd. in September, 2000 with the aim of reducing the amount of time between the reporting of an emergency and the arrival of rescue services, in order to save more lives. When an accident or sudden illness occurs during vehicle operation, information on the vehicle's position and registration number is communicated either automatically or manually from the vehicle to a service centre via the mobile telephone network. The information is then relayed to the nearest rescue service (police, fire department, etc.). Toyota Motor Corporation has developed two types of on-board devices to take advantage of the HELPNET service. The first is an air bag interlock device that can notify the service centre automatically when an air bag is activated. The second is a one-touch device for the purpose of manual reporting in the event of a sudden illness. Both devices went on sale in the fall of 2000 [18].

EUROPE

"BMW Assist" is a car complement which is integrated into the car's communication and audio systems. It works in conjunction with the navigation system or uses its own GPS equipment. Originally it worked with the AMS cellular network for data transmission and voice communication, but current BMW Assist system works using more advances CDMA, TDMA or GSM technologies.

The car communicates via the cellular network with a Back-end system that receives and analyses the information. Both voice and data are transmitted. The information is routed to a BMW call-centre.

The BMW Assist System is disposable in all the series of BMW cars. It includes the automatic or manual emergency call functions, road assistance and information about the traffic state.

First systems were installed in Germany, but nowadays this service operates in all around Europe [19].

"Mercedes-Benz Tele Aid"

The Mercedes-Benz TeleAid system integrates hardware and software from Motorola. The innovative TeleAid system offers three distinct kinds of services accessible at the touch of a button. For emergency help, there´s a «SOS» button on the rear-view mirror. Pushing the SOS button will immediately establish voice contact with the call-centre. Pressing this button also transmits crucial information about the customer, including the precise location of the vehicle (through the GPS tracking). If voice contact is not established (e.g., the customer is unable to respond), the call-centre will call the emergency services.

If a collision deploys any airbag, the system automatically establishes contact with the call-centre, relaying all pertinent information.

This system has been available since the spring of 2004 in Germany, Austria, Belgium Luxembourg, Italy, France, Spain, Holland,and Switzerland., in some of its classes.[20].

Volvo on Call: Volvo on Call system generates an automatic alarm in case of accident. When the air bags or the Seat Belt Emergency Tensioning Device are activated, a notice is send to the Volvo On Call Central. In that moment the operator opens a voice line with the vehicle for having knowledge of the state of the occupants, in case of not getting in touch with the occupants the emergency services would be notified and be sent to the place of the accident, thank to the GPS system [21].

2.2 Openmoko

2.2.1 Openmoko project

Openmoko is a project which encompasses two related sub-projects, with the aim of creating a family of open source mobile phones [6][7]. The project is sponsored by Openmoko Inc. In one hand is Openmoko Linux, a Linux based operating system designed for mobile phones built using free software, in the other hand is the development of hardware devices on which Openmoko Linux runs. The first device released was the *"Neo 1973"*, which was followed up by the *"Neo FreeRunner"*.

2.2.2 Neo Freerunner

The "*Neo FreeRunner"*, as it has been commented before is a mobile phone, which gives it connectivity via GSM/GPRS, it is provided with a GPS chip-set receiver and antenna, which gives the possibility to access to the GPS position information, but also has incorporated two 3 axis accelerometers, with which the detection of the accident will be carry out (See *Annex I*). Due to its equipment and having the advantage of being open-source, it is the device which during the development of the project will be used.

Figure 3: Neo FreeRunner

3 PREVIOUS WORK

Before starting to develop any application, the first days were dedicated to the familiarization with the device, by developing different simple programs in C, and after, compiling and implementing them in the "*Neo FreeRunner"*.

As it has been explained before, the global project can be divided in three sections. The first part is the one that gets the position, then there is the one that detects the accident, and finally the one which notifies it. In this section the applications for getting the GPS position and for sending a SMS are going to be explained. After having corroborated their correct work, they were integrated, achieving an application which sent a SMS with the position of the "*Neo FreeRunner"*. Then in the Chapter 4 (Development of the project), the work made for detecting the accidents will be explained.

3.1 Getting the position

As it has been commented previously, the Openmoko is provided with a GPS receiver, concretely an *"Ublox Antaris 4 chip"* [22]. It is a single chip receiver which power consumption is ultra low and has 4 Hz position update rate.

The first algorithm developed gets the data from the GPS receiver and inserts it in a file. In the next flowchart there is the explanation of it.

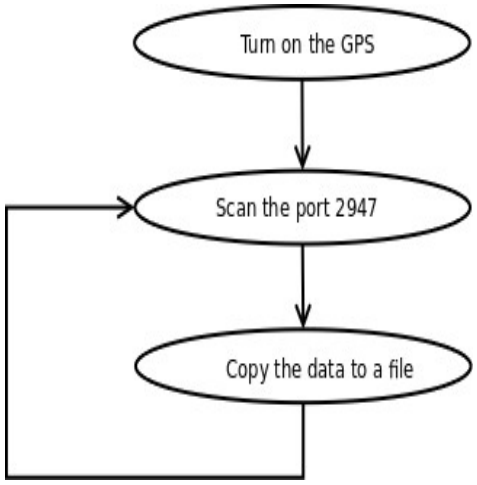

Diagram 1: Flowchart of the algorithm for getting data

The steps are very simple, first the GPS receiver chip is turned on. Then a scanning of the port to which the information is send has to be made, for finally copying the data to a file. This process is continuously executing, till the program is finished.

3.2 Sending SMS

The second application designed for the global project is the one which sends a SMS. Following there is the diagram which shows the different steps of the algorithm.

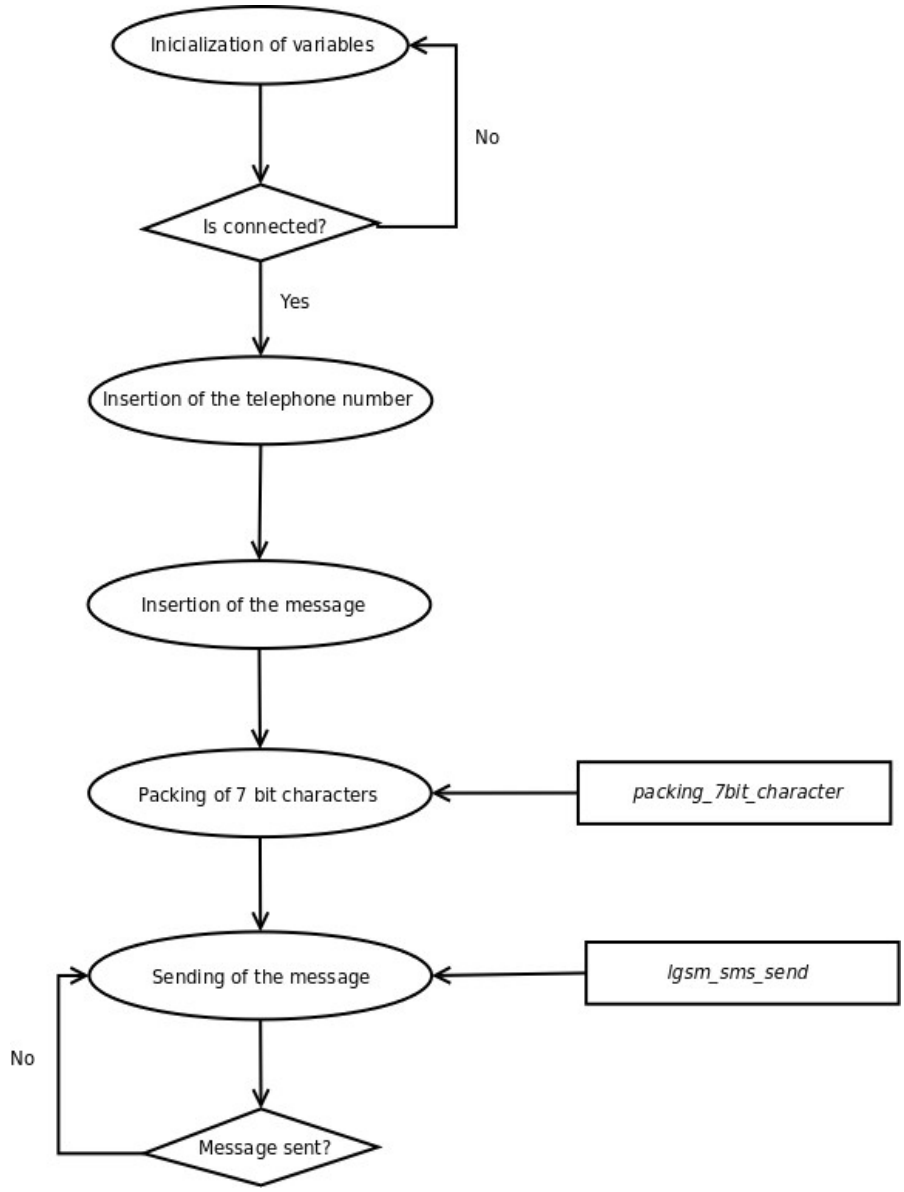

Diagram 2: Flowchart of the algorithm for sending SMS

In the flowchart all the process carried out for sending a message is shown. The first step is to initialize the variables. Then a verification of the connectivity is made. After the telephone number and the message are inserted. In the next step a packing of 7 bit characters is made, with the function *packing_7bit_character*, which gives it the SMS format. Following the message is sent using the function *lgsm_sms_send.* This function sends the SMS and returns a bit telling if it has been a successfully sending. Finally the checking of the sending is made, and in case of not having been sent the previous step is repeated.

3.3 Final algorithm, integration of the two algorithms

The last step, in this previous work, is to join the two algorithms in one. This means that the message sent by the SMS algorithm is going to be composed of the GPS data.

In the next image is plotted the flowchart of the global algorithm.

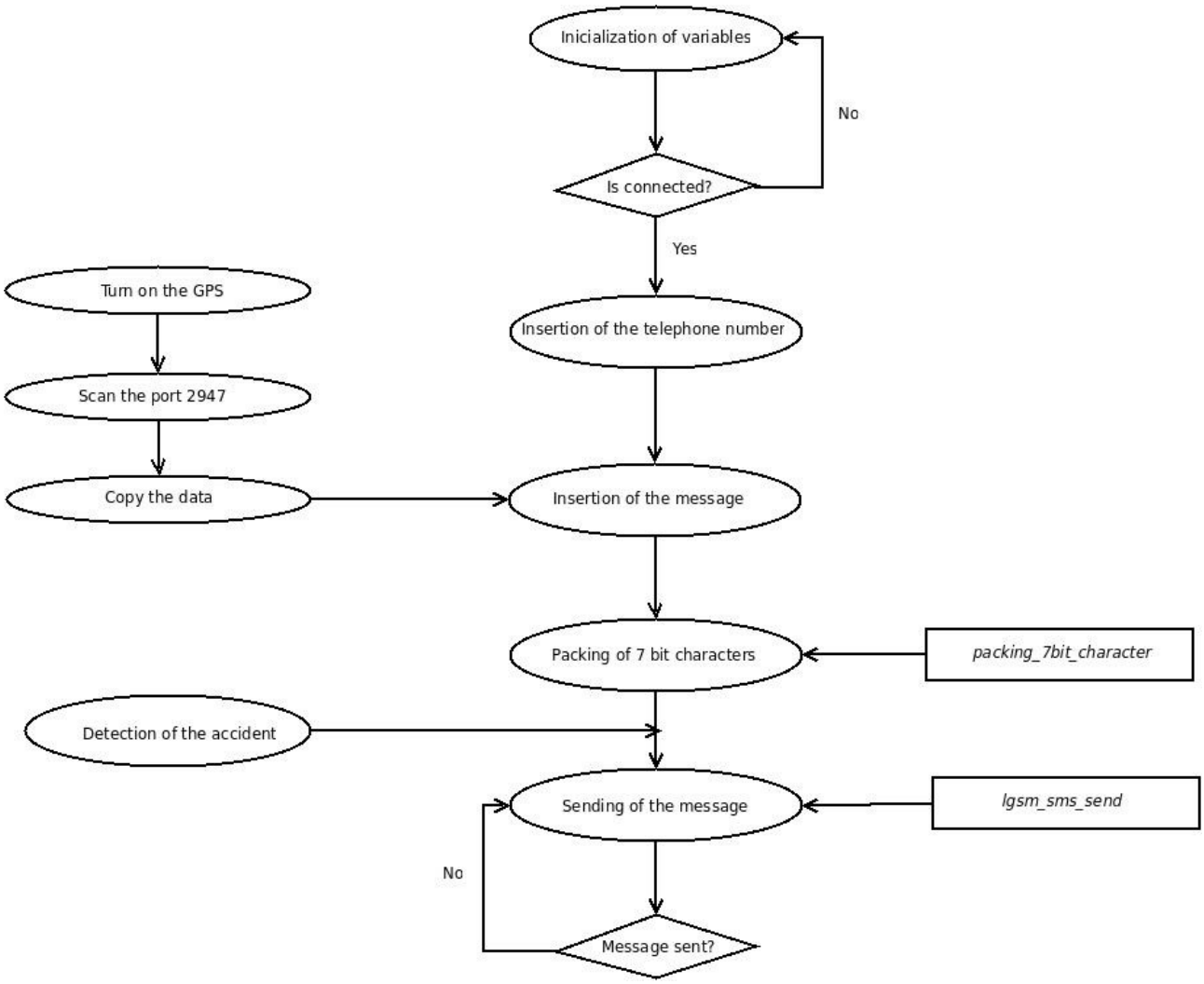

Diagram 3: Flowchart of global algorithm for sending a message with the GPS position

The process is the same as the one explained in the case of sending a SMS, but in this case the message is the position gotten by the GPS receiver.

4 DEVELOPMENT OF THE PROJECT

4.1 Accelerometers

An accelerometer is a sensing element that measures the acceleration it experiences relative to free-fall. The acceleration is measured as a vector that has magnitude and direction. Single and multi-axis models are available to detect magnitude and direction of the acceleration as a vector quantity, and can be used to sense orientation, vibration and shock.

Its measurement is equivalent to inertial acceleration minus the local gravitational acceleration, where inertial acceleration is understood in the Newtonian sense of acceleration with respect to a fixed reference frame, which the Earth is often considered to approximate.

As a consequence, quite counter-intuitively, an accelerometer at rest on the Earth's surface will actually indicate 1 g upwards along the vertical axis. To obtain the inertial acceleration (due to motion alone), this gravity offset must be subtracted. Along all horizontal directions, the device yields acceleration directly. Conversely, the device's output will be zero during free-fall, where the acceleration exactly follows gravity.

The reason for the appearance of a gravitational offset is Einstein's equivalence principle, which states that the effects of gravity on an object are indistinguishable from acceleration of the reference frame. When held fixed in a gravitational field by, for example, applying a ground reaction force or an equivalent upward thrust, the reference frame for an accelerometer (its own casing) accelerates upwards with respect to a free-falling reference frame. The effect of this reference frame acceleration is indistinguishable from any other acceleration experienced by the instrument.

There are a number of types of accelerometers [23]. What differentiates the types is the sensing element and the principles of their operation.

Capacitive accelerometers sense a change in electrical capacitance, with respect to acceleration. The accelerometer senses the capacitance change between a static condition and the dynamic state.

Piezoelectric accelerometers use materials such as crystals, which generate electric potential from an applied stress. This is known as the piezoelectric effect. As stress is applied, such as acceleration, an electrical charge is created.

Piezoresistive accelerometers (strain gauge accelerometers) work by measuring the electrical resistance of a material when mechanical stress is applied Hall Effect accelerometers measure voltage variations stemming from a change in the magnetic field around the accelerometer.

Magnetoresistive accelerometers work by measuring changes in resistance due to a magnetic field. The structure and function is similar to a Hall Effect accelerometer except that instead of measuring voltage, the magnetoresistive accelerometer measures resistance.

Heat transfer accelerometers measure internal changes in heat transfer due to acceleration. A single heat source is centred in a substrate and suspended across a cavity. Thermoresistors are spaced equally on all four sides of the suspended heat source. Under zero acceleration the heat gradient will be symmetrical. Acceleration in any direction causes the heat gradient to become asymmetrical due to convection heat transfer.

MEMS-Based Accelerometers
MEMS (Micro-Electro Mechanical System) technology is based on a number of tools and methodologies, which are used to form small structures with dimensions in the micrometer scale (one millionth of a meter). This technology is now being utilized to manufacture state of the art MEMS-Based Accelerometers.

Future Accelerometer Advancements
In the next decade, NANO technology will create new applications and dramatically reshape this area of technology.

*"Neo FreeRunner"*s accelerometers are LIS302DL, MEMS-Based Accelerometers. They are ultra compact low-power three axes linear accelerometers. The sensing element, capable of detecting the acceleration, is manufactured using a dedicated process developed by ST to produce inertial sensors and actuators in silicon.

The LIS302DL has dynamically user selectable full scales of ± 2g/± 8g and it is capable of measuring accelerations with an output data rate of 100 Hz or 400 Hz. It is guaranteed to operate over an extended temperature range from -40 °C to +85 °C [24].

4.1.1 Data acquisition

To understand the values provided by the accelerometers, the first step is to understand how the sensors are oriented.

In the following images the orientations of the two sensors are shown.

Figure 4: Orientation of the first accelerometer

Figure 5: Orientation of the second accelerometer

As it can be seen in the images, the Z axis is pointing from the display downwards to the back of the Openmoko, this applies to both of the sensors. The X and Y axis are in the same plane as the screen, while the Z, as it has been commented previously is pointing into the screen. The second accelerometer has the X and Y axes rotated 45 degrees around the Z axes, but there are in the same plane as previous one.

Following the way to access the data provided by the accelerometers is going to be explained.

Data structure

The data is given with the next structure:

```
struct input_event {
struct timeval time;
__u16 type;
__u16 code;
__s32 value;
};
```

So the structure of the accelerometer's data has four different fields. It consists of a structures with the time when the data has been obtained, the type which concretes the kind of data, if it is accelerometer's data or a synchronization package, the code which concretes more this information and finally the value.

The data is written to the stream message by message.

The following block-size is an example of the accelerometer data, divided into the used sections.

Typical accelerometer data:

```
|----- time ------|  |type| |code|  |-value-|
8163 49da 6d62 000d   0000   0000   0000 0000
8163 49da 91d8 000d   0002   0000   0048 0000
8163 49da 9231 000d   0002   0001   0012 0000
8163 49da 9251 000d   0002   0002   03ba 0000
8163 49da 9270 000d   0000   0000   0000 0000
8163 49da b6cf 000d   0002   0000   0036 0000
```

Following each field is going to be explained:

Time Structures

The time structure contains the time information.

Event types

The types categorize the incoming messages. This could have two different values:

0x00
According to *linux/input.h* this event is called *EV_SYN*. It signals the wish to synchronize. Normally this event is used in combination with code 0x00 to mark the send data complete and therefore applicable.

0x02
This event is called *EV_REL* and signals *relative movement*. It is used to transmit the acceleration the sensors encounter. The definition should not be taken too seriously in this context, because the data values provided by the accelerometer always represent the absolute acceleration measured at the given time.

Event codes

Synchronization event codes

The synchronization event may use quite a lot of codes, but the only used one is the 0x00 code.

0x00
This code is referred to as SYN_REPORT. It means that the last dataset was completely transmitted. Therefore the before transmitted set of data values can be considered complete. This means if this message is received you may process the given data further.

Relative movement event codes

The amount of possible codes for this event type is quite big. The only ones used are explained following .

0x00
REL_X - Acceleration in x direction

0x01
REL_Y - Acceleration in y direction

0x02
REL_Z - Acceleration in z direction

Value of the acceleration

The last block of data contains the value of the acceleration.In case of being a synchronization package, the value is 0.

A typical message block

The typical message block consists of 3 messages containing the acceleration data for every of the three axis followed by a synchronization message to signal the end of the block and to verify the correction of the 3 previous messages.

The following example is a message block with explanation of its different messages and data sections.

```
8c66 4819 99e6 0006   0002   0000   0048 0000
|------Time-------|  EV_REL  REL_X  |-Value-|
(Measured acceleration in x axis direction of 72) ──────────► x(n)

8c66 4819 9a36 0006   0002   0001   0024 0000
|------Time-------|  EV_REL  REL_Y  |-Value-|
(Measured acceleration in y axis direction of 36) ──────────► y(n)

8c66 4819 9a50 0006   0002   0002   0396 0000
|------Time-------|  EV_REL  REL_Z  |-Value-|
(Measured acceleration in z axis direction of 918) ─────────► z(n)

8c66 4819 9a57 0006   0000   0000        0000 0000
|------Time-------|  EV_SYN  SYN_REPORT  |-Value-|
(The transmitted data block is complete you may process the given data)
```

Data acquisition

Once having explained the data structure, following it is going to be commented the developed application for acquiring the data.

The information from both of the accelerometers is exported through two different input event based file mappings. These devices nodes can be opened by the default file systems calls for reading files. The data can be read from the stream as soon as the sensor measures it.

In the next figure, there is the flowchart of the application.

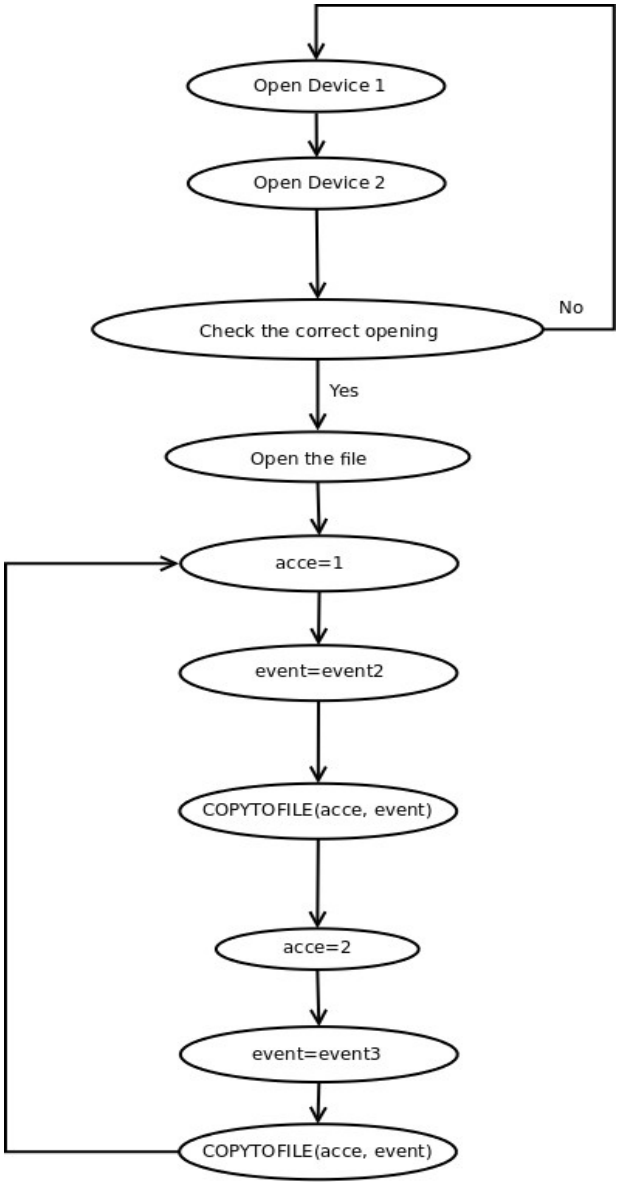

Diagram 4: Flowchart of the application for getting data from the accelerometers

First the devices nodes are opened, and a checking of the correct opening is made. After, the file where the data is going to be saved is opened. Then the specification of which accelerometer is going to be read is made, in the first time, the first accelerometer. The next step is to call the *"copytofile"* function, which is going to be explain following, but in general, it takes the data and copy to the file. Finally the same process is carried out, but this time with the second accelerometer. This process is continually executing.

Following, there is the flowchart of the *"Copytofile"* function.

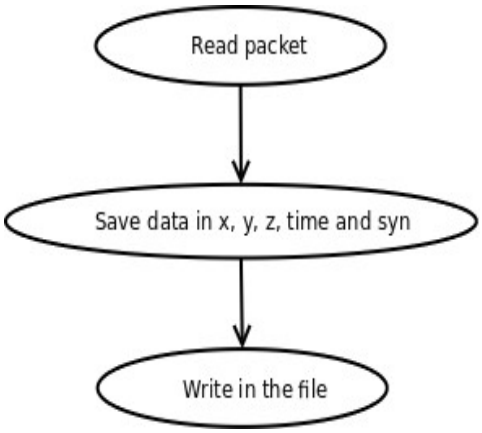

Diagram 5: Flowchart of the "Copytofile" function

The “Copytofile” function, reads the packets, from the device node. After it takes the data of the acceleration in the different axes (x, y and z), the time and the synchronization data, and it writes them in a file.

The sample frequency of the data of the accelerometers is 400 Hz, as it has been commented previously. Its bandwith is of 200 Hz and sixteen bits per sample has been used.

In the next graphic it is the plotted of the data of the second accelerometer.

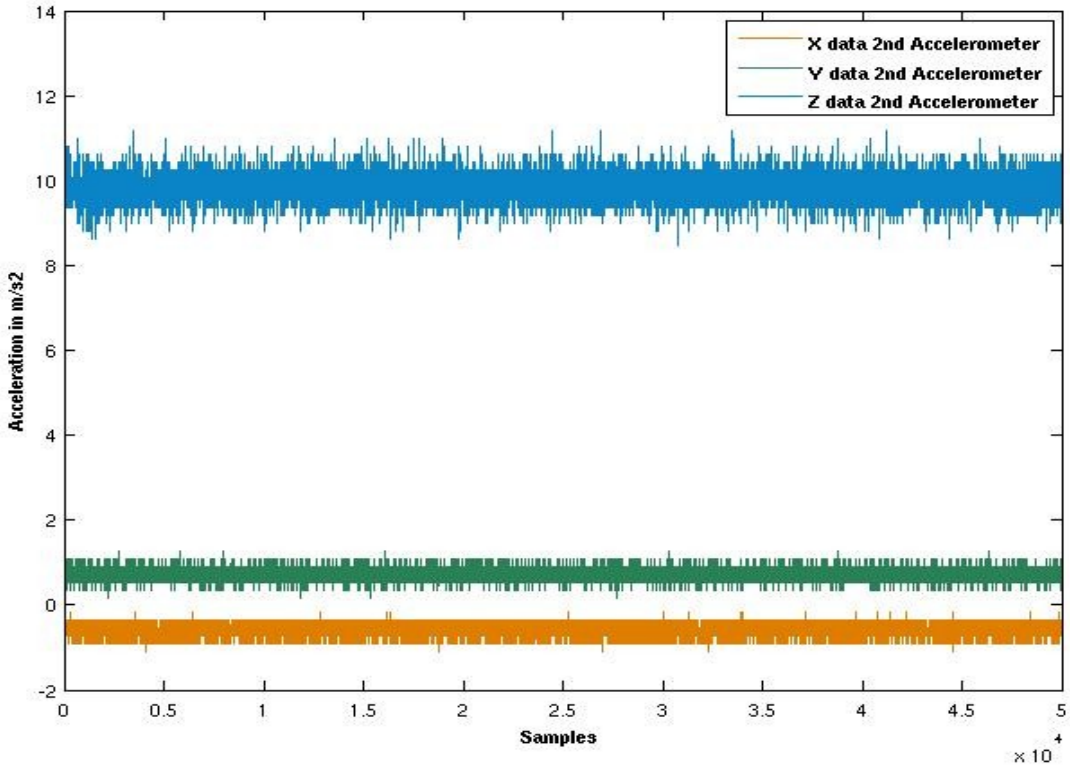

Figure 6: Data of the three axis of the second Accelerometer

Analysing the data, some errors in the packages were detected. Some of them were out of order so a study of the errors was made for discarding the wrong packages, taking 50000 packages for each accelerometer.

The problem was that some packages were mixed up, so instead of having the value of the synchronization bits, were the values of the accelerometers or of the accelerations. For ruling out this wrong packages, the synchronization bit was studied checking that the value of it was 0. In the following graphics the distribution of these errors are plotted, where value '1' is for the right packages, and value '0' for the wrong ones:

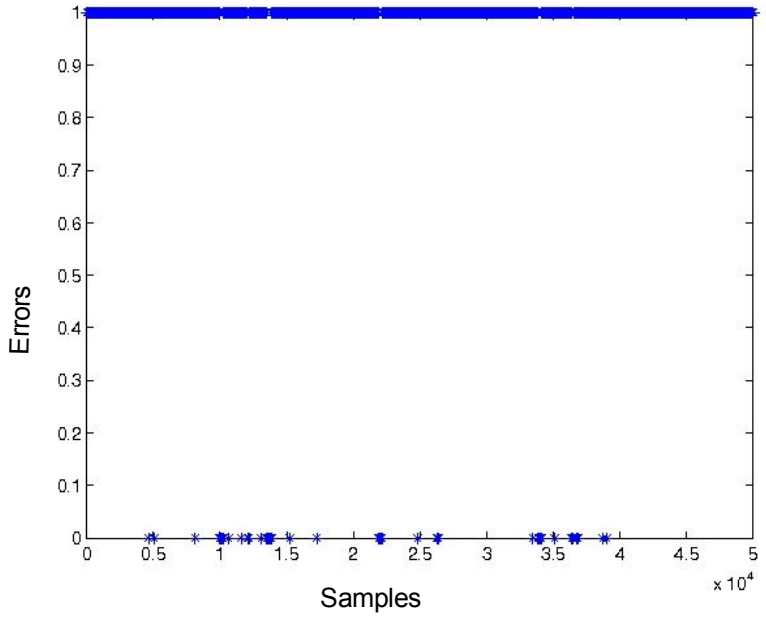

Figure 7: Distribution of the errors of the first accelerometer

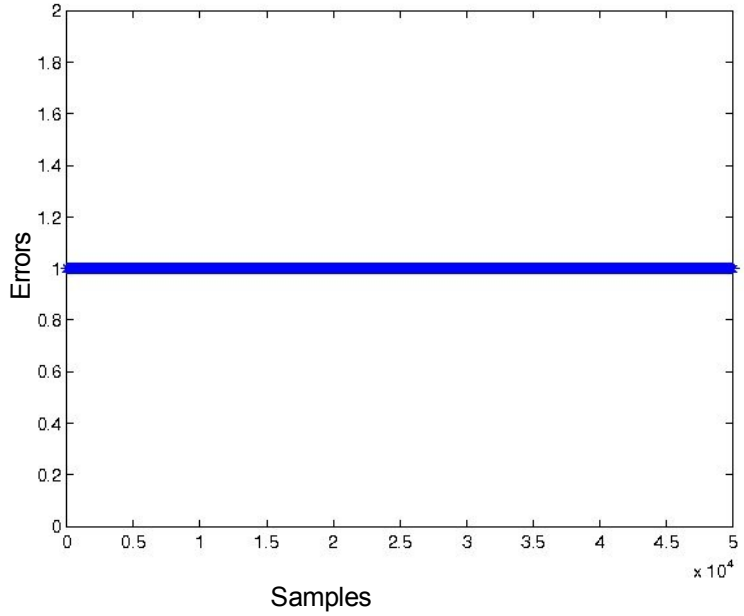

Figure 8: Distribution of the errors of the second accelerometer

Observing the figures can be concluded that whereas in the second accelerometer there is no error, in the first a 3,58% of the total data arrived wrong, this means 1790 packages. These errors will affect the later work of calculating the correlation coefficients. Although all these are distributed among the 50000 samples, in the last 10000, there is no error, so the decision of using these last 10000 samples of the two accelerometers to go on working was taken.

4.1.2 Noise in accelerometer data

Once being sure that the data is correct for continuing, the next step is to analyse it. Observing the data*(Figure 6)*, the first conclusion made is that there is a great noise. The values of the X and Y axes should be 0, and the values of the Z axis have to be 1. Instead of this values, in the Figure 6, can be seen that the values vary from 9,5 to 11 in the case of Z axis. The data of the accidents with which the later analyse will be done, has been taken with some accelerometers with higher quality than the "*Neo FreeRunner"* 's ones, and so with less noise,so the first step is to characterize the noise of the LI LIS302DL. This characterization is made by calculating the different correlations: the autocorrelation, the cross-axis and the cross-sensor coefficient correlation.

The autocorrelation is the measure of similarity of a signal with itself as a function of a time-lag applied to one of them. It is the similarity between observations as a function of the time separation between them.

The following expressions have been used for achieving the desired results. The first one calculates the self-correlation coefficient with bias, and the second one without it.

$$\hat{R}(m)_{xx} = \frac{\sum_n [(x(n)\,x(n+m))]}{\sum_n [x(n)^2]}$$ Expression for self-correlation with bias

$$\check{R}(m)_{xx} = \frac{\sum_n [(x(n))(x(n+m))]}{\sum_n [x(n)^2]} \frac{N}{(N-m)}$$ Expression for self-correlation without bias

In these expressions x(n) is called to data without the mean. As we can notice the only difference between them, is a N/(n-m) factor.

In the next tables there are some values of the autocorrelation for different numbers of sample:

Correlation lag (m)	$\hat{R}(m)_{xx}$	$\check{R}(m)_{xx}$	$\hat{R}(m)_{yy}$	$\check{R}(m)_{yy}$	$\hat{R}(m)_{zz}$	$\check{R}(m)_{zz}$
1	1	1	1	1	1	1
37	-0,0483	-0,0484	-0,0061	-0,0061	0,0026	0,0026
1805	-0,0021	-0,0025	0,0014	0,0017	0,0037	0,0045
2414	0,0040	0,0053	0,0044	0,0058	0,0057	0,0075
3506	0,0013	0,0020	-0,0028	-0,0042	0,0062	0,0095
4738	0,0020	0,0037	0,0133	0,0254	0,0020	0,0038
5963	0,0122	0,0301	0,0044	0,0110	0,0006	0,0016
6890	-0,0026	-0,0084	-0,0069	-0,0223	-0,0033	-0,0105
7253	-0,0016	-0,0057	-0,0046	-0,0168	-0,0096	-0,0351
8370	0,0017	0,0105	0,0059	0,0364	0,0016	0,0099
9589	0,0044	0,1063	0,0000	0,0001	0,0000	-0,0009

Table 1: Values of autocorrelation of the first accelerometer

Correlation lag (m)	$\hat{R}(m)_{x2x2}$	$\check{R}(m)_{x2x2}$	$\hat{R}(m)_{y2y2}$	$\check{R}(m)_{y2y2}$	$\hat{R}(m)_{z2z2}$	$\check{R}(m)_{z2z2}$
1	0,9999	0,9999	1	1	0,9999	0,9999
37	-0,0123	-0,01	-0,0042	-0,0042	-0,0007	-0,0007
1805	0,0215	0,0262	0,0049	0,0060	-0,0116	-0,0142
2414	0,0143	0,0188	-0,0009	-0,0013	-0,0023	-0,0031
3506	0,0075	0,0115	0,0102	0,0157	0,0100	0,0154
4738	-0,0081	-0,0154	0,0040	0,0076	-0,0036	0,0038
5963	0,0065	0,0160	-0,0047	-0,0118	0,0040	0,0098
6890	-0,0070	-0,0226	0,0054	0,0174	-0,0101	0,0326
7253	-0,0066	-0,0239	-0,0085	-0,0309	-0,0102	-0,0370
8370	0,0019	0,0119	-0,0015	-0,0093	-0,0005	-0,0034
9589	-0,0014	-0,0349	-0,0015	-0,0371	0,0004	0,0103

Table 2: Values of autocorrelation of the second accelerometer

The values of the autocorrelation falls down quite fast, so in the sample 37 the values are of the order of a 4 % in higher case.

After having calculated the autocorrelations for the 3 axes of the two accelerometers, the next step is to determinate if there is any linear relation between them. For determining it, the Cross-axes and

Cross-sensor correlations have also been calculated. Cross-correlation is a measure of the interdependence of two variables.

So the cross-sensor correlation coefficients are:

$$R_{xx2}=\frac{\sum_n[(x(n)x_2(n))]^2}{\sum_n[x(n)^2]\sum_n[x_2(n)^2]} \qquad R_{yy2}=\frac{\sum_n[(y(n)y_2(n))]^2}{\sum_n[y(n)^2]\sum_n[y_2(n)^2]} \qquad R_{zz2}=\frac{\sum_n[(z(n)z_2(n))]^2}{\sum_n[z(n)^2]\sum_n[z_2(n)^2]}$$

The cross-axis correlation coefficients are the following ones:

$$R_{xy}=\frac{\sum_n[(x(n)y(n))]^2}{\sum_n[x(n)^2]\sum_n[y(n)^2]} \qquad R_{xz}=\frac{\sum_n[(x(n)z(n))]^2}{\sum_n[x(n)^2]\sum_n[z(n)^2]} \qquad R_{yz}=\frac{\sum_n[(y(n)z(n))]^2}{\sum_n[y(n)^2]\sum_n[z(n)^2]}$$

$$R_{x2y2}=\frac{\sum_n[(x_2(n)y_2(n))]^2}{\sum_n[x_2(n)^2]\sum_n[y_2(n)^2]} \qquad R_{x2z2}=\frac{\sum_n[(x_2(n)z_2(n))]^2}{\sum_n[x_2(n)^2]\sum_n[z_2(n)^2]} \qquad R_{y2z2}=\frac{\sum_n[(y_2(n)z_2(n))]^2}{\sum_n[y_2(n)^2]\sum_n[z_2(n)^2]}$$

Where, x(n) is a sample of the X axis of the first accelerometer y(n) is the sample of the Y axis of the second accelerometer z(n) is a sample of the Z axis of the first accelerometer, $x_2(n)$ is a sample of the X axis of the second accelerometer, $y_2(n)$ is the sample of the Y axis of the second accelerometer and $z_2(n)$ is a sample of the Z axis of the second accelerometer.

In the following table there are the different coefficients:

Cross-Sensor Coefficient	R_{xx2}	-0,0033
	R_{yy2}	-0,0110
	R_{zz2}	0,0026
Accelerometer 1 Cross- Axis Coefficient	R_{xy}	0,1039
	R_{xz}	-0,0055
	R_{yz}	-0,0251
Accelerometer 2 Cross-Axis Coefficient	R_{x2y2}	0,0659
	R_{x2z2}	0,0138
	R_{y2z2}	-0,0221

Table 3: Coefficients of cross-correlation

The coefficients in the case of Cross-sensor correlation are quite small, being the higher one of the order of 0,01. The case of Cross-axis coefficients is different. In one hand there are some values as the R_{xz} coefficient and the R_{yz} coefficient and the R_{x2z2} and the R_{y2z2} coefficients, these are the cross sensor coefficient between the X and Z axes and between the Y and Z axes of the two accelerometers, that are quite low, suggesting that it could not be a linear relation between them. But in the case of the R_{xy} coefficient , and in the R_{x2z2} these are higher, implicating a bigger correlation.

As it has been mentioned before, after having analysed the signals, the next step is to design a noise model generator. For designing it in M*atlab*®, first of all a white noise has been introduced, with the same number of samples as the. After the "*Monte Carlo method"*has been used, which is commonly used for simulating systems with correlated variables [25]. With this method, the autocorrelation matrix is decomposed to give a lower-triangular matrix, using "*Cholesky method*". Some values of this autocorrelation matrices are shown in Tables 1 and 2. So :

$$\overline{R}_{xx} = \overline{H}_x \overline{H}_x'$$

In this case, the M*atlab*®'s function gives the upper-triangular, but the lower one is the complex conjugate transpose of the upper one. Applying this to the white noise vectors,(w_x, w_y and w_z), produces three results vector with the correlation properties of the system being modelled. So the resulting vectors are the next ones:

$$\overline{u}_x = \overline{H}_x' \overline{w}_x$$

$$\overline{u}_y = \overline{H}_y' \overline{w}_y$$

$$\overline{u}_z = \overline{H}_z' \overline{w}_z$$

Where w_x, w_y and w_z are the vectors of white noise and H is the matrix with the properties of the autocorrelation.

The next step is to multiply it by a gain, for compensating the variance of the resulting vector and the real one. Finally the observed bias has been added, obtaining the next expressions for the different axis and the different accelerometers.

First accelerometer

$$\overline{v}_{x1} = \overline{H}_{x1}' \overline{w}_{x1} + b_{x1}$$

$$\overline{v}_{y1} = \overline{H}_{y1}' \overline{w}_{y1} + b_{y1}$$

$$\overline{v}_{z1} = \overline{H}_{z1}' \overline{w}_{z1} + b_{z1}$$

Second accelerometer

$$\overline{v}_{x2} = \overline{H}_{x2}' \overline{w}_{x2} + b_{x2}$$

$$\bar{v}_{y2} = \bar{H}_{y2}' \bar{w}_{y2} + b_{y2}$$

$$\bar{v}_{z2} = \bar{H}_{z2}' \bar{w}_{z2} + b_{z2}$$

In the following lines and figures there are explained the obtained results of the first accelerometer. In the *Annex II* there are the images of both accelerometers, of all the process.

In the following figures, the obtained spectrum with the real one is compared:

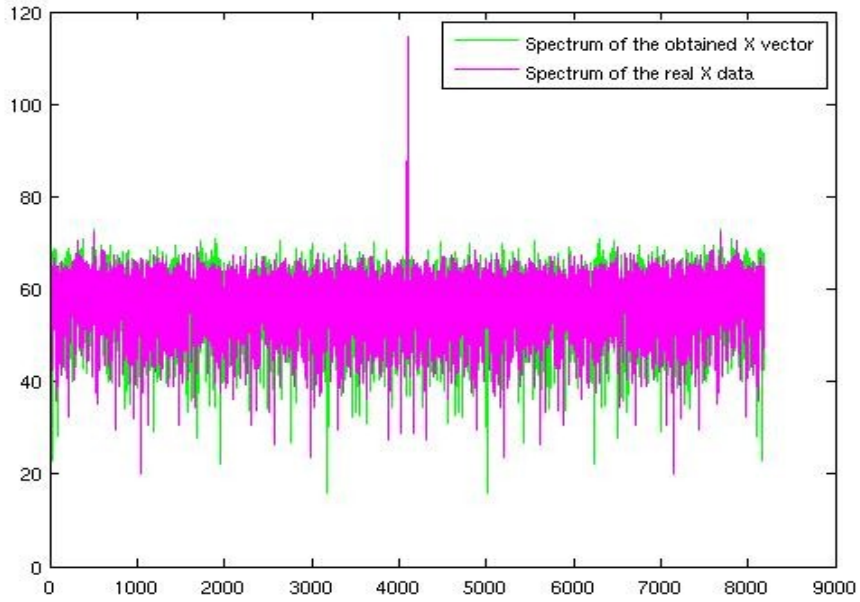

Figure 9: Comparison between the obtained X axis spectrum and the real one

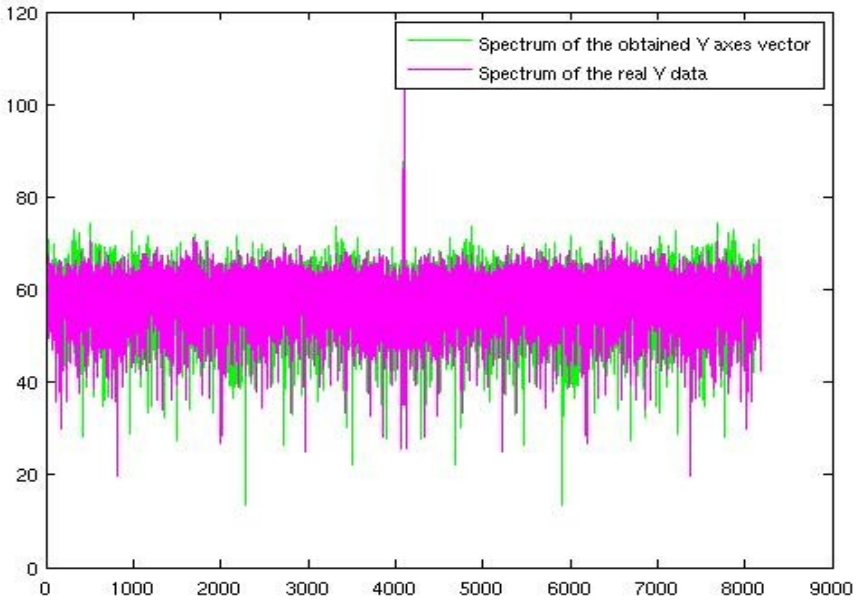

Figure 10: Comparison between the obtained Y axis spectrum and the real one

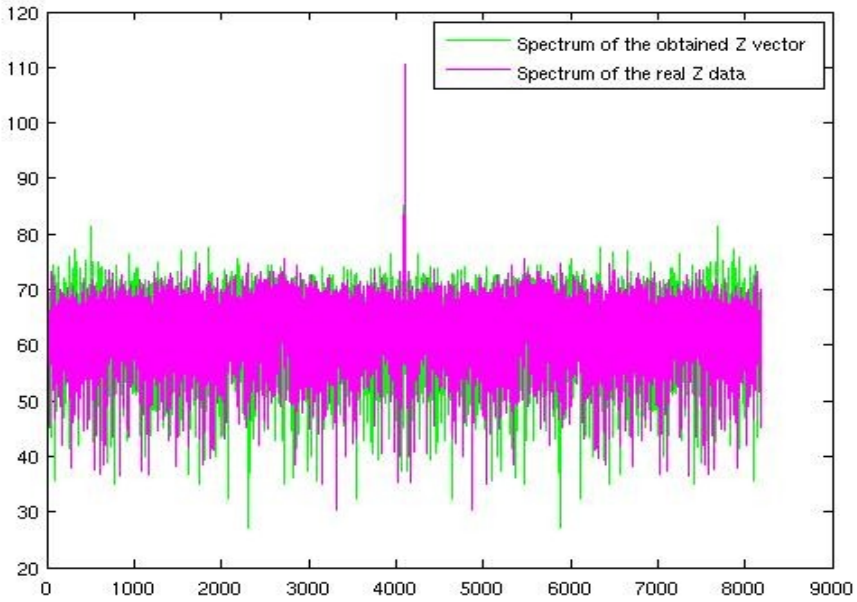

Figure 11: Comparison between the obtained Z axis spectrum and the real one

Analysing the results, although not been equals, they are similar, and comparing with the spectrum of the white noise, they bear a certain resemblance to the desired one.

The autocorrelations of the obtained vector have also been compared to the real ones. In the next figures there are shown.

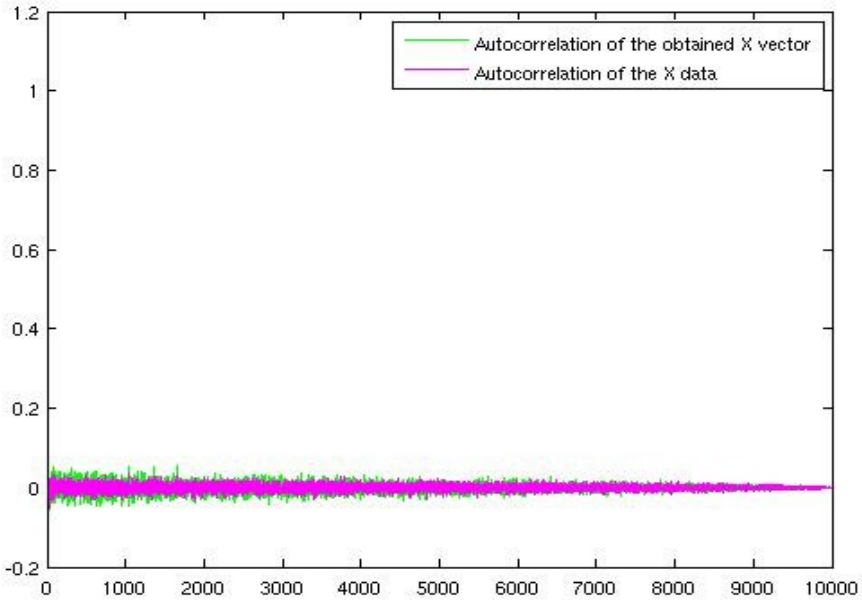

Figure 12: Comparison between the autocorrelation of the obtained X axis and the autocorrelation of the X data

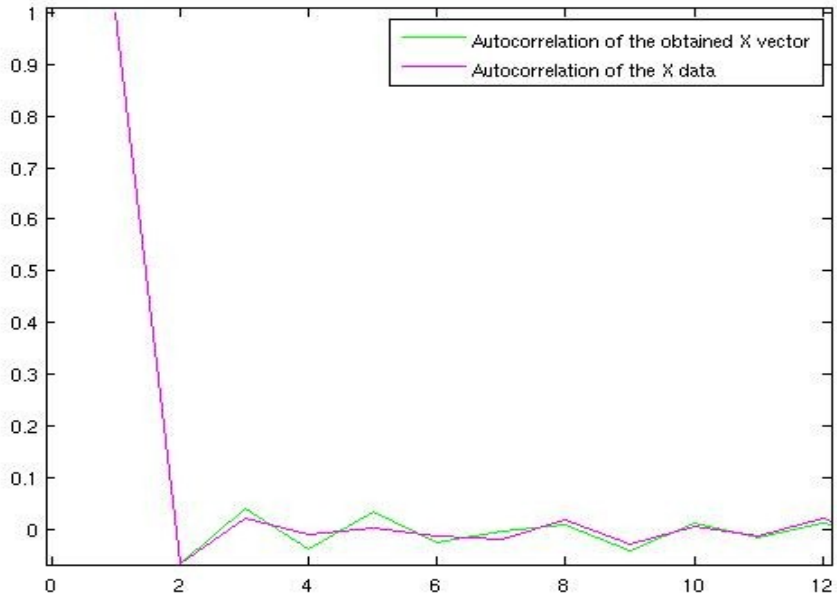

Figure 13: Zoom of the 10 first samples, of the comparison between the autocorrelation of the obtained X axis and the autocorrelation of the X data

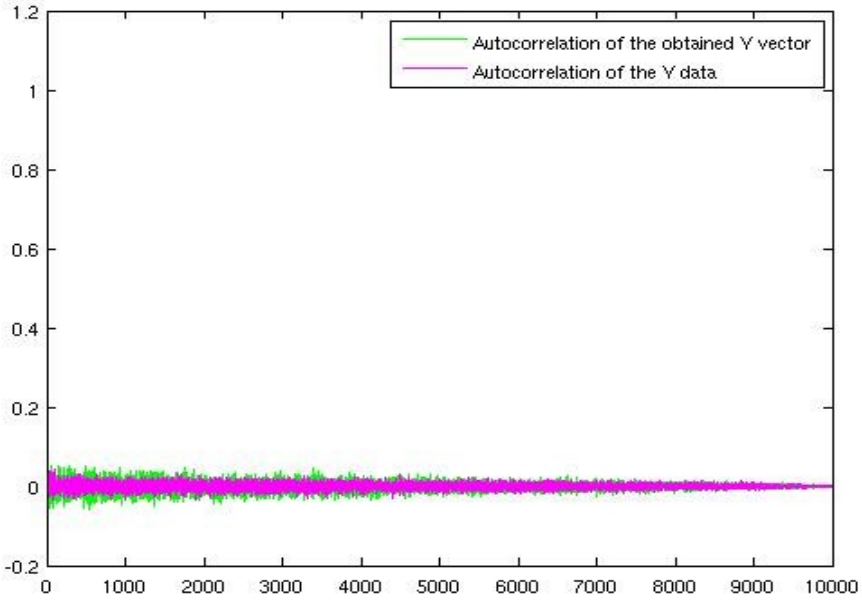

Figure 14: Comparison between the autocorrelation of the obtained Y axis and the autocorrelation of the Y data

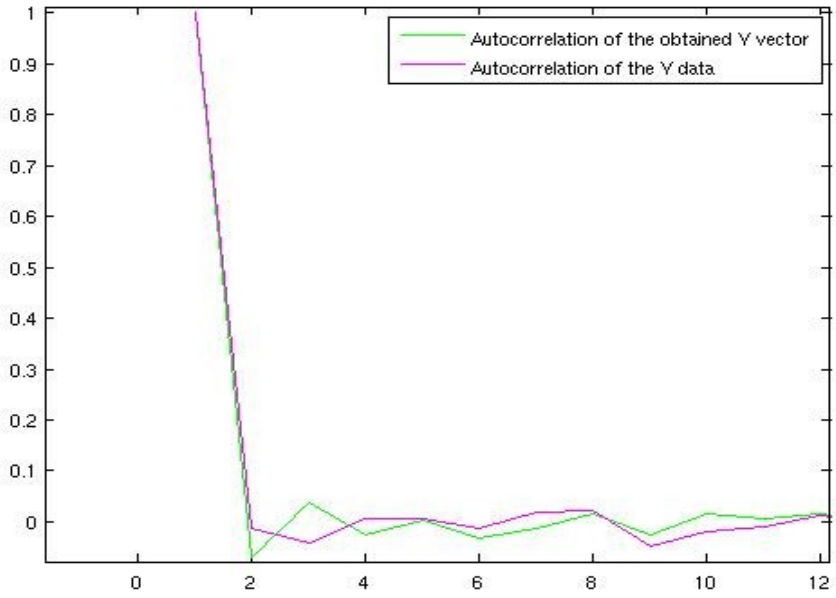

Figure 15: Zoom of the 10 first samples, of the comparison between the autocorrelation of the obtained Y axis and the autocorrelation of the Y data

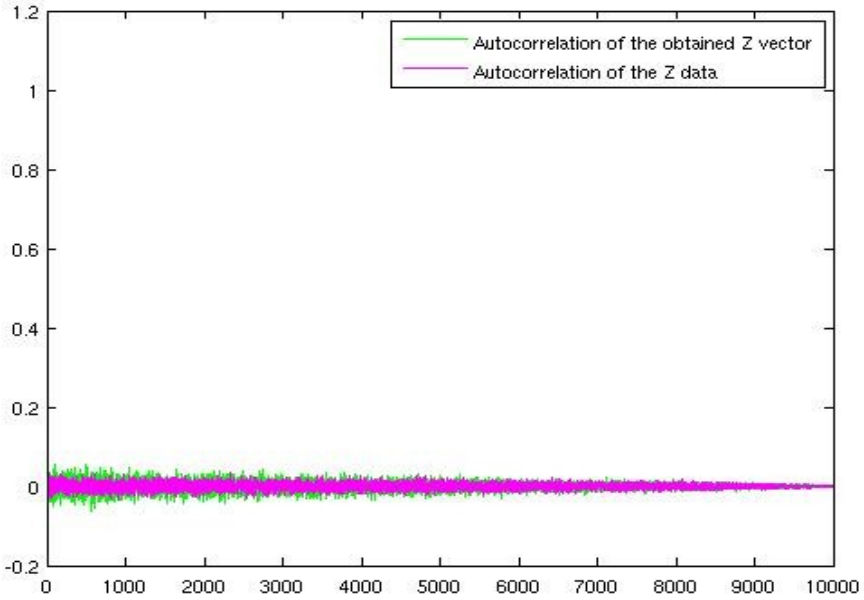

Figure 16: Comparison between the autocorrelation of the obtained Z axis and the autocorrelation of the Z data

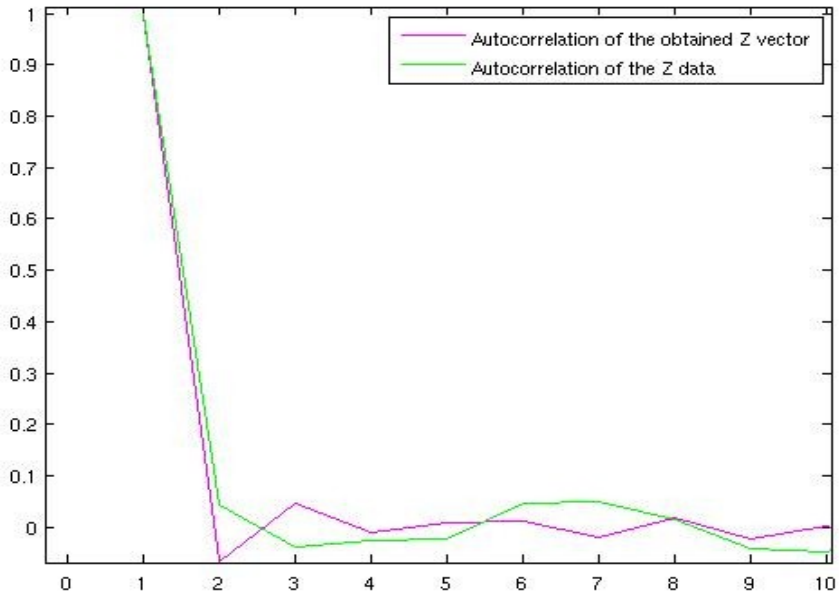

Figure 17: Zoom of the 10 first samples, of the comparison between the autocorrelation of the obtained Z axis and the autocorrelation of the Z data

With the autocorrelations the same conclusions can be obtained, thought not been identical, their resemblance is remarkable.

The noise of the accelerometer's data is always changing. This makes suspect that this could be caused by a hardware failure. Depending on which devices where turned on, different signals where strained. So the possible cause of this problem could be a hardware failure, which makes that different signals of different frequencies were strained, affecting the study of the noise.

4.2 Driving and accident models

4.2.1 Driving models

For performing the detection of possible crashes, the first step is to study different data. In one hand the data of a normal driving, and in the other one the data of accidents. The data of a driving model have been obtained from two different ways, the first one from a model called “Artemis model” [26], representative for typical European driving, the second one, instead, has been taken from some expressions used for dynamic process modelling [27].

As it has been commented previously, the Artemis model represents a typical European driving model,modelling different situations of real-world driving and on different roads. It only has the acceleration of the X axis, and it has been supposed, that in the other two axis the acceleration is 0. Although this is not truth in the Y axis, in the Z axis it comes true, in case of flat road and after having subtracted the gravity. In the graphics, the acceleration versus the time is plotted.

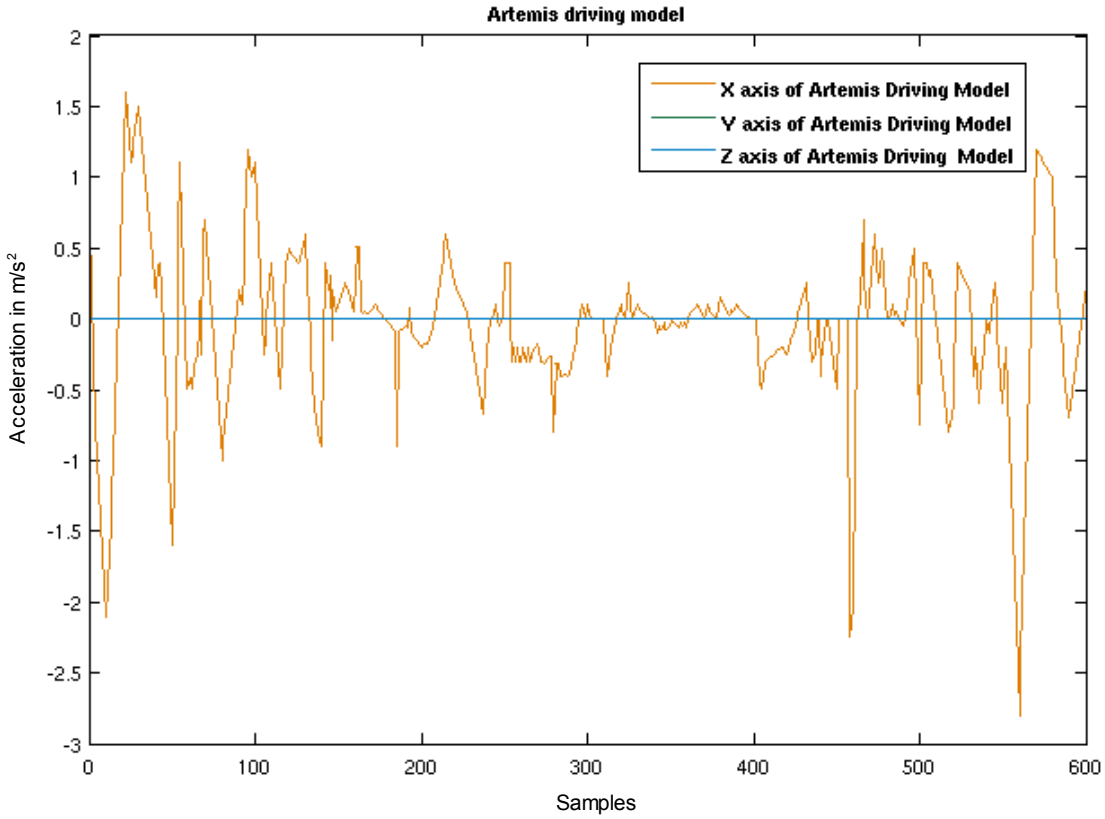

Figure 18: Artemis driving model

As can be seen in the image, the acceleration is limited between 1,6 m/s^2 and -2,8 m/s^2. This means that the car would achieve a speed of 60 km/h more or less, in 10 seconds or in the other hand, that for stopping a car going on 60 km/h 6 seconds would be needed,. The first 100 seconds, corresponds, to a driving in a city, with great acceleration and deceleration moments. From second 100 to 450, would correspond to a driving in a motorway, and finally it goes back to the city.

The second driving model, has been taken from expressions used in dynamic process modelling [27]. This expressions, established the acceleration in the X and the Y axis. This is enough, because the acceleration in the Z axis in the case of a flat road, should be null.

$$v_x = A_{max} * (\cos(0{,}1t) + 0{,}2 * \Phi_1)$$
$$v_y = A_{max} * (\sin(0{,}1t) + 0{,}2 * \Phi_2)$$

Where A_{max} is the magnitude indicating the maximum acceleration and Φ_1 and Φ_2 uniformly distributed random variables in the interval of [0 1].

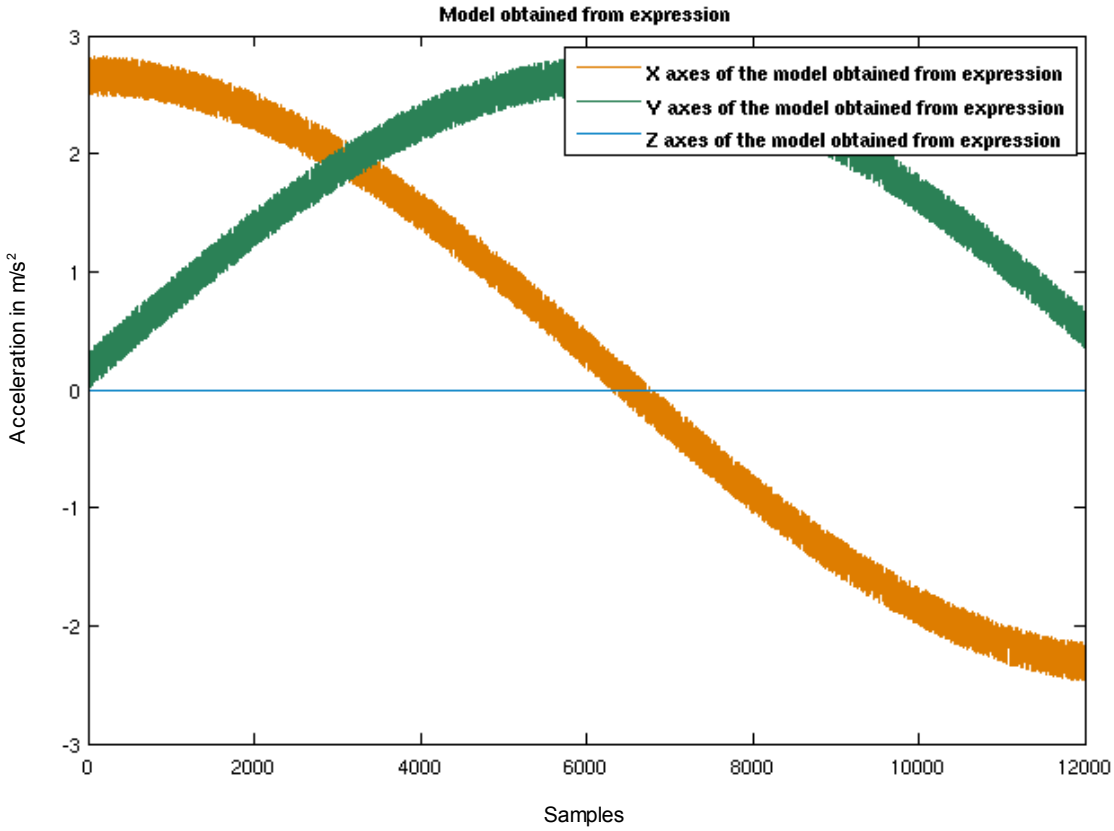

Figure 19: Model obtained from expressions

This model just consists of two sinusoids with an added noise. The maximum value of acceleration is 2,9 m/s^2, and the minimum, is the same but negative. This means that in one second a stopped car will achieve a speed of 10,44 km/h.

4.2.2 Accident models

The data of the crashes, have been taken from the web of NTHSA [28], which is an administration focused on vehicle safety, and it has a public crash test database, in which different data are saved. This data have been taken with different devices situated in different places, and different types of accidents. Although being a lot of different kinds of crashes, the only ones which are valid for the analysis are those, which have the data of the tri-axis accelerometers situated in the engine of the car, and which have the data of the three axis.

The accelerometers take a sample each 75 μs, that means that the sample frequency is of 13333 Hz. The sensors have been oriented following the global coordinate system for the vehicle, which is shown in the *Figure 20*. [29-30]

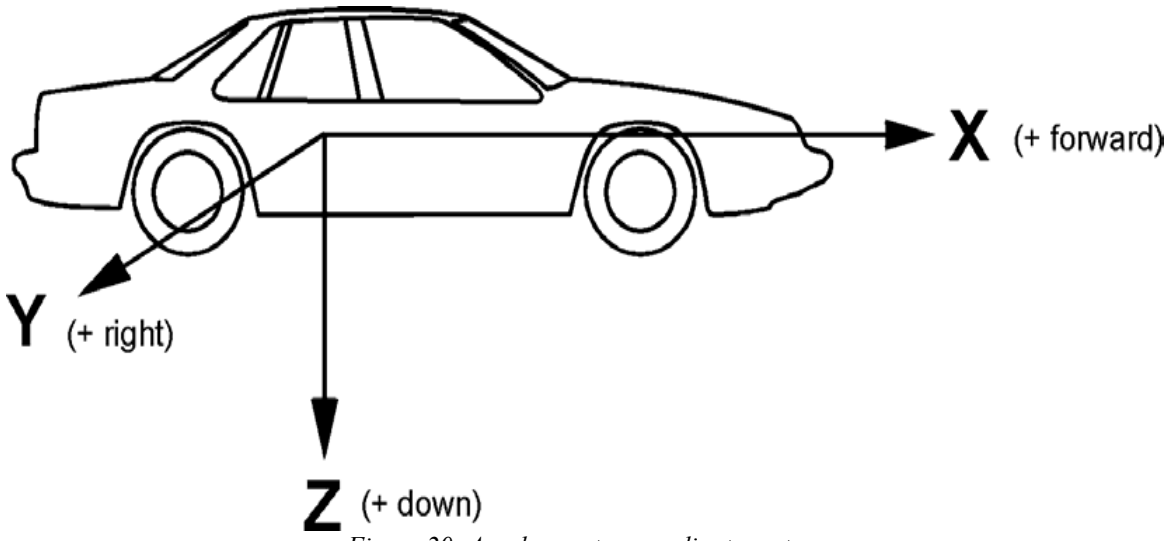

Figure 20: Accelerometer coordinate system

In the next table, there are the characteristics of the different accidents, which are going to be analysed later. For seeing more accident data go to *Annex III*.

Test Number	***Type of accident***	***Impact Angle (degrees)***	***Closing speed (kph)***
Accident 2	Vehicle into vehicle	300	48,1
Accident 107	Vehicle into vehicle	60	48
Accident 400	Vehicle into vehicle	0	98,8

Table 4: Characteristics of the different accidents

In the next pictures, there are some examples of the acceleration on the different axes in some crashes.

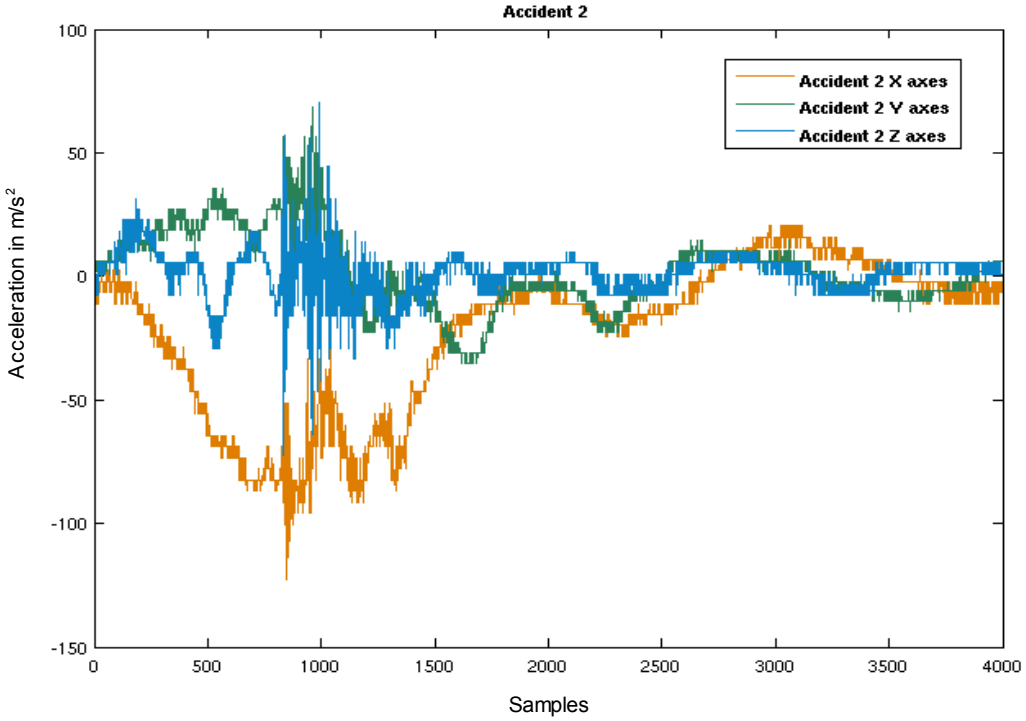

Figure 21: Accident 2

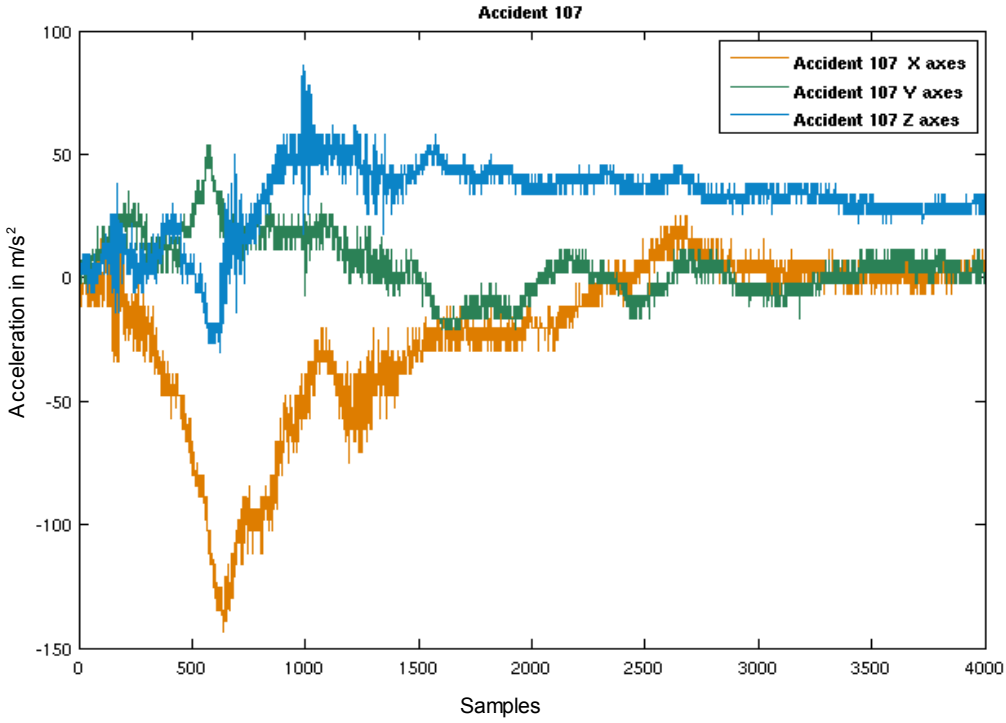

Figure 22: Accident 107

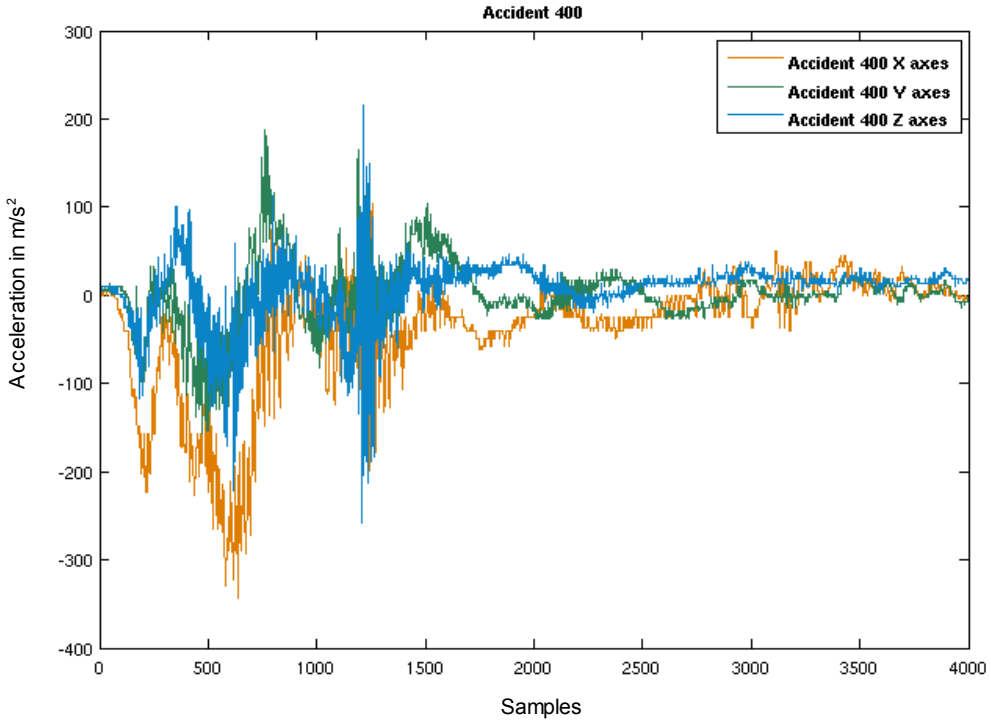

Figure 23: Accident 400

In the images can be seen, that the accelerations are very high compared to the driving models. Observing the graphics, it is remarkable, the great deceleration that occurs in a first moment in the X axes, which in all the cases exceeds from the 100 m/s^2. The great difference between the Accident 400 and the others two is also interesting, this is due to the difference between the closing speeds, which in the accident 400 duplicates the other two cases (See *Table 4*). With this difference, it is noticed that although having some patterns of some accidents, and even these being very similar, each crash may be different from the others.

4.3 Detection of the accidents

4.3.1 Study of the accident data

As the sampling frequencies of the accelerometers of the "Neo FreeRunner" and the ones used for getting the accidents data are different, (the accelerometers maximum sampling frequency is 400 Hz and accident data have been taken with a frequency of 13333 Hz) the data have to be downsampled. For analysing if a filter is necessary or not, a study of the spectrum have been made.

At the time of analysing the spectrum, a rectangular window has been used. This is constant inside the window interval, and zero elsewhere. This window has been chosen, for no affecting the signal.

For getting the spectrum, a discrete Fourier transform (DFT) have been used using 2^{13} samples, computed with a fast Fourier transform algorithm (FFT). Then the output have been rearranged by moving the zero frequencies to the centre.

In the next figures there are the spectrum of different accidents, algorithmic plotted have been used:

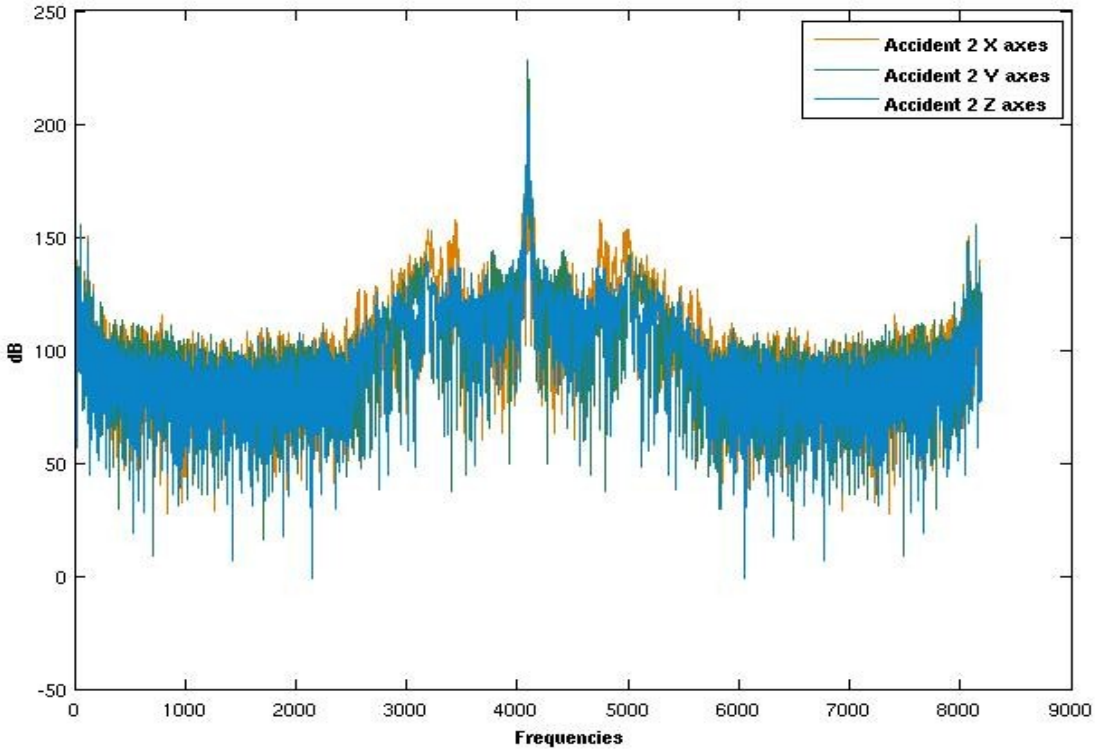

Figure 24: Spectrum of data of Accident 2

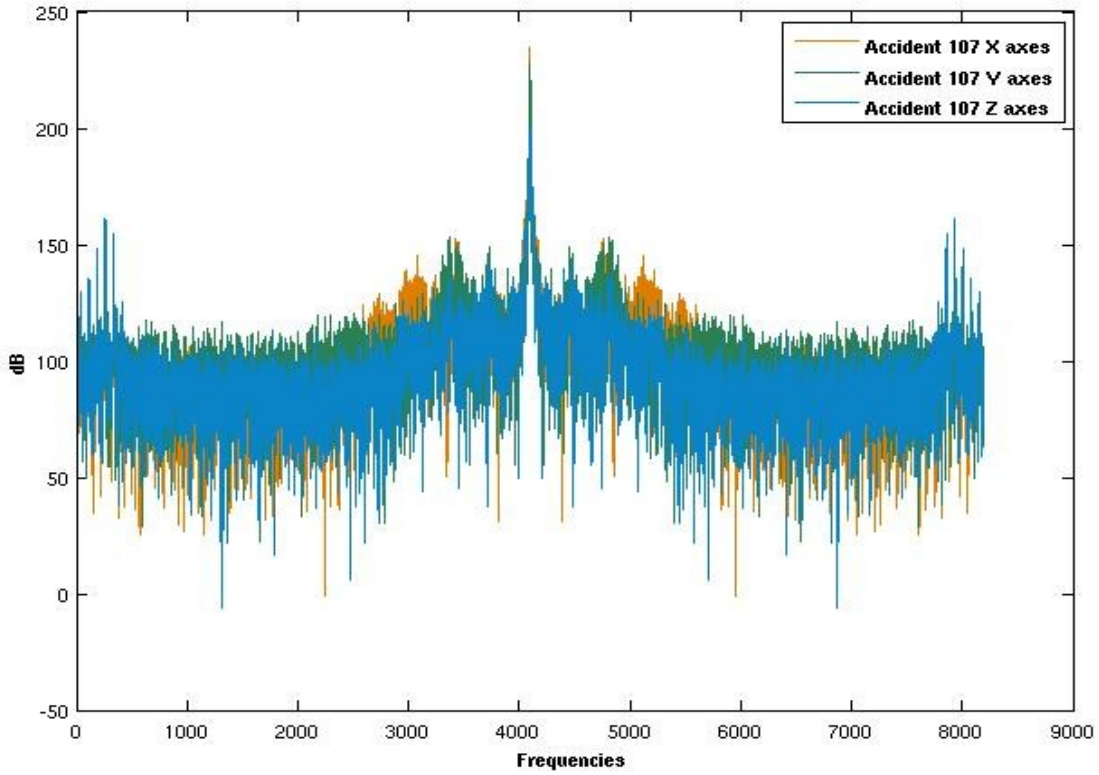

Figure 25: Spectrum of data of Accident 107

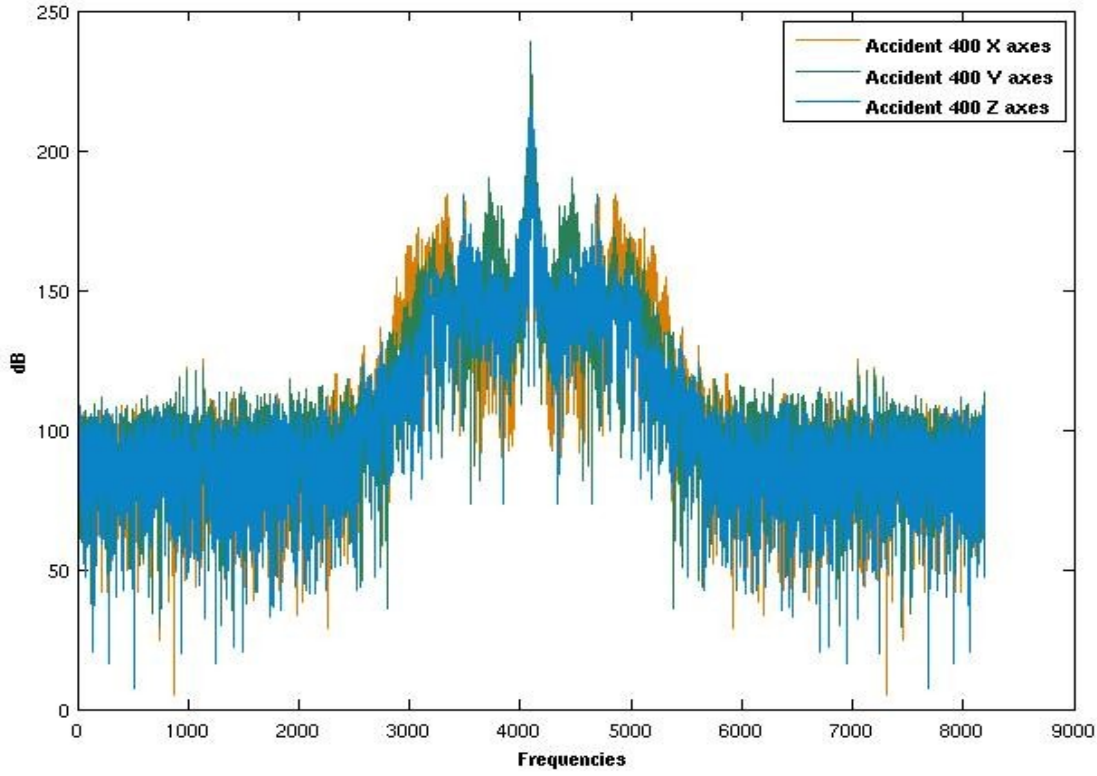

Figure 26: Spectrum of data of Accident 400

In the figures can be seen that in all of them there are spectral components until 1800 Hz. So the Shannon-Nyquist sampling theorem [31], is not satisfied and the resulting signal will have aliasing. To ensure that the sampling theorem is satisfied, a low-pass filter has been used as an anti-aliasing filter to reduce the bandwidth of the signal before the signal is down-sampled. So the process is the next one:

- Filter the signal to ensure that the sampling theorem is satisfied.
- Reduce the data by picking out every Mth sample. In this case M=33.

All the process, including the two steps, is called decimation.

The cut-off frequency of the antialiasing filter is 200 Hz. As the Downsampling factor is 33, the following the cu-off frequency should be Fs/2M, and that is 200 Hz.

The filter has been design with Matlab®'s fdatool, which stands for Filter Design and Analysis Tool [32].

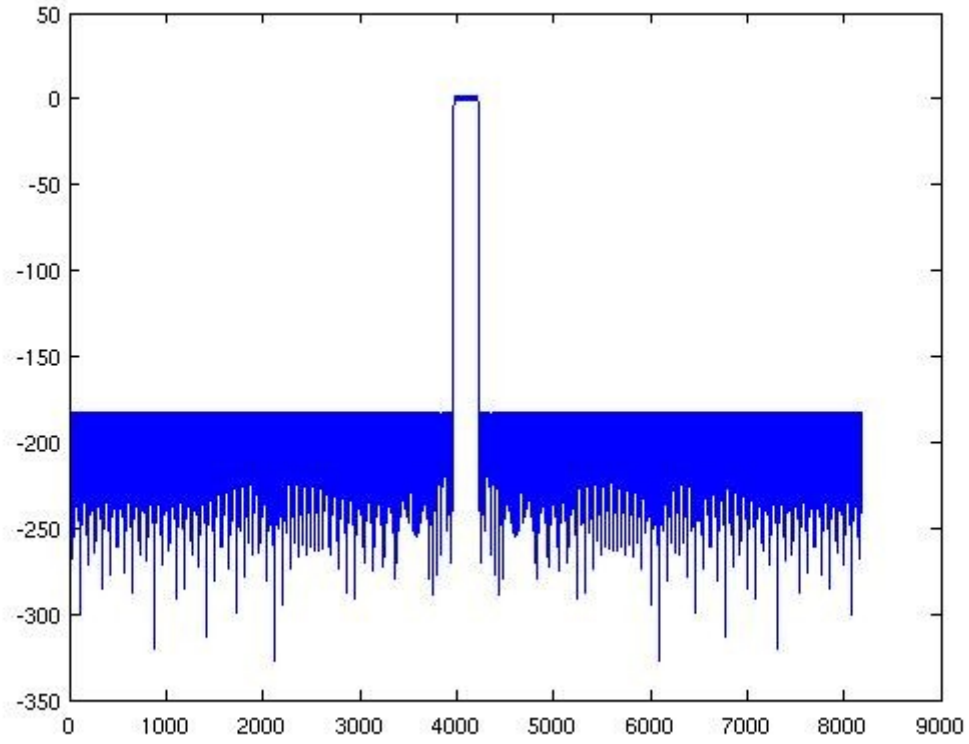

Figure 27: Anti-aliasing filter

As it is already known, after filtering the signal with the filter in *Figure 27*, all the frequencies out of the bandwidth of the filter must be attenuated, while the frequencies which are inside the bandwidth, should continue with the same form. As it is shown in the next figure:

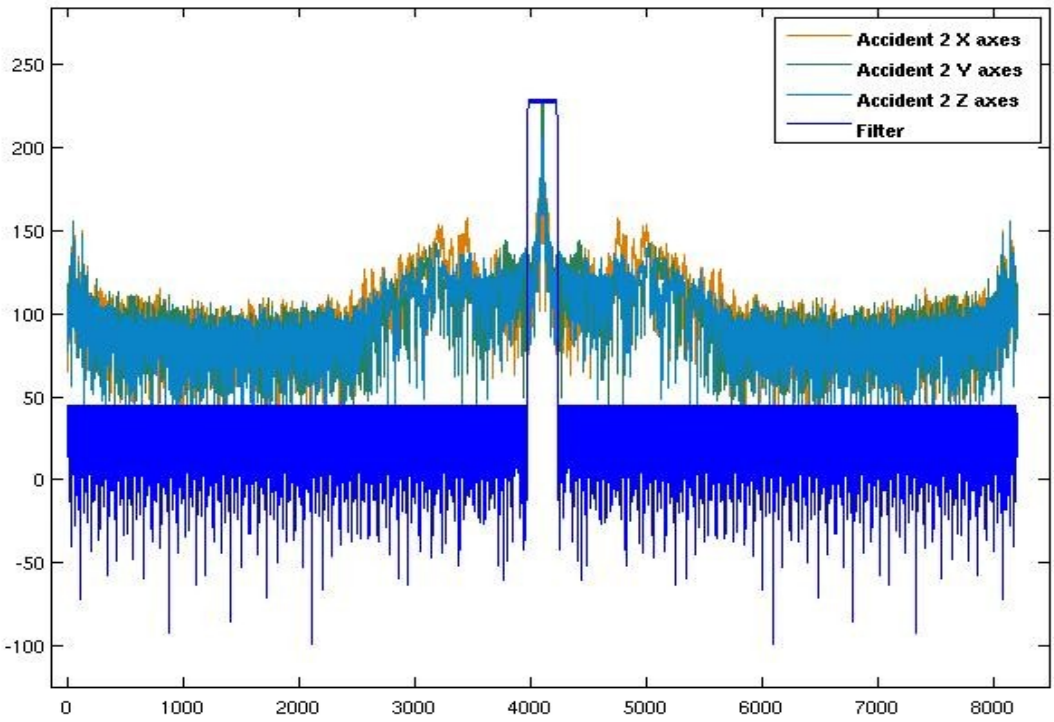

Figure 28: Spectrum of data of Accident 2 and Filter

The obtained results are shown in the following figures:

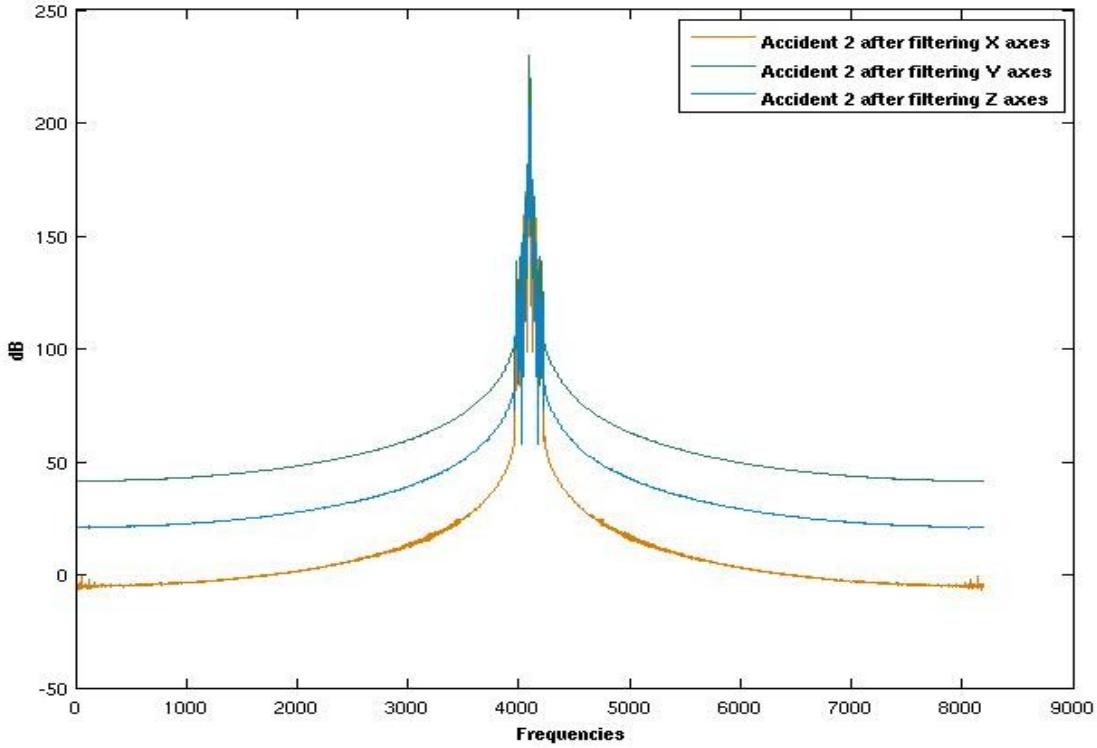

Figure 29: Spectrum of Accident 2 after filtering the signal

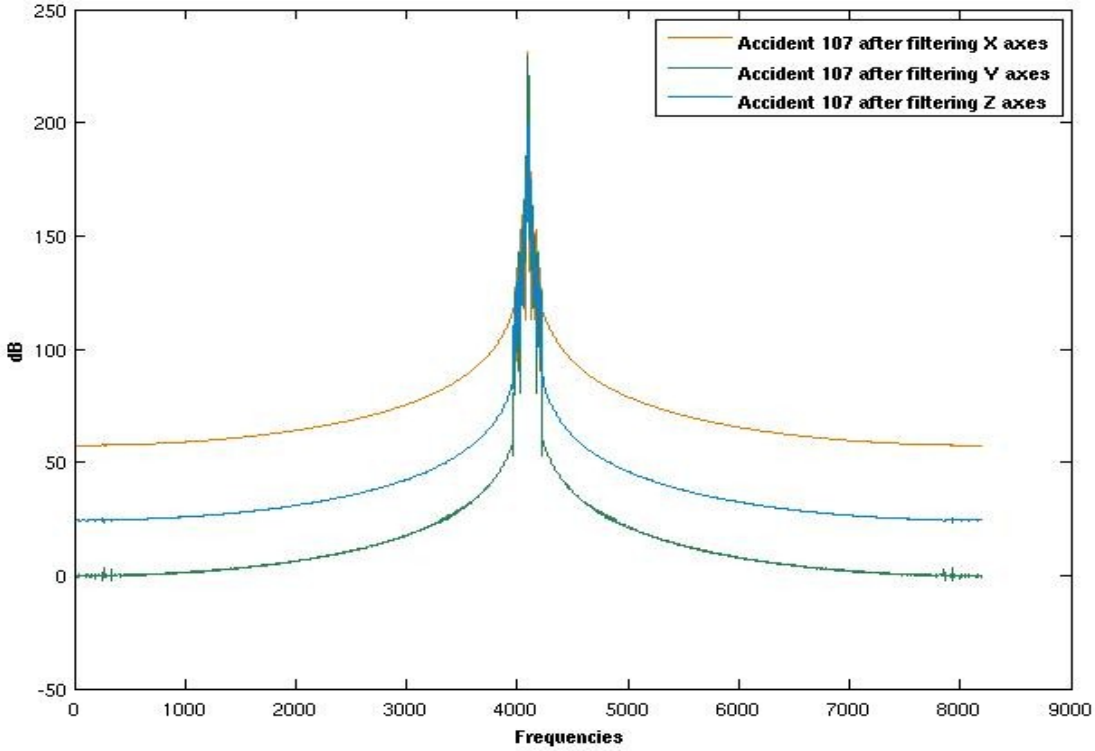

Figure 30: Spectrum of Accident 107 after filtering the signal

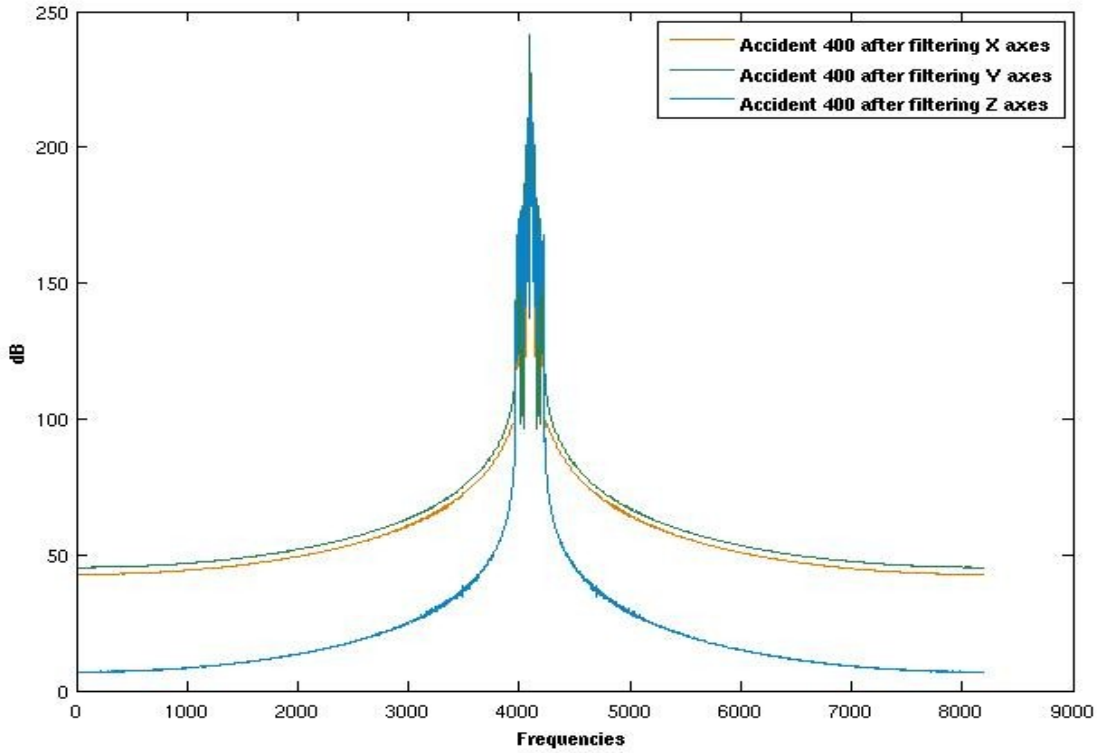

Figure 31: Spectrum of Accident 400 after filtering the signal

The obtained filtered data is just as the expected one, attenuating the frequencies out of the band.

In the following figures there is the comparison between, the spectrum of the down-sampled data filtered and not filtered.

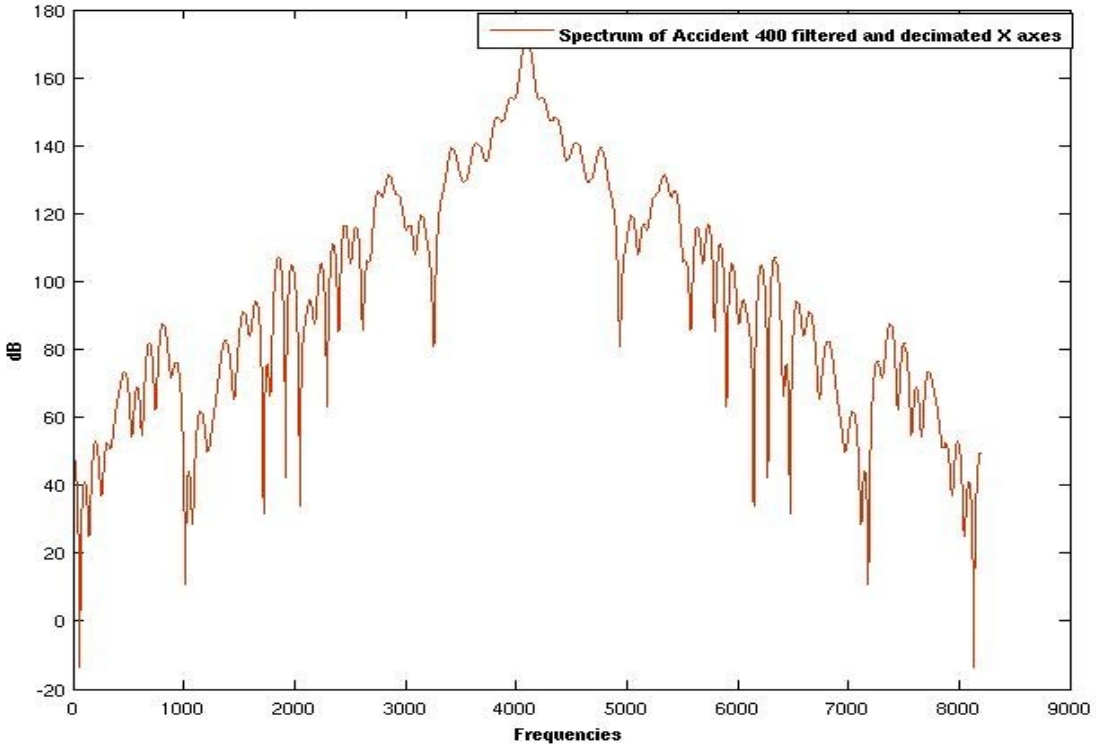

Figure 32: Comparison between the X axes data of the Accident 400 with and without filtered.

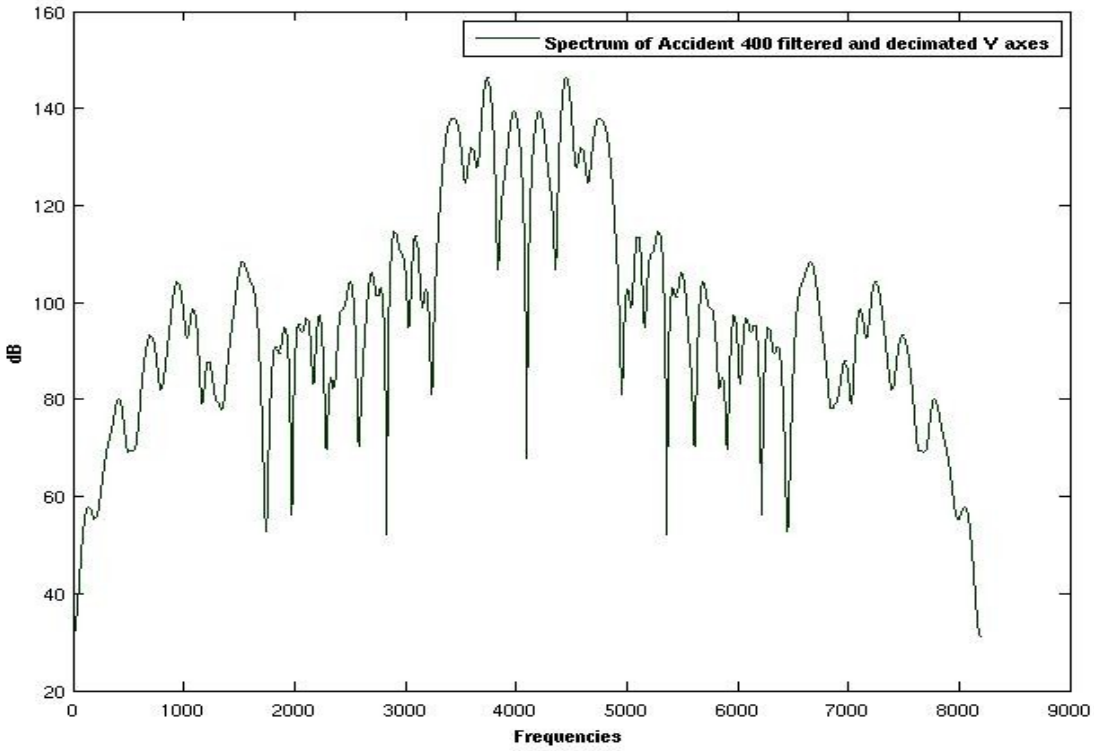

Figure 33: Comparison between the Y axes data of the Accident 400 with and without filtered.

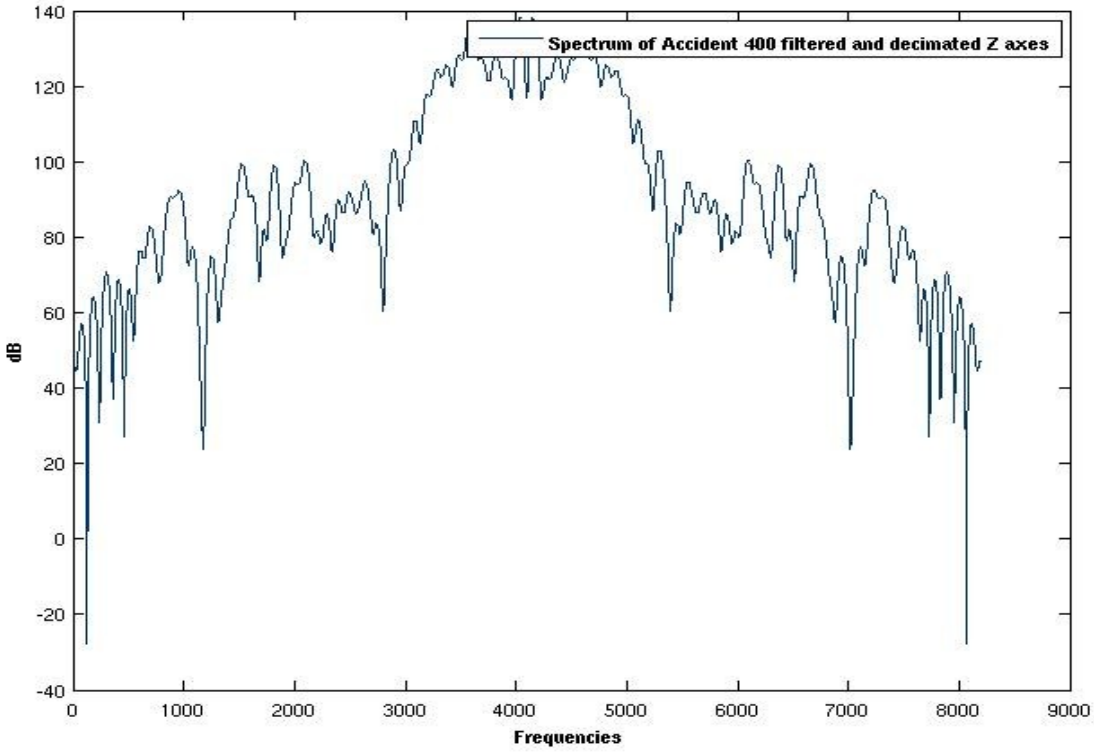

Figure 34: Comparison between the Z axes data of the Accident 400 with and without filtered.

Observing the images, the correct functionality of the filter can be observed. After having filtered and downsampled the data, the frequencies from 200 in advance are cancelled, while the others are conserved, as happened in previous figures, without downsampled.

After having compared the spectrum of the different accidents filtered and not filtered and having confirmed the right operation of the filter, the next step is to analyse the data itself. Comparing the data, the first conclusion made is that the filter introduces a lag to the signal. This is due to the type of the filter used, an IIR filter, with a huge number of coefficients, of the order of 100. The order is not an inconvenient because this filter is used only for the theoretical study. It is also remarkable, that as the signal is filtered with a low pass filter, the great peaks of the accident data, are softened.

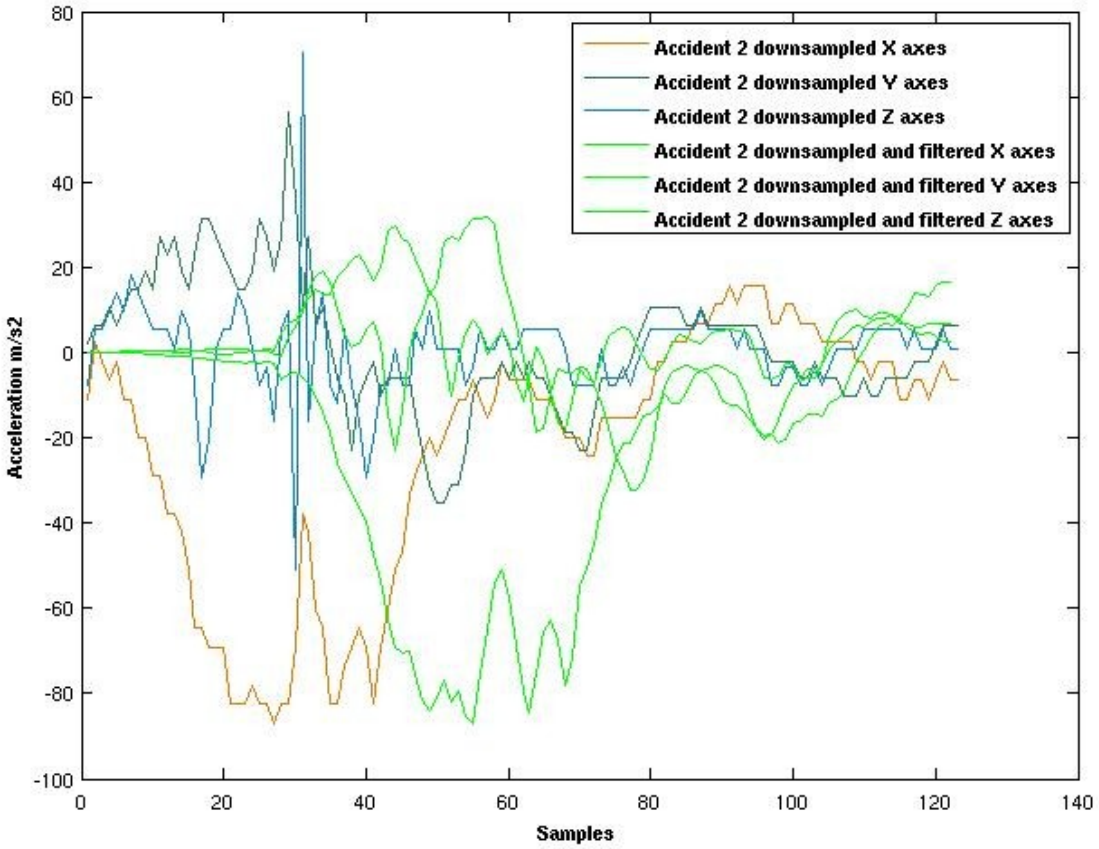

Figure 35: Comparison of the data of the Accident 2 downsampled with and without filtered

In the figure 35 is observed the gap introduced by the filter. The data is very similar, with less peaks, but there is a gap of 26 samples in all the axes. As the filter is used only for the theoretically study, it does not matter, because for analysing the data, this has been delayed. In the next images,the accident 2, the accident 107 and the accident 400 downsampled without being filtered, and after filtering and gaping them are plotted.

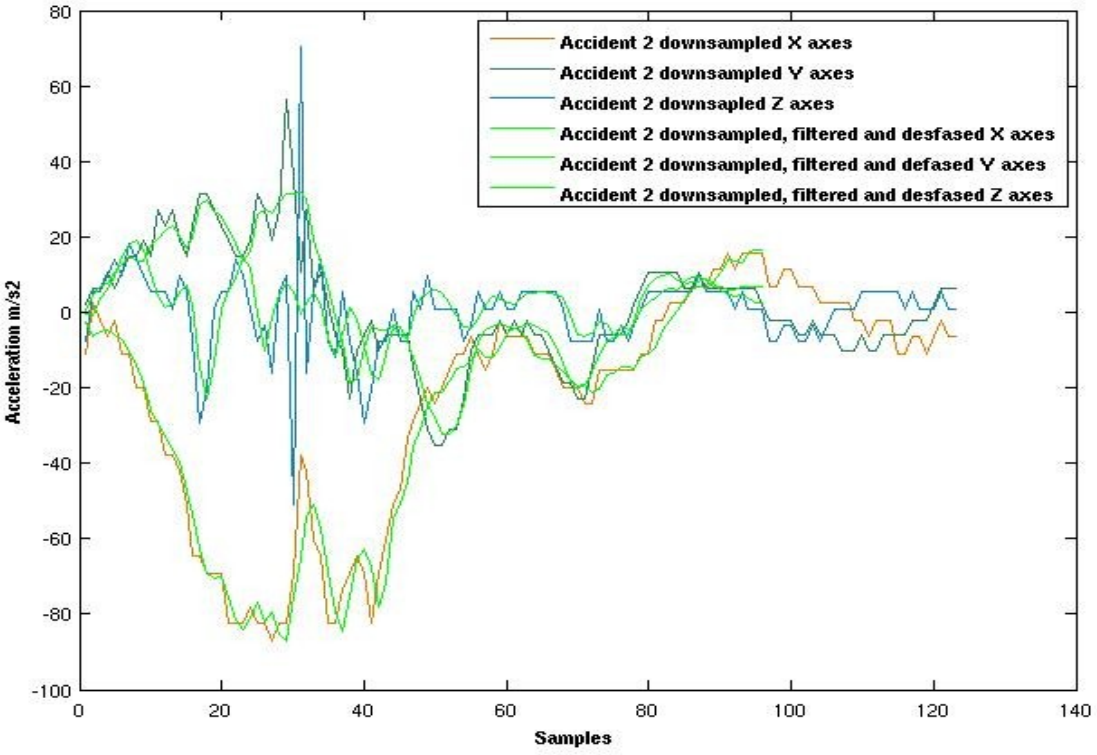

Figure 36: Accident 2 downsampled without being filtered, and after filtering and gaping it.

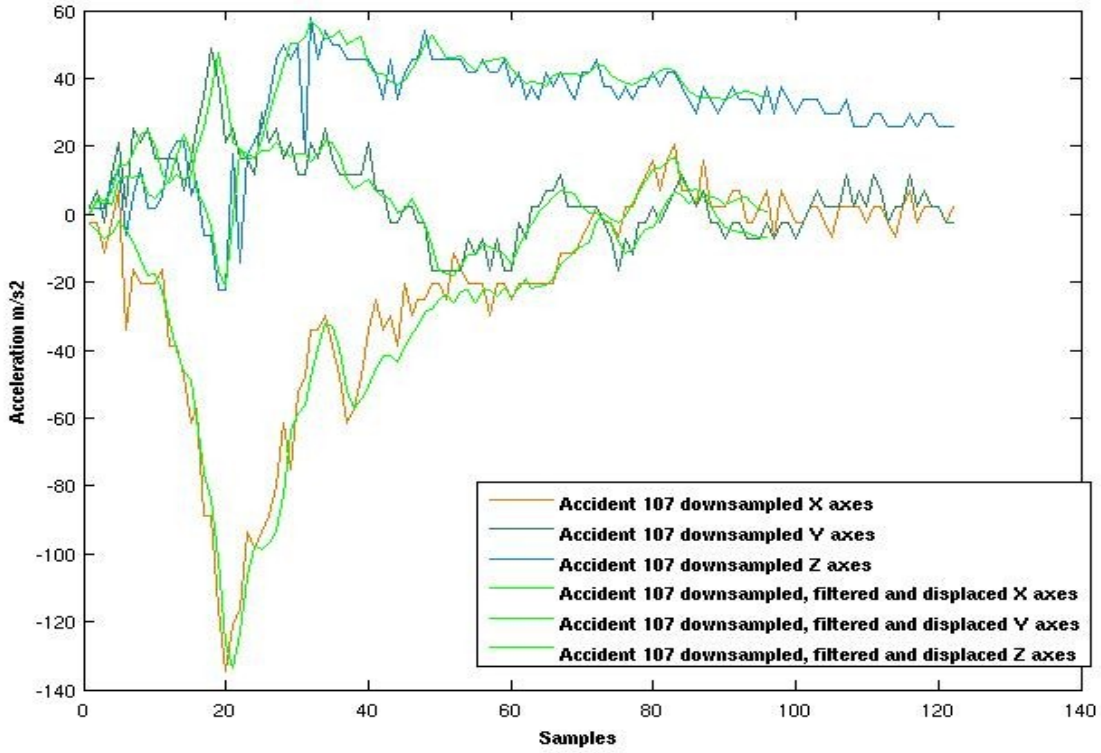

Figure 37: Accident 107 downsampled without being filtered, and after filtering and gaping it.

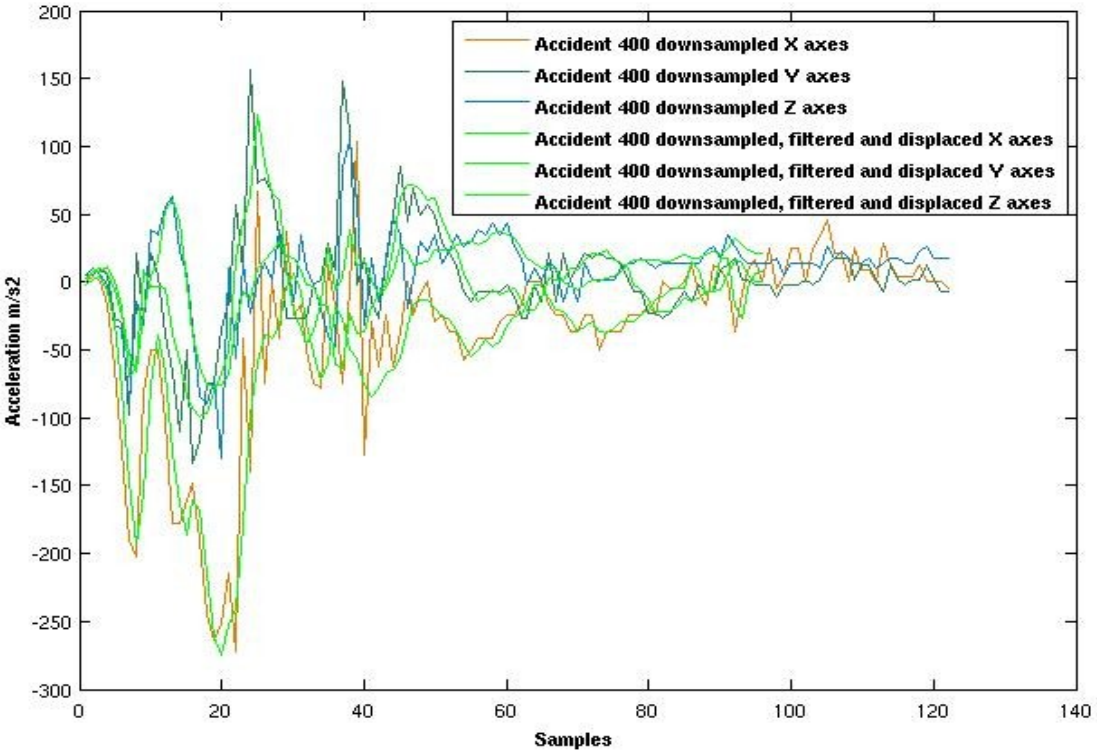

Figure 38: Accident 400 downsampled without being filtered, and after filtering and gaping it.

In the images, there are plotted the different axes of the three accidents without filtering with different colours. In green there are the data of the different axes, after filtering and having moved 26 samples, the gap introduced by the filter.

There are very similar but the filtered data have changes, the more significant one is the less abrupt, than the data,this means that the peaks are not so remarkable, this may produce that the probability of detection would be worst, as it is shown in the next section.

4.3.2 Election of the threshold

For choosing the threshold a probability of false alarm has been fixed in one false alarm per year. Supposing that a driver uses the car two hours per day in a year he would drive during 730 hours.

$$2\,hours/day * 365\,day = 730\,hours$$

730 hours are 2628000 seconds. As the accelerometer of the "*Neo FreeRunner"* is able of taking 400 samples per second, the total number of samples is 1051200000.

.

$$2628000\,seconds * 400\,samples/second = 1051200000\,samples$$

As the probability of false alarm has been fixed in one per year, this is 10^{-9}.

The probability of false alarm, is the probability of the data of being higher or equal to the threshold.

$$P_{fa} = P(|X| \geq T)$$

Where X is the signal of normal conduction having added the noise, and T is the Threshold.
A assumption of the noise distribution has been made, supposing this to be Gaussian.

Gaussian distribution $f(x) = 1/(\sigma * \sqrt{(2*\pi)}) * e^{\frac{-(x-\mu)^2}{(2*sigma^2)}}$

$$P_{fa} = \int_t^{\infty} f(x)\,dx = 1 - \int_0^T f(x)\,dx$$

$$\int_0^T f(x)\,dx = \frac{1}{2} * \left[1 + erf\left(\frac{(x-\mu)}{(\sigma * \sqrt{2})}\right)\right]$$

$$P_{fa} = 1 - \frac{1}{2} * \left[1 + erf\left(\frac{(x-\mu)}{(\sigma * \sqrt{2})}\right)\right]$$

Where x is T, this means the threshold.

$$P_{fa} = 10^{-9} = 1 - \frac{1}{2}\left[1 + erf\left(\frac{(T-\mu)}{(\sigma/\sqrt{2})}\right)\right] = \frac{1}{2} * erfc\left(\frac{-(T-\mu)}{(\sigma * \sqrt{2})}\right)$$

$$2 * 10^{-9} = erfc(A)$$

Observing to the table of the complementary error function:

$$A=4,4$$

$$A=\frac{(T-\mu)}{(\sigma*\sqrt{2})}$$

$$T=A*\sigma*\sqrt{2}+\mu$$

Where σ is the variance 1 as the power of measured noise, and μ is the maximum value in the acceleration of the normal driving, which has been taken a value of 2,8. This is a very conservative approximation, because most of the driving data has lower value of acceleration than it, so the obtained threshold is going to be higher than the real one. So the threshold:

$$T=4,4*\sqrt{2}+2,8$$

$$T=8,9$$

If a detection of a sample is considered an accident , the threshold must been set to 9 for having the probability of false alarm pre-established to 10^{-9}.

The other rule taken into account was that instead of detect an accident sample, and deduce that an accident was occurring, 2 of 3 accident samples must arrive to take the accident decision. This rule is very used in the area of communications, in GPS receiver, when they are looking for satellites for example.

Taking into account this rule, the necessary threshold for achieving the probability of false alarm previously set, would be lower.

So the total probability of false alarm would be 10^{-9} , but the probability of each sample would be lower, enabling to use a lower threshold.

$$P_{fa}(X)=\binom{3}{2}*(P_{fa}(x))^2*(1-P_{fa}(x))=10^{-9}$$

$$P_{fa}(x)=1,8257*10^{-5}$$

With this new probability of false alarm, a new value of A and a new threshold has been calculating:

$$A'=3,$$

$$T'=\sqrt{2}*A'+\mu$$

$$T'=\sqrt{2}*3+2,8$$

$$T'=7$$

So the probability of detection would be higher than using the Threshold of 9.
In the next sections the probabilities of the accident detections are going to be studied.

4.3.3 Algorithm and results using one accelerometer

The next step is to explain the process carried out and the obtained results with just one accelerometer. In the following image there is the diagram of the process using one accelerometer.

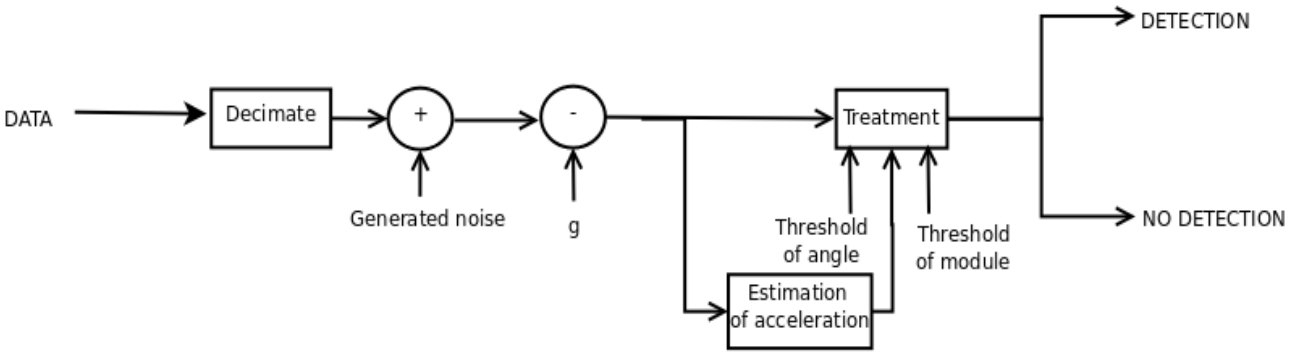

Diagram 6: Diagram of the process using one accelerometers

The process is the next one, in the first step there is the data. In the case of being the accident data, this has to be decimated, because its sample frequency is of 13333 Hz, whereas the one which is going to be used is of 400 Hz. After having taken one of each 33 sample, the next step is to add to the data the generated noise, which have been calculated for the accelerometers of the "*Neo Freerunner*". Then the gravity is subtract, because the accelerometers measure the acceleration relative to free fall, so the accelerometers in the Earth's surface indicate 1 g along the vertical axis, where it should be 0. This happens during free fall, where the acceleration is the same as the gravity, so to measure the real acceleration in the 3 axes, 1 g of the Z axis have to be subtracted. This will be the data which the process will be made with. These data are stored in an array, for calculating an estimation of the acceleration, which the data will be compared with. The estimated acceleration is calculated with a maximum of 1000 samples.

In the treatment block, the angle between the estimation of the acceleration (g in the Figure 39) and the data itself is calculated.

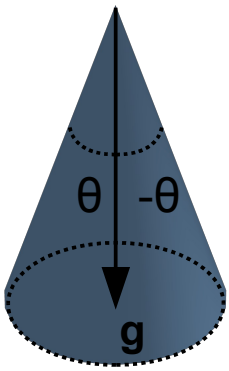

Figure 39:Explanation of the treatment block.

In case of been this higher than a threshold, the module of the acceleration data is calculated. If the measured acceleration is out of the cone, delimited by the angle threshold, this result is also compared with another threshold, and after the decision is taken.

In the following sections the obtained probabilities of false alarm and of detection are going to be studied, but first a little explanation of them is going to be made.

As it has been commented before, for any threshold the detection is simplified to yes/no detection. The observation itself is put in one of two categories. H is going to denote hits, this means the accident is detected and it is an accident, F false alarm, the accident is detected but it is not an accident, M missed accident, the detection is not made although having been an accident and Z all correct non-accident.

In this case the probability of detection it is :

$$POD = \frac{H}{H + M} 100$$

It measures the fraction of observed events that were correctly detected.

The probability of false alarm it is:

$$POFA = \frac{F}{F + H} 100$$

It gives the fraction of accident events that were observed to be non detections.

So in the following sections, this parameters are studied.

4.3.3.1 Probability of false alarm

In the next figures, there are the probabilities of false alarm of the two different models(Y axis), using different thresholds from 0 to 10 with steps of 0,5 (X axis). As the threshold goes up, the probability of false alarm decrease, but as it is going to be shown later, the probability of detections in the case of crashes, also decrease.

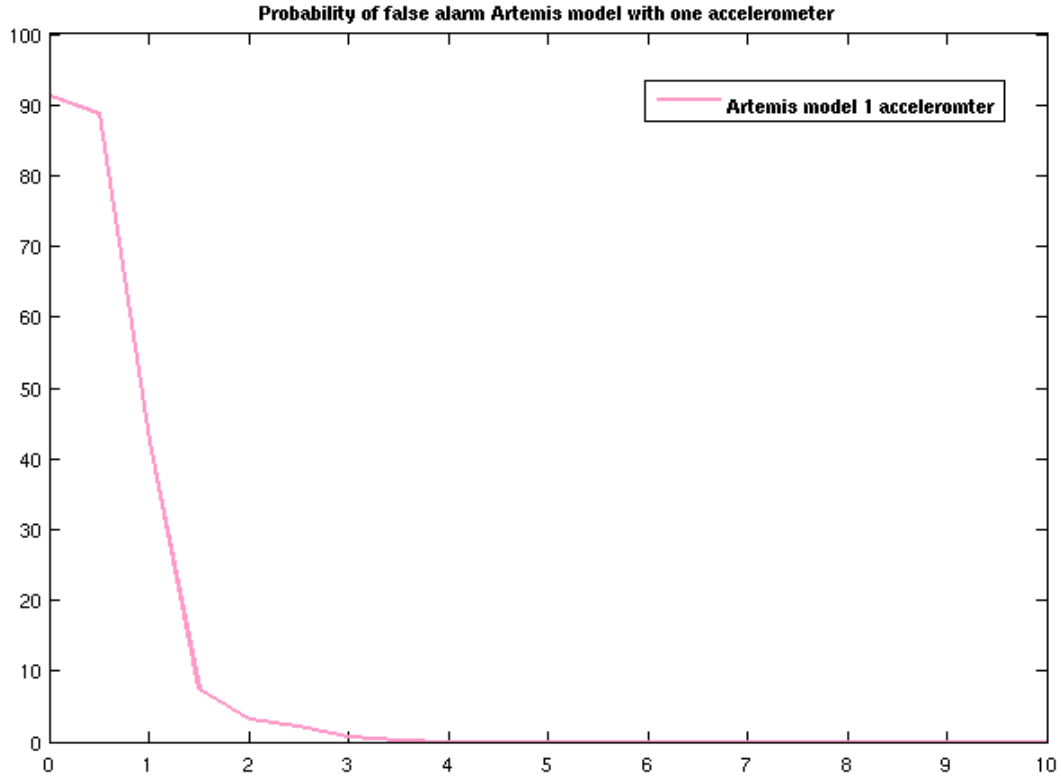

Figure 40: Probability of false alarm of Artemis model using one accelerometer and with different thresholds

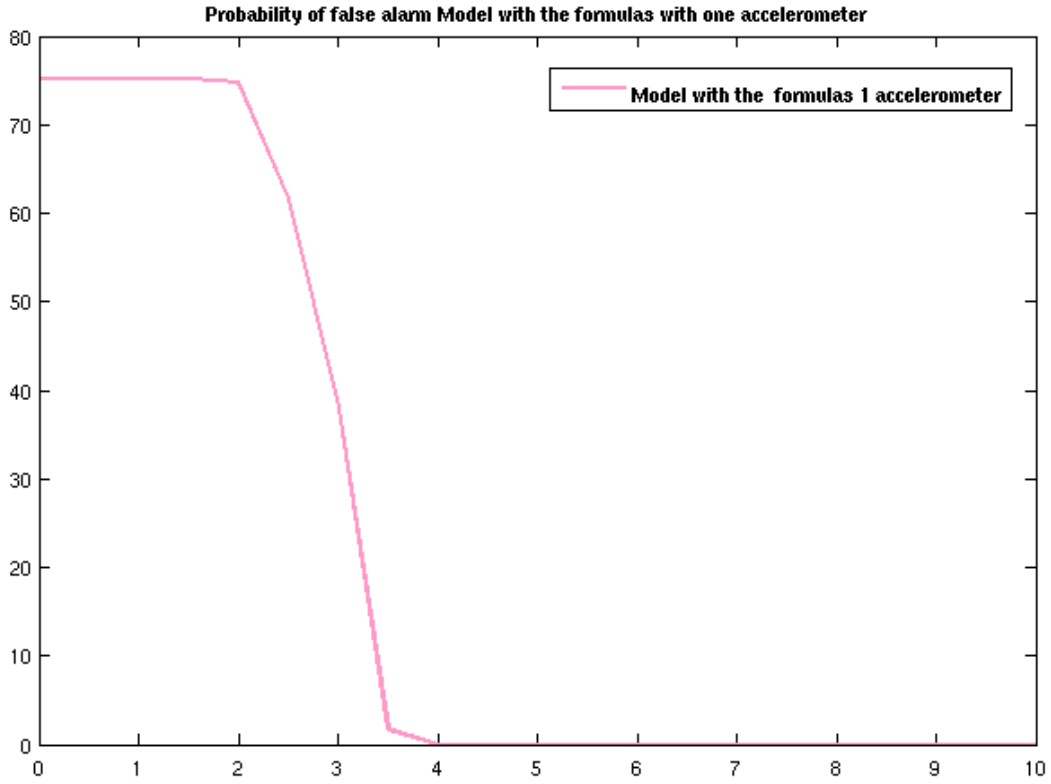

Figure 41: Probability of false alarm of the Model with the formulas using one accelerometer and with different thresholds

In the figures, the differences between the two models, can be seen. Whereas, in the Artemis model with a threshold of 2 the probability of false alarm goes down to the 5 %, in the model generated with the formulas, the probability is around the 75 %. In the first model, there is a remarkable inflection point around the threshold of 1,5 where is an important fall of probability of false alarm, while in the second model, this change occurs around the threshold of 3.5.

4.3.3.2 Probability of detection

Following there are the figures showing the probabilities of detections in three different accidents, these probabilities are of one decimated part of all the data of the crashes. The first plots show the probability of detection of the accidents without having filtered the data, and then there is a comparison between them and having filtered them. As in the previous ones, in the X axis, there are the different thresholds, from 0 to 10, with steps of 0,5, and in the vertical axis there is the probability of detection.

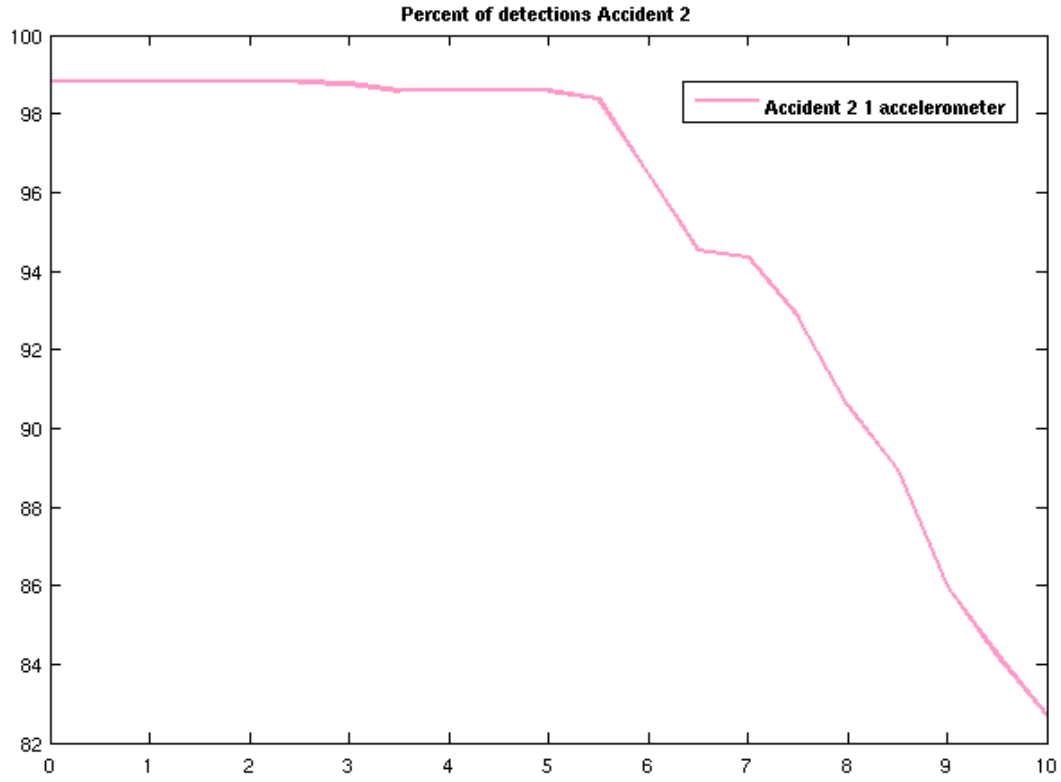

Figure 42: Probability of detection of Accident 2 with different thresholds

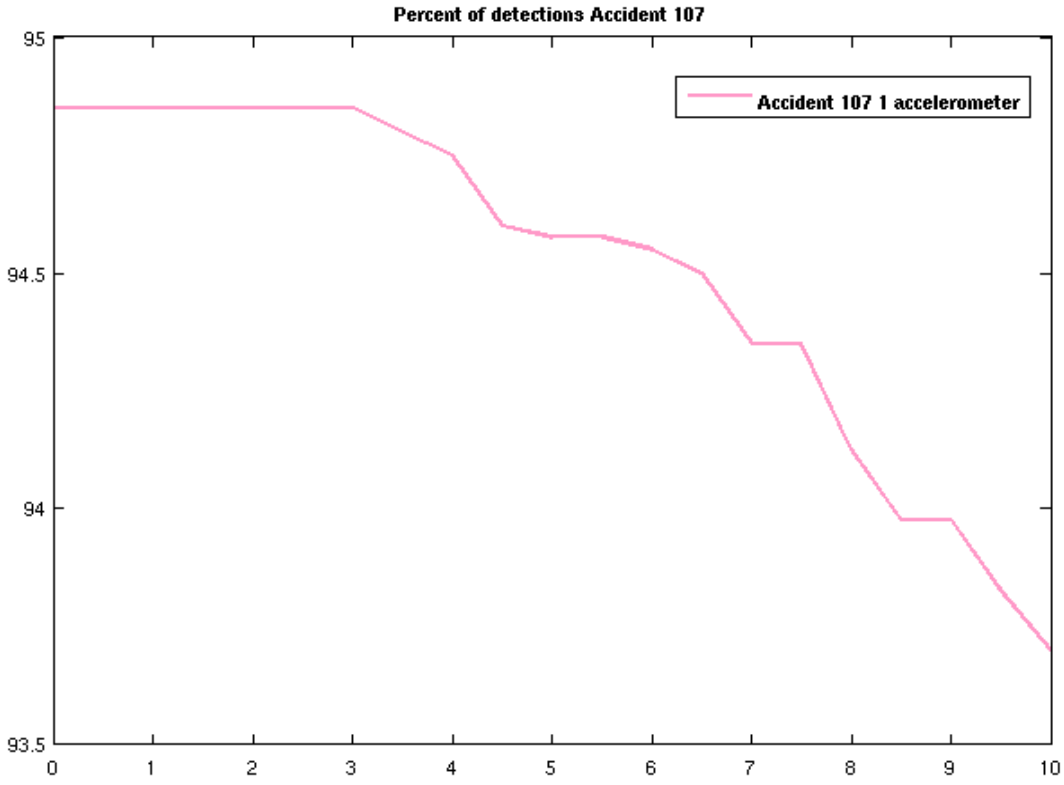

Figure 43: Probability of detection of Accident 107 with different thresholds

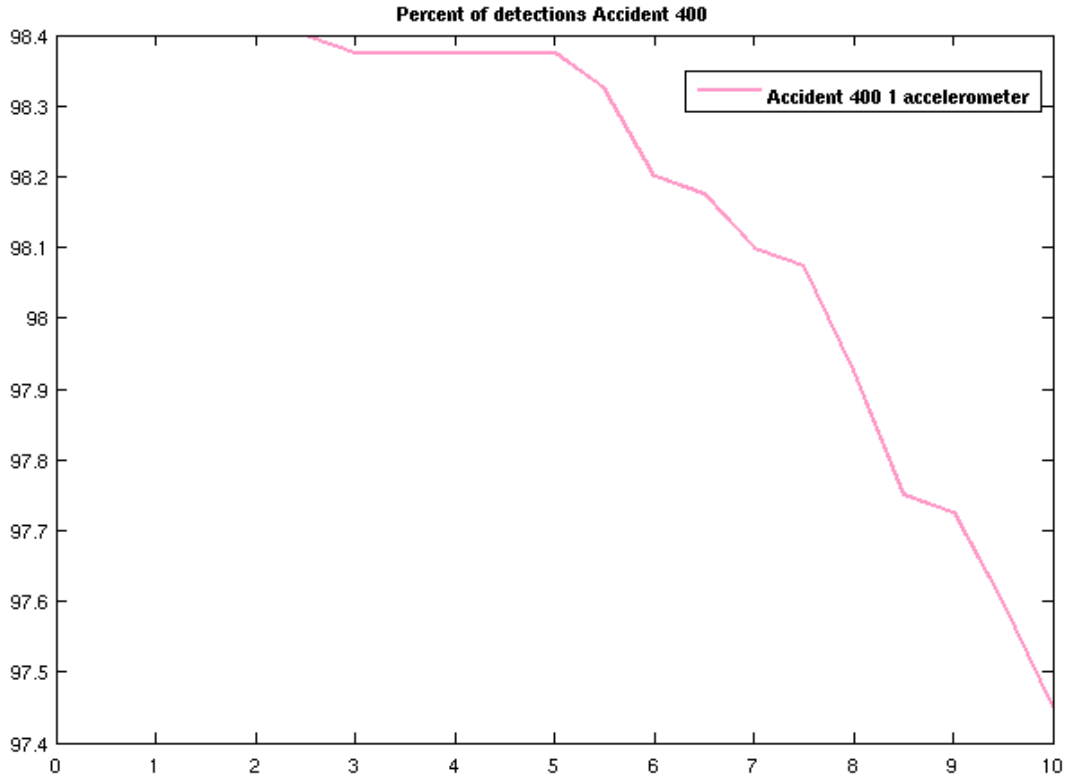

Figure 44: Probability of detection of Accident 400 with different thresholds

As it has been previously commented, the data of the accident has to be filtered and downsampled before analysing them, due to the difference of sampling frequency of the accelerometers used for getting the accidents data and the accelerometers of the *"Neo FreeRunner"*. The figures above, show the probabilities of detection of the accidents, without filtering the data. As aliasing could be produced, it has been introduced the filter previously mentioned (see section *4.3.1.1 Study of the spectrum of the accident data*). Following the are the tables, in which the probabilities between the two cases are compared.

ACCIDENT 2		
	PROBABILITY OF DETECTION WITHOUT FILTERING	***PROBABILITY OF DETECTION FILTERING THE SIGNAL***
Threshold 5,5	98,38	95,87
Threshold 6	96,47	95,87
Threshold 6,5	94,53	92,78
Threshold 7	94,35	92,78
Threshold 7,5	92,85	89,58
Threshold 8	90,58	89,58
Threshold 8,5	88,95	86,41
Threshold 9	85,95	83,33
Threshold 9,5	84,22	81,25
Threshold 10	82,7	81,25

Table 5: Comparison of Probabilities of detection of Accident 2 without and with filter

ACCIDENT 107		
	PROBABILITY OF DETECTION WITHOUT FILTERING	***PROBABILITY OF DETECTION FILTERING THE SIGNAL***
Threshold 5,5	94,58	93,81
Threshold 6	94,55	93,81
Threshold 6,5	94,5	93,81
Threshold 7	94,35	93,81
Threshold 7,5	94,35	93,81
Threshold 8	94,12	93,81
Threshold 8,5	93,97	92,78
Threshold 9	93,97	92,78
Threshold 9,5	93,83	92,78
Threshold 10	93,7	92,78

Table 6: Comparison of Probabilities of detection of Accident 107 without and with filter

ACCIDENT 400		
	PROBABILITY OF DETECTION WITHOUT FILTERING	***PROBABILITY OF DETECTION FILTERING THE SIGNAL***
Threshold 5,5	98,33	95,87
Threshold 6	98,2	95,87
Threshold 6,5	98,17	95,87
Threshold 7	98,1	95,87
Threshold 7,5	98,08	95,87
Threshold 8	97,92	95,87
Threshold 8,5	97,75	95,87
Threshold 9	97,72	95,87
Threshold 9,5	97,6	95,87
Threshold 10	97,45	95,87

Table 7: Comparison of Probabilities of detection of Accident 107 without and with filter

Observing the tables, it is remarkable the reduction of the probabilities of detection having filtered previously the data. This is due to the reduction of the peaks, because the filter has soften the signal making the high changes less abrupt. This decrement of detections is up to a 2% of the data in some cases. But this is what would happen in the real situation.

4.3.3.3 ROCs (Receiver Operating Characteristic curves)

Receiver Operating Characteristic curves are graphical plots of the different parameters (in this case 1-probability of detection versus false alarm), as its discrimination threshold is varied, in this process it is varied from 0 to 10 with steps of 0.5.

Through these curves a comparison of classifiers may be done. The area under the ROC is a very important parameter, in this case the lower the area is, the better results are. But the area is not the only important point, in some cases the area may be misleading. To use a compare different situations an operating point, a threshold, has to be chosen, and then the probabilities, must be compared. So the ROCs curves, are a complementation for the false alarm probabilities curves, and for the detection probabilities curves.

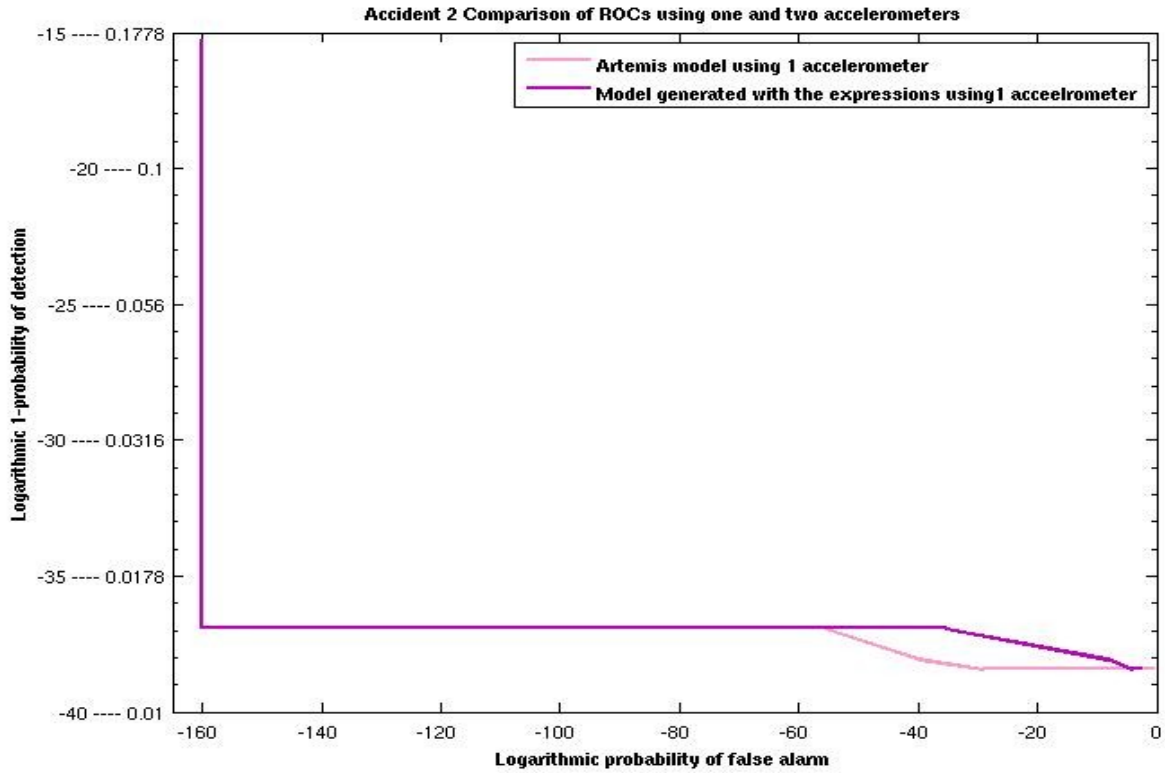

Figure 45: Comparison of ROCs using data of Accident 2 and the two different driving models

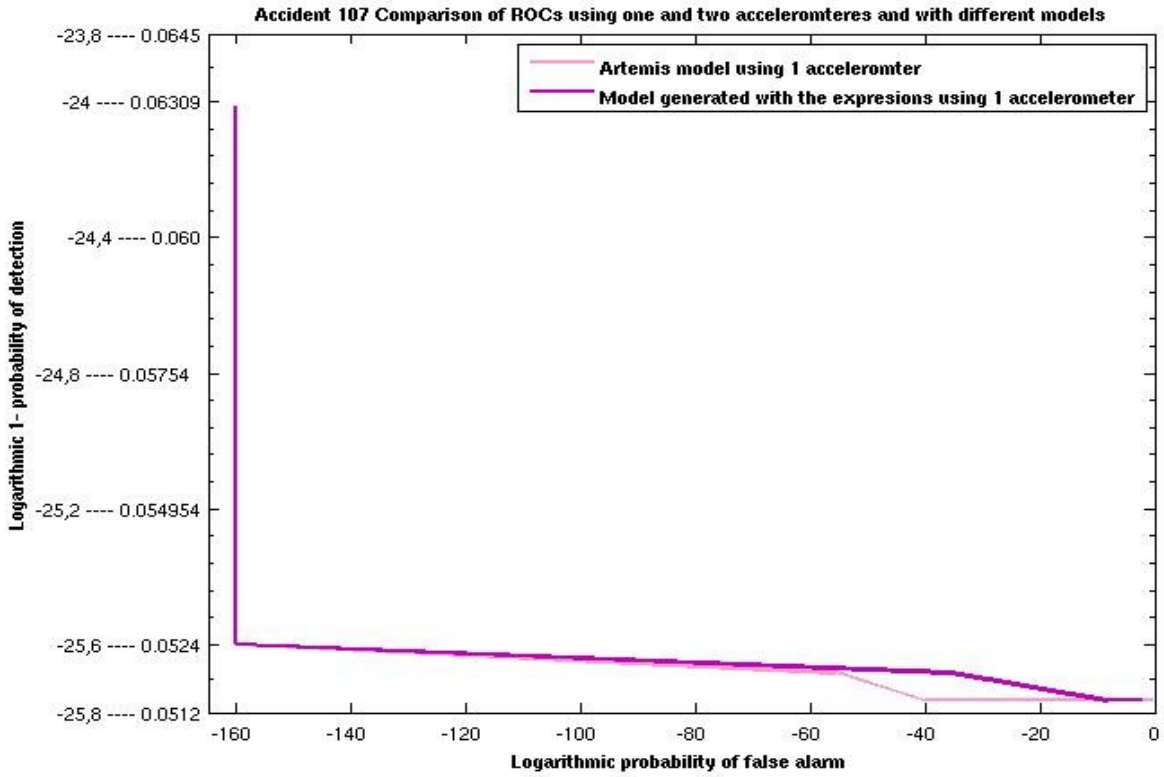

Figure 46: Comparison of ROCs using data of Accident 107 and the two different driving models

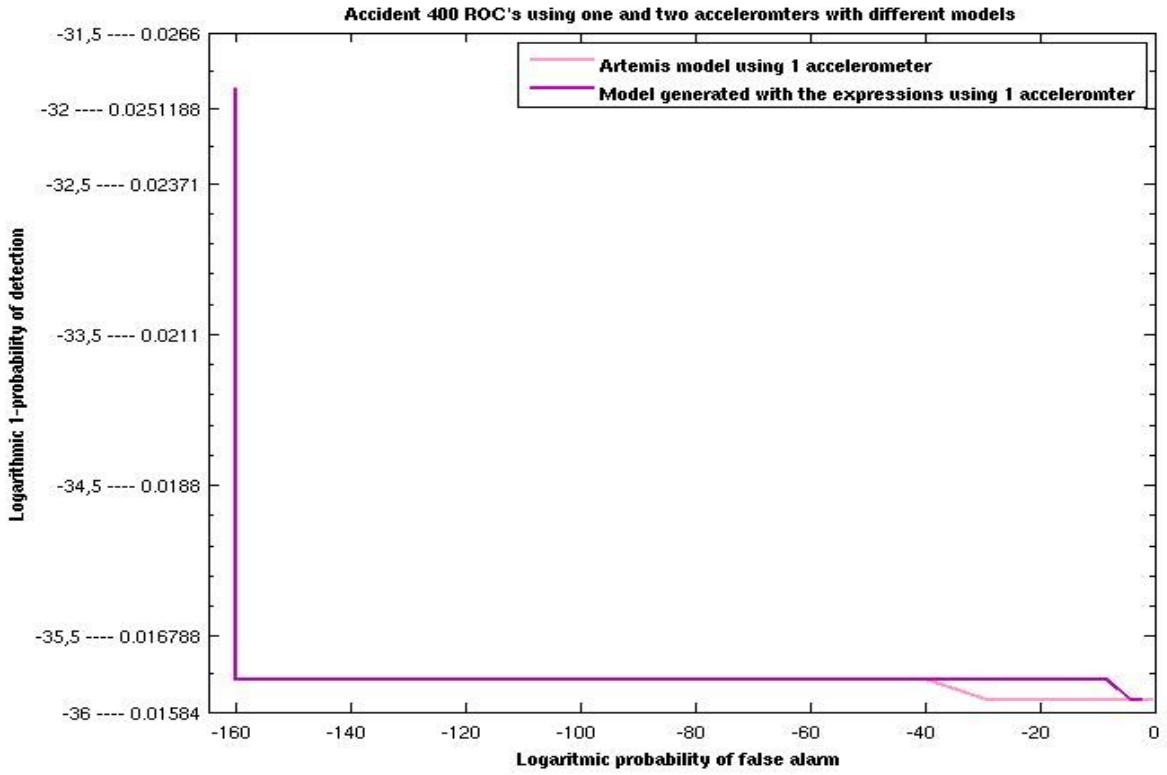

Figure 47: Comparison of ROCs using data of Accident 400 and the two different driving models

In the ROC curves, the differences between the two models, can be noticed. As it has been commented before, with Artemis model better results are achieved: This is due to the difference, between the maximum acceleration of the models, and because, while in the Artemis model the maximum accelerations are peaks, in the model generated with expressions the maximum accelerations carry on during more time.

In the case of the data filtered and without filtered, the ROC curves are very similar, due to the probability of false alarm does not change, and although the probability of false alarm changes, this changes are not so big, to make a great change in the curves.

4.3.4 Algorithm and results using two accelerometers

The device used , the *"Neo Frerunner*", is provided with two accelerometers. Once having analysed the process made with the data of one accelerometer, and the obtained results, the next step is to make a similar analysis, but this time, using the two accelerometers.

The two accelerometers are orientated differently, the second sensor is turned 45 degrees around the Z axis, as it is shown in the following images.

Figure 48: Orientation of the first accelerometer

Figure 49: Orientation of the second accelerometer

The next diagram, shows the process which has been carried out, this is very similar to the previous one made with one accelerometer, but with some modifications.

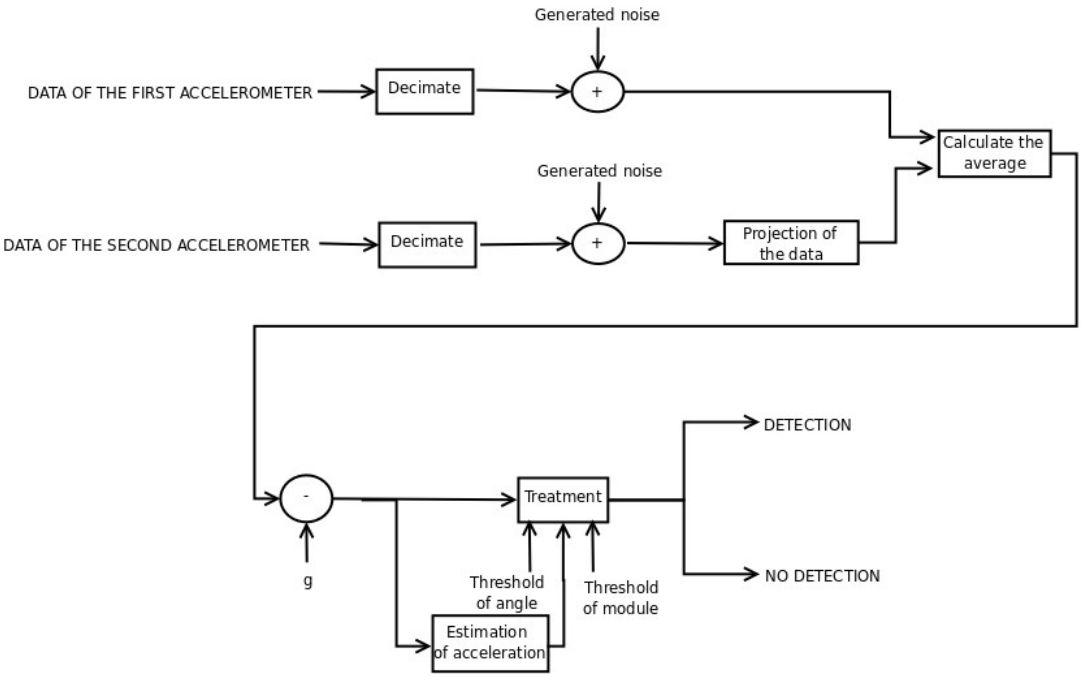

Diagram 7: Diagram of the process using two accelerometers

The more important modifications are made with the data, which are studied. In this case the treatment will be done with two different sets of data. After having decimating them, the first step is to simulate the data of the second accelerometer, this is made by projecting the data of the first accelerometer without noise, in the new axes. After, a different noise is added to this new data, and it is in this point where the real data of the second accelerometer are simulated. Finally for making the average with the first accelerometer's data, the obtained data are projecting again, in the axes of the other accelerometer. The rest of the process is the same, as with one accelerometer.

4.3.4.1 Probability of false alarm

Following, there are the images comparing the results obtained of the probability of false alarm of the two different models, using one and two accelerometers.

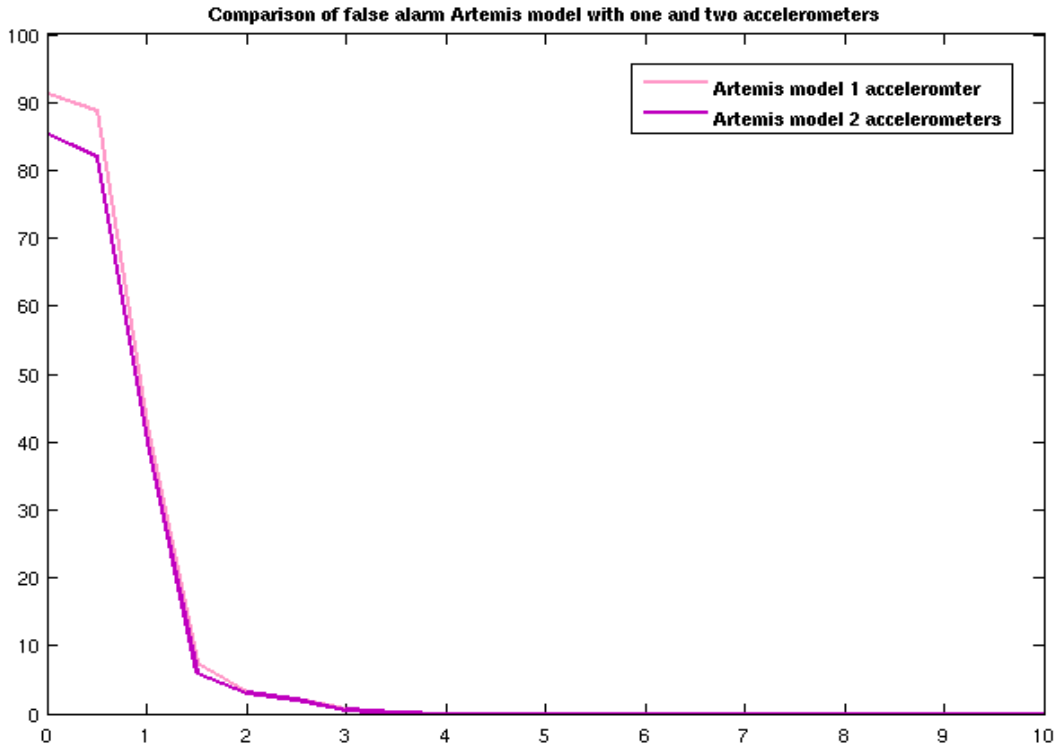

Figure 50: Comparison of probability of false alarm of Artemis model using one and two accelerometers

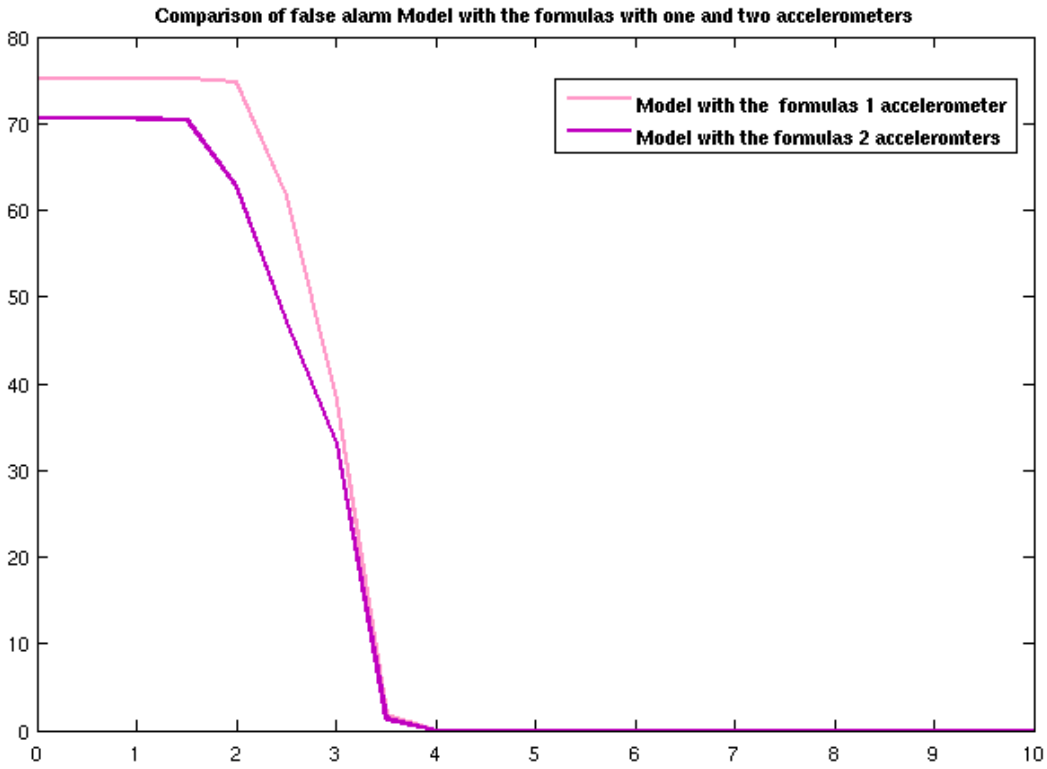

Figure 51: Comparison of probability of false alarm of the model generated using the formulas with one and two accelerometers

In the graphics, can be observed that the probability of false alarm improves using two accelerometers. While in the Artemis model, this improvement is lower, a 5% with the two first thresholds, in the generated model, the improvement is also of the order of a 5%, but until the threshold has grown up to 3.

4.3.4.2 Probability of detection

Following there are the figures showing the probabilities of detection in three different accidents using one and two accelerometers. As in the previous ones, the thresholds are in the X axis, whereas in the vertical axis there is the probability of detection.

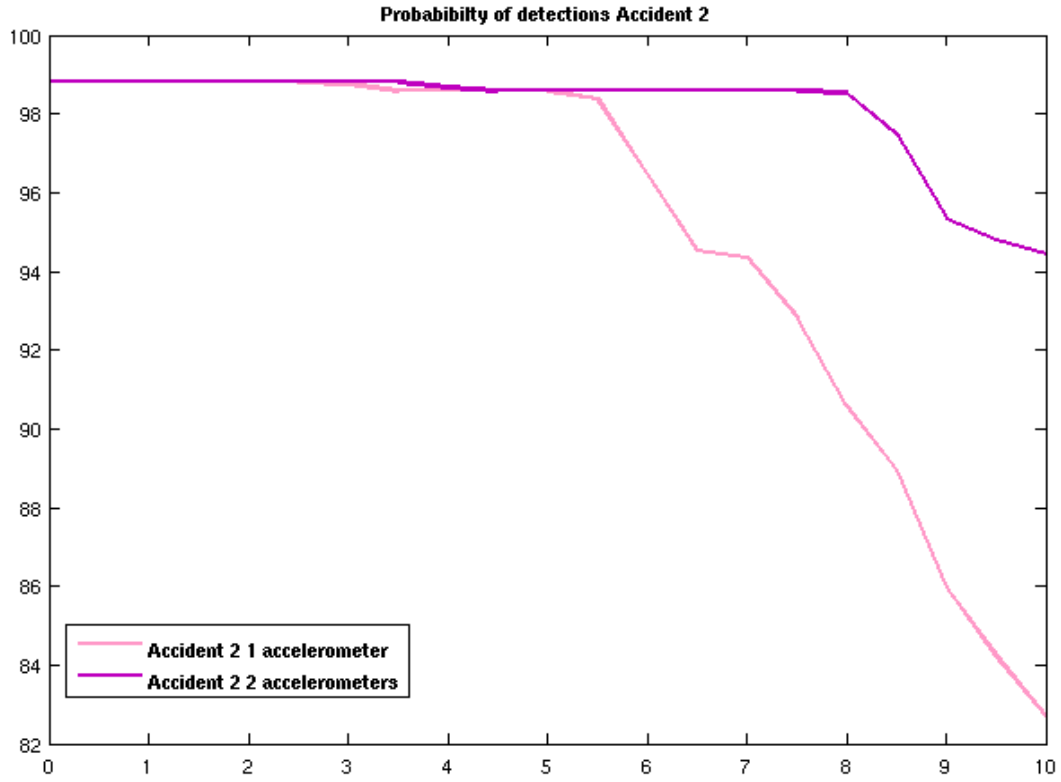

Figure 52: Comparison of probabilities of detections with one and two accelerometers Accident 2

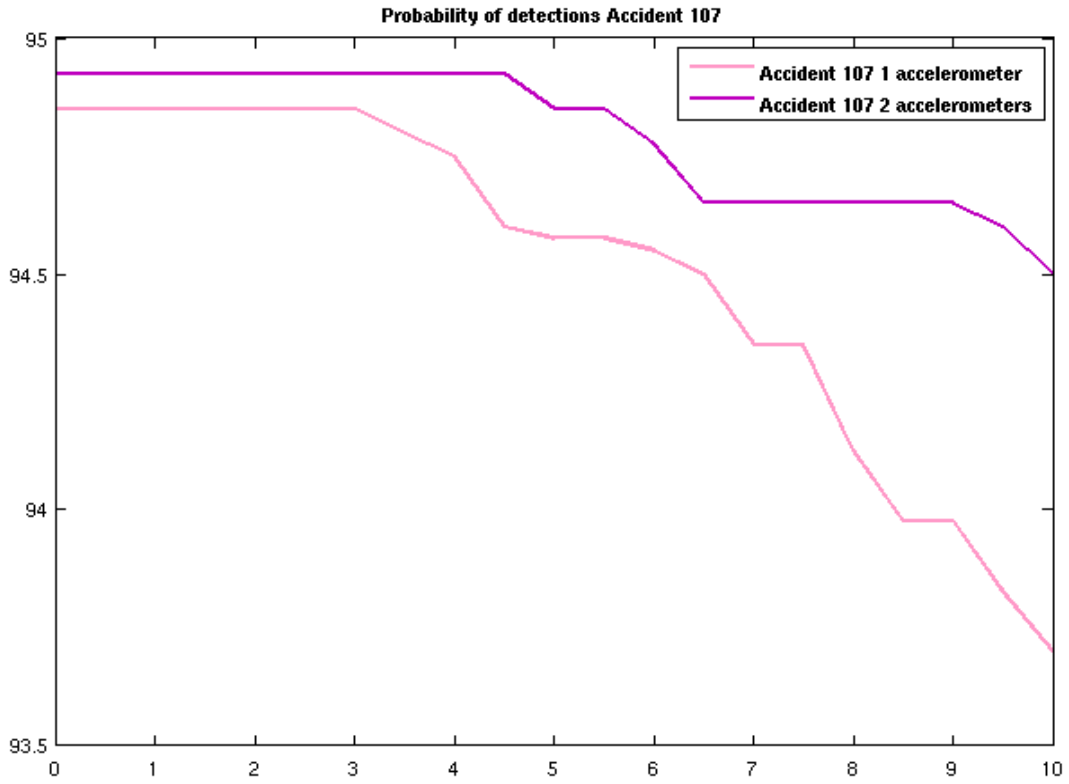

Figure 53: Comparison of probabilities of detections with one and two accelerometers Accident 107

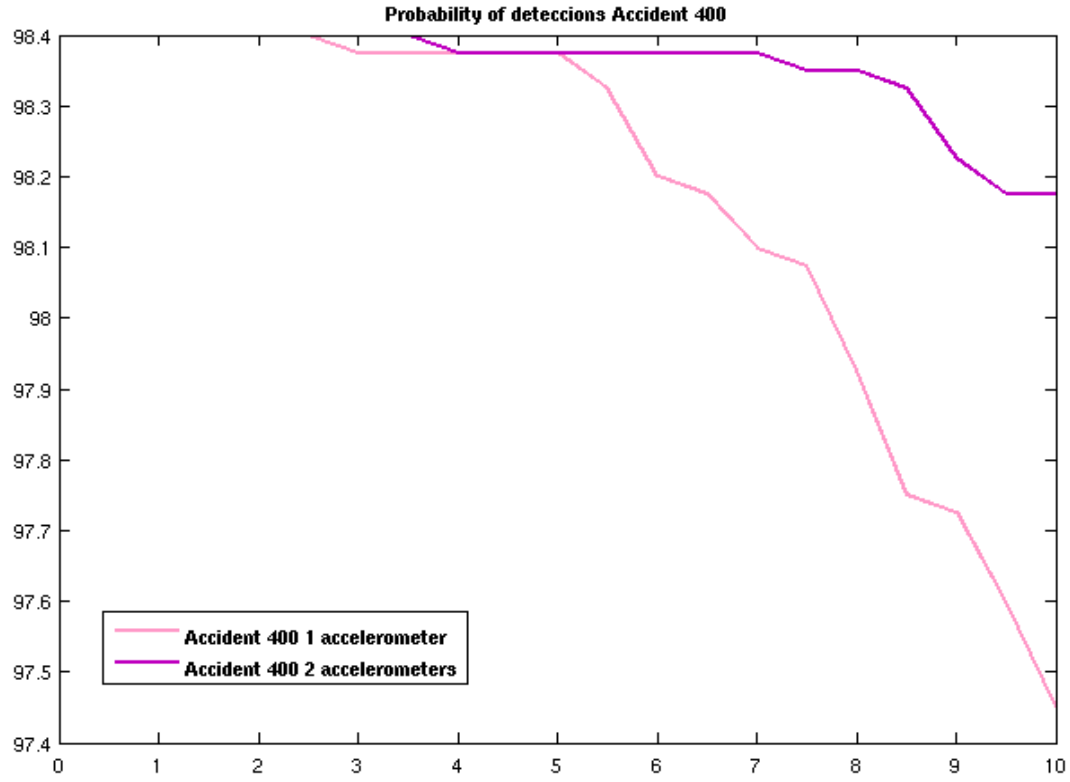

Figure 54: Comparison of probabilities of false alarm with one and two accelerometers Accident 400

The probability of detection also improves using two accelerometers .The higher the threshold is, the improvement more remarkable is, achieving a 11% in the case of Accident 2 with a threshold of 10.
In the following tables there are the comparisons of the probabilities of detection with and without filter.

ACCIDENT 2		
	PROBABILITY OF DETECTION WITHOUT FILTERING	***PROBABILITY OF DETECTION FILTERING THE SIGNAL***
Threshold 5,5	98,58	95,87
Threshold 6	98,58	95,87
Threshold 6,5	98,58	95,87
Threshold 7	98,58	95,87
Threshold 7,5	98,58	95,87
Threshold 8	98,53	93,81
Threshold 8,5	97,5	93,81
Threshold 9	95,35	90,63
Threshold 9,5	94,8	90,63
Threshold 10	94,42	90,63

Table 8: Comparison of probabilities of detection of Accident 2 using two accelerometers with and without filter

ACCIDENT 107		
	PROBABILITY OF DETECTION WITHOUT FILTERING	***PROBABILITY OF DETECTION FILTERING THE SIGNAL***
Threshold 5,5	94,85	93,81
Threshold 6	94,78	93,81
Threshold 6,5	94,65	93,81
Threshold 7	94,65	93,81
Threshold 7,5	94,65	93,81
Threshold 8	94,65	93,81
Threshold 8,5	94,65	93,81
Threshold 9	94,65	93,81
Threshold 9,5	94,6	92,78
Threshold 10	94,5	92,78

Table 9: Comparison of probabilities of detection of Accident 107 using two accelerometers with and without filter

ACCIDENT 400		
	PROBABILITY OF DETECTION WITHOUT FILTERING	***PROBABILITY OF DETECTION FILTERING THE SIGNAL***
Threshold 5,5	98,38	97,94
Threshold 6	98,38	97,94
Threshold 6,5	98,38	97,94
Threshold 7	98,38	97,94
Threshold 7,5	98,35	96,91
Threshold 8	98,35	96,91
Threshold 8,5	98,33	96,91
Threshold 9	98,22	96,91
Threshold 9,5	98,17	96,91
Threshold 10	98,17	96,91

Table 10: : Comparison of probabilities of detection of Accident 400 using two accelerometers with and without filter

4.3.4.3 ROCs

As it has been made with the obtained results using only one accelerometer, the obtained results using the two accelerometers are going to be plotted using the ROCs.

In this case 4 different data are going to be compared, the results using one accelerometer and the two models, and the obtained results using two accelerometers.

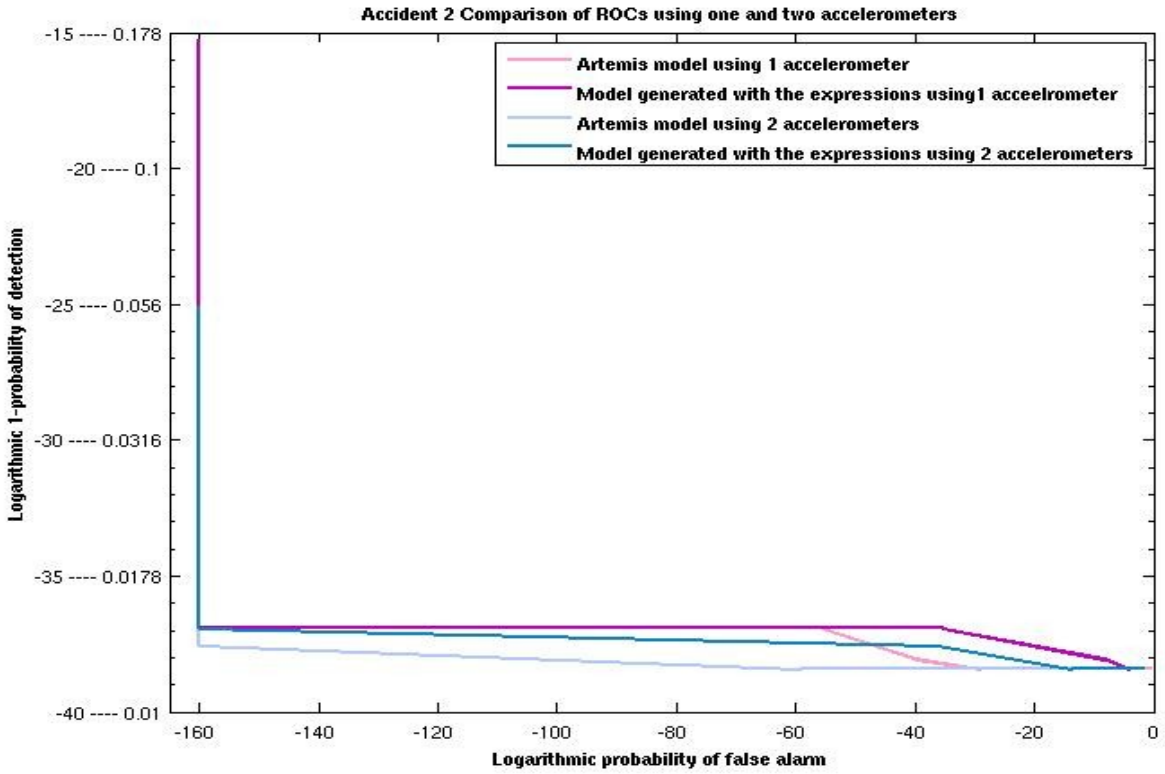

Figure 55: Comparison of ROCs using data of Accident 2, the two different driving models and 1 and two accelerometers

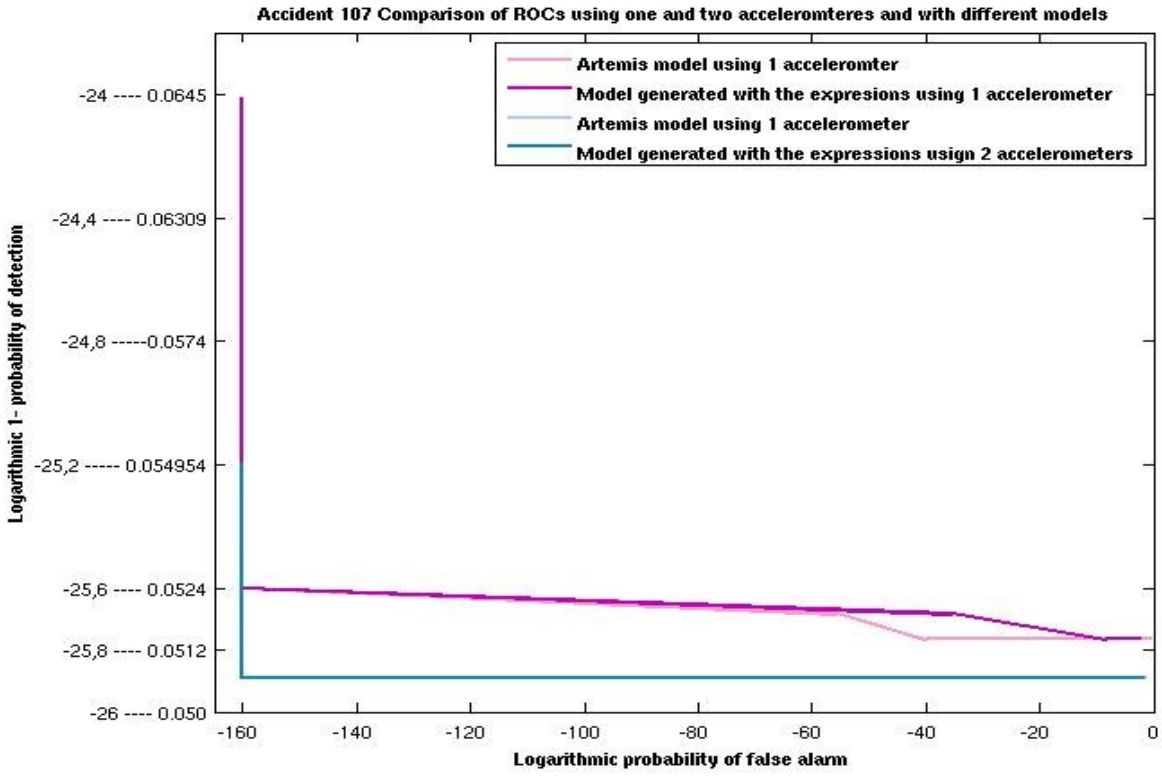

Figure 56: Comparison of ROCs using data of Accident 107, the two different driving models and 1 and two accelerometers

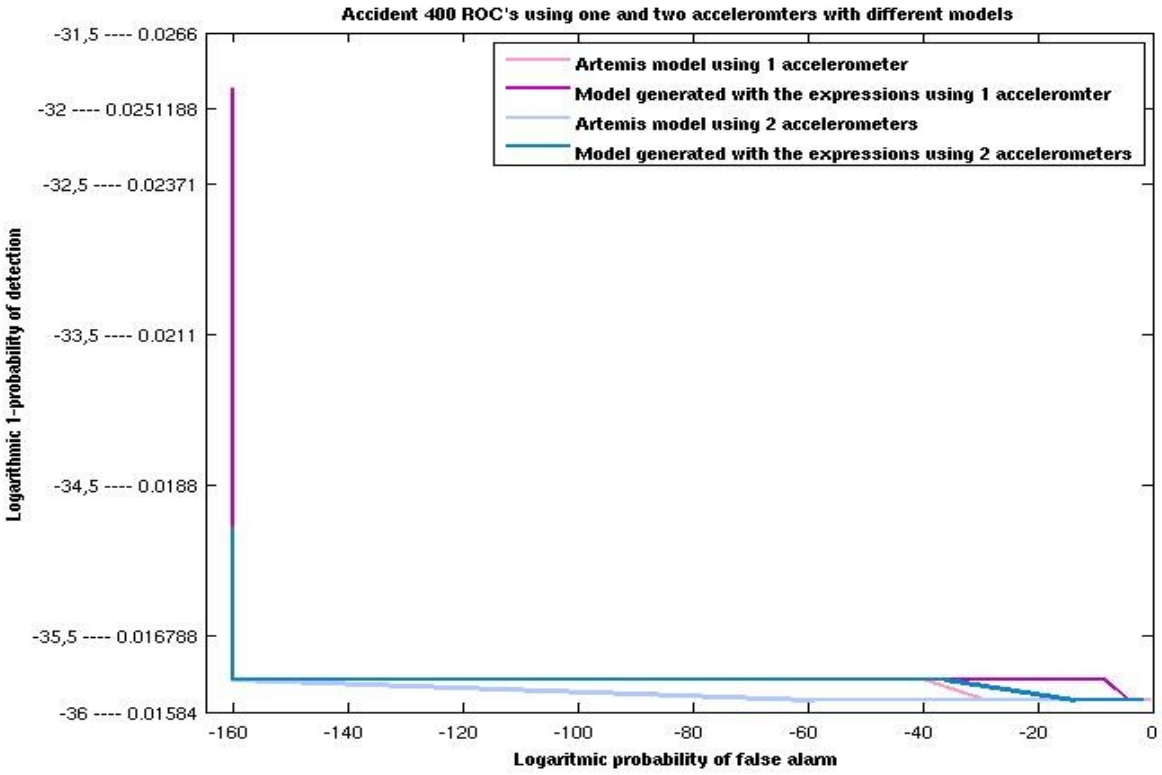

Figure 57: Comparison of ROCs using data of Accident 400, the two different driving models and 1 and two accelerometers

As in the curves of false alarm and of detection, in ROC curves, there can be also seen the achieved improvement using two accelerometers instead of one. As it has been mentioned before, the lower the area under the ROC curve is, the better results are. So comparing the results using Artemis model, with one and two accelerometers, though the difference is not very remarkable, the results in the second case are better than in the first one. This occurs also, with the model generated from the expressions.

4.4 Model of normal driving followed by an accident

The previous study of the probabilities of detection and of false alarm has been made with models of accident in one hand and of normal driving in the other. In the following lines a model consisting of a normal driving followed by an accident has been analysed.

This model is exactly what would happen in the real life, because the accident would occur after a process of normal driving. The estimation of gravity is supposed to be better than in the case of only accident, because in this case, as the model is composed of normal driving the estimation is going to be made with this data.

Another important improvement is that for calculating the estimation of the acceleration, the first 1000 samples have been ignored. During this time the algorithm is supposed to be training. This is possible, due to the higher number of samples. First the analysis have been made using 10000 number of samples of a normal driving, and the samples of the accidents and later, the number of samples of the normal driving has been increased obtaining the same results. The following figure shows, a normal driving during 10000 samples followed by the accident 2.

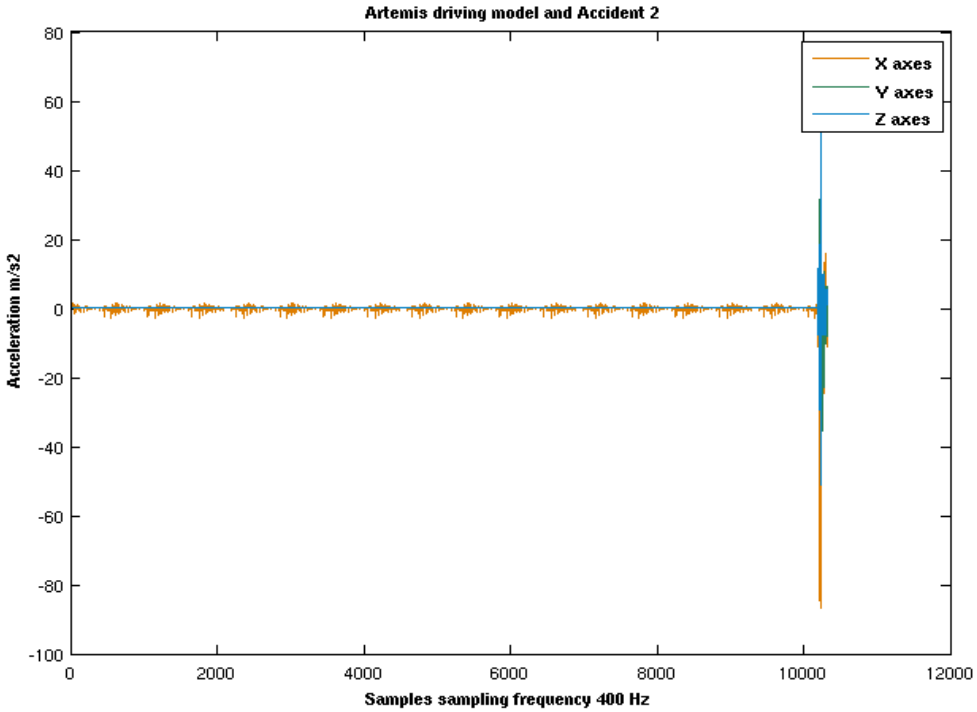

Figure 58: Artemis driving model and Accident 2

In the next tables, there are the probabilities of detection using 10000 samples of the Artemis driving model followed by an accident, and .taking advance of the two accelerometers

Model consisting of 10.000 samples of Artemis driving model and accident 2

PROBABILITY OF DETECTION										
Threshold	5,5	6	6,5	7	7,5	8	8,5	9	9,5	10
Probability	97,54	97,54	97,54	97,54	97,54	95,08	95,08	92,62	92,62	92,62

Table 11: Probability of detection using Artemis driving model of 10000 and the Accident 2

Model consisting of 10.000 samples of Artemis driving model and accident 107

PROBABILITY OF DETECTION										
Threshold	5,5	6	6,5	7	7,5	8	8,5	9	9,5	10
Probability	95,08	95,08	95,08	95,08	95,08	95,08	95,08	94,53	94,53	92,62

Table 12: Probability of detection using Artemis driving model of 10000 and the Accident 107

Model consisting of 10.000 samples of Artemis driving model and accident 400

PROBABILITY OF DETECTION										
Threshold	5,5	6	6,5	7	7,5	8	8,5	9	9,5	10
Probability	98,36	98,36	98,36	98,36	97,54	97,54	97,54	97,54	97,54	97,54

Table 13: Probability of detection using Artemis driving model of 10000 and the Accident 400

The probabilities of false alarms cannot be simulated due to the huge number of samples needed.

More proves with more number of samples have been made obtaining very similar results, concluding that the number of samples has no influence on the probabilities of false alarm and of detection.

The same process has been carried out with the model generated with the expressions. The obtained results in these cases has also been very similar.

4.5 Analysis of the Time to the First Detection

Another important point in the analysis of the accident detections is the Time to the First Detection, this means, when is the accident detected.

During an accident, in case of been a great one, the damages caused to the car, and so to everything inside it, could be devastating. Because of that the time to the first detection is going to be studying, due to the lower the time is, the more probabilities would be to notify the accident before a possible destruction of the device.

So an analysis for detecting the first detection have been made. In the next graphics the probabilities of the first detections versus the time is plotted. In one hand there are the probabilities of detection of the accident using one sample with threshold 9 and in the other the probabilities of detection taking 2 of 3 samples, using threshold 7.

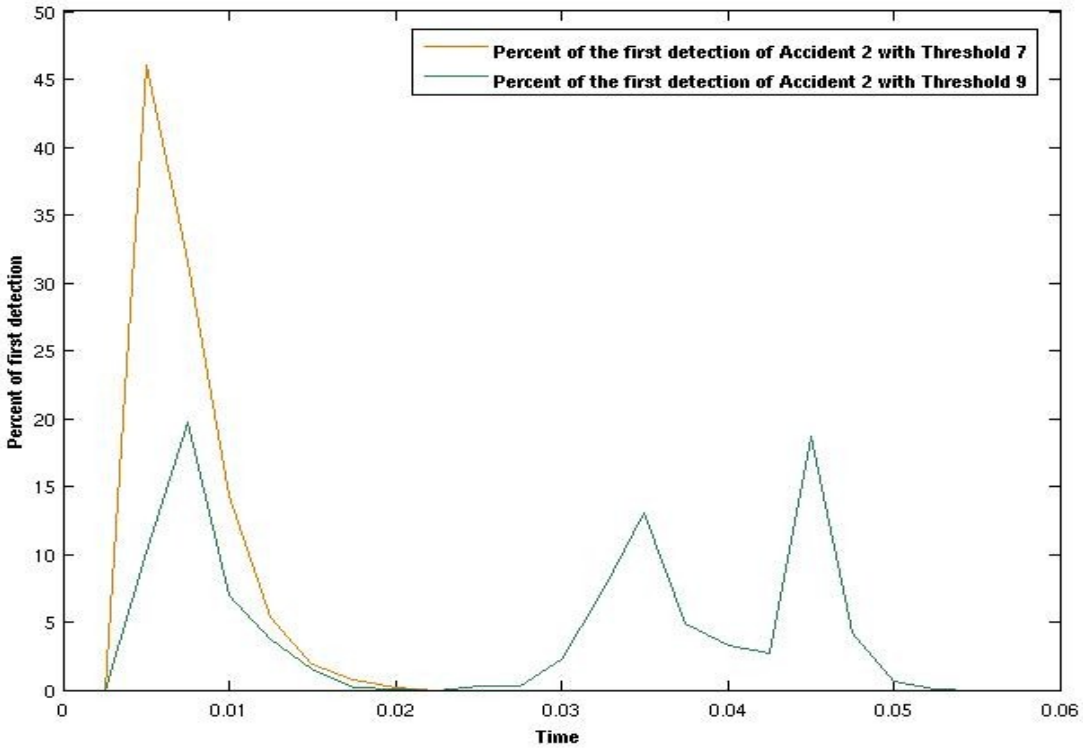

Figure 59: Percent of the First detection versus time of Accident 2

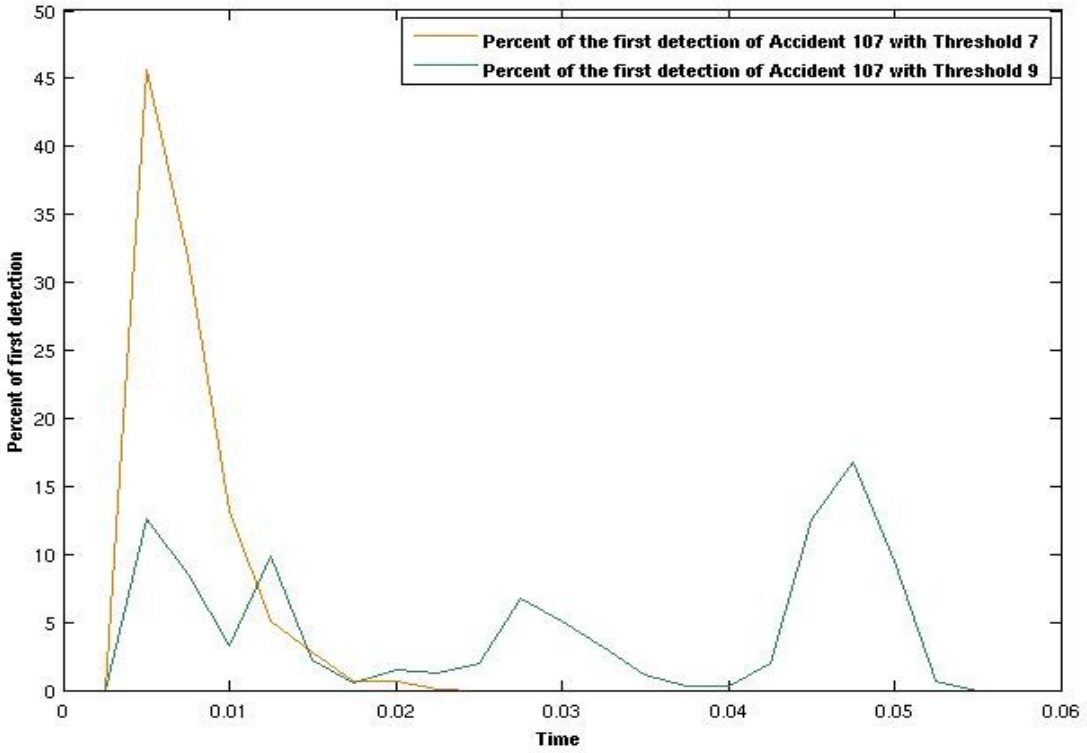

Figure 61: Percent of the First detection versus time of Accident 107

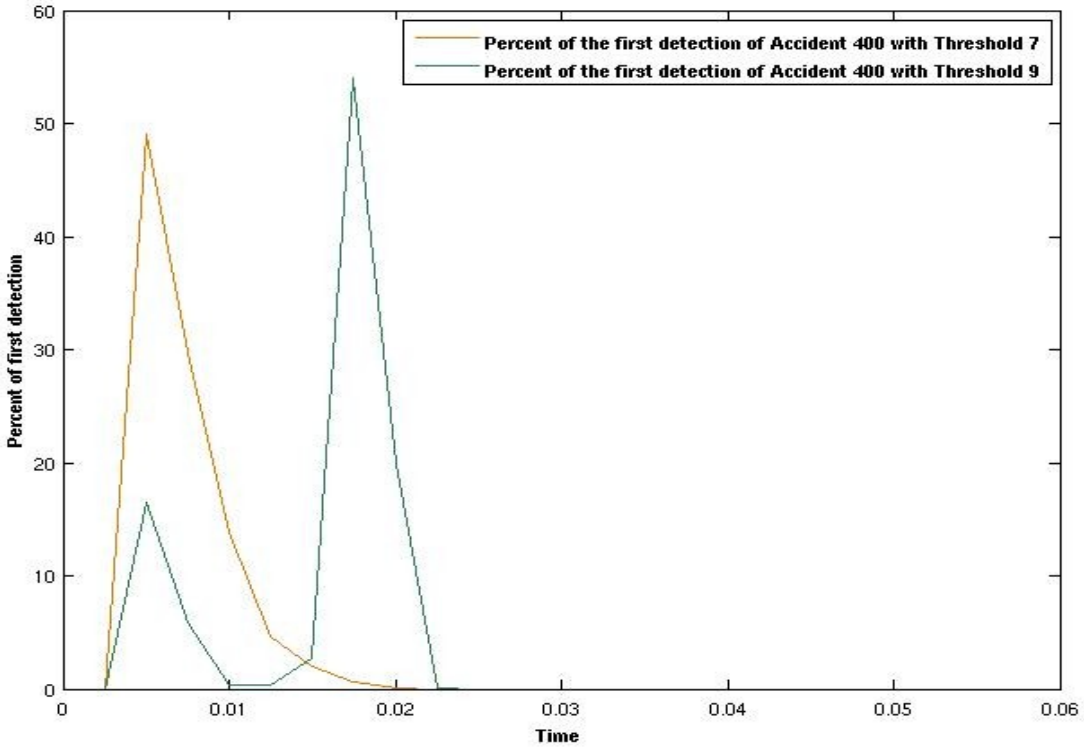

Figure 60: Percent of the First detection versus time of Accident 400

Analysing the images, the obtained conclusion is that using the threshold 7 the results are better than in the case of threshold 9, as it was supposed.

In almost all the cases using 2 of three samples and the threshold 7, the first detection has been made before the 10 milliseconds, which is a good result. In the case of threshold 9, the time of the first detection is not so constant. In some cases it is detected before the 25 milliseconds, as in the Accident 400, but in some others, the accident is not detected until the 50 milliseconds. So using the rule of 2 out of 3 some seconds are gained for sending the SMS.

4.6 Decision of accident

The last characteristic, which have to be established, is how the decision of the accident would be taken. This mean what is going to be considered an accident.

Different rules for deciding if the obtained data corresponds to an accident have been taking into account. The first consideration has been made with the detection of just one accident data. This means, if an accident data is detected, the decision of accident will be taken. The advantage of this rule is that the probabilities of detection will be the highest one could ever achieve. In all the cases studied would be of %100, because in all the accidents at least one sample is detected. While in the case of the probabilities of false alarm, it will be the same as the calculated ones.

The other rule taken into account is that instead of detect an accident sample, and deduce that an accident was occurring, 2 of 3 accident samples must arrive to take the accident decision. This rule is very used in the area of communications, in GPS receivers when they are looking for satellites, for example.

In the following tables the comparisons of the probabilities of detection using just one sample or using 2 of 3 samples are shown. The study made in section *4.3.2 Election of the threshold* showed that in case of using just one sample, the threshold that should be used for achieving the established probability of false alarm is 7 and in case of taking 2 of 3 samples, this should be of 10.

ACCIDENT 2		
	PROBABILITY OF DETECTION FILTERING THE SIGNAL	PROBABILITY OF DETECTION FILTERING THE SIGNAL TAKING 2 OF 3
Threshold 5,5	97,54	93,75
Threshold 6	97,54	93,75
Threshold 6,5	97,54	93,75
Threshold 7	97,54	93,75
Threshold 7,5	97,54	93,75
Threshold 8	95,08	90,62
Threshold 8,5	95,08	90,62
Threshold 9	92,62	87,5
Threshold 9,5	92,62	87,5
Threshold 10	92,62	87,5

Table 14: Comparison of probabilities of detection of Accident 2 using two accelerometers with filter

ACCIDENT 107		
	PROBABILITY OF DETECTION FILTERING THE SIGNAL	PROBABILITY OF DETECTION FILTERING THE SIGNAL TAKING 2 OF 3
Threshold 5,5	95,08	93,62
Threshold 6	95,08	93,62
Threshold 6,5	95,08	93,62
Threshold 7	95,08	93,62
Threshold 7,5	95,08	93,62
Threshold 8	95,08	93,62
Threshold 8,5	95,08	93,62
Threshold 9	94,53	90,62
Threshold 9,5	94,53	90,62
Threshold 10	92,62	87,5

Table 15: Comparison of probabilities of detection of Accident 107 using two accelerometers with filter

ACCIDENT 400		
	PROBABILITY OF DETECTION FILTERING THE SIGNAL	PROBABILITY OF DETECTION FILTERING THE SIGNAL TAKING 2 OF 3
Threshold 5,5	98,36	96,88
Threshold 6	98,36	96,88
Threshold 6,5	98,36	96,88
Threshold 7	98,36	96,88
Threshold 7,5	97,54	93,65
Threshold 8	97,54	93,65
Threshold 8,5	97,54	93,65
Threshold 9	97,54	93,65
Threshold 9,5	97,54	93,65
Threshold 10	97,54	93,65

Table 16: Comparison of probabilities of detection of Accident 400 using two accelerometers with filter

Observing the differences between the probabilities of detection using one sample with threshold 9, and taking 2 of 3 samples, with threshold 7, the obtained conclusion is that in the first case, the results are better than in the second one.

Joining all the final information obtained, the time to the first detection and the probabilities of detection, the decision has to be taken. Analysing the differences of the probabilities of detection, the higher difference occurs in the case of Accident 107 obtained a better a difference of 0,91%. In the case of Time to the First Detection, better results are obtained using 2 of 3 samples. The differences in this parameter are higher than in the probabilities of detection. So finally the rule of 2 of 3 samples, would be use. This means an accident is going to be detected if 2 of 3 samples of accident arrives.

4.7 Vibrations

Another point to have into account are the vibrations of the cars. These generates an additional acceleration in the model of Normal driving and in the accidents. In the following lines, it is going to make an analysis and it is going to generate a model of them.

4.7.1 Mechanics of vibration

A vibration, in its simplest form, can be considered as the oscillation or the repetitive motion of an object around a position of equilibrium. The equilibrium position is the position the object will attain when the excitation force acting on it is zero. The extent of the oscillation determines the magnitude of the vibration and the repetition rate of the cycles of oscillation determines the frequency of the vibration.

The vibratory motion of a car can be completely described as a combination of individual motions of the three orthogonal directions x, y and z.

The vibration of an object is always caused by an excitation force. This force may be externally applied to the object, or it may originate inside the object. The frequency and magnitude of the vibration of a given object is completely determined by the excitation force, direction, and frequency [34].

4.7.2 Classification of vibration

It is possible to distinguish two types of excitation functions, namely, deterministic and nondeterministic, where the latter is also known as random. Deterministic functions may be further subdivided in harmonic, periodic and non periodic.

The common characteristic of the deterministic functions is that their values can be determined for any future time. The response of systems to deterministic excitations is also deterministic. There are many physical phenomena, however, that do not lend themselves to explicit time description. The implication is that the value at some future time of the variables describing these phenomena cannot be predicted. Phenomena whose outcome at a future instant of time cannot be predicted are classified as nondeterministic and referred to as random. A typical example of such phenomena is the jet engine noise [35].

The sources of vibrations in a vehicle are many, including the engine, driveline, road surface, brakes, wind and type of car. Many problems are generated as either vibration or noise, transmitted via a variety of paths. Due to this complex combination of factors, the vibration of a car is supposed to be a random vibration, with a maximum value of 0,8 m/s^2 .[36]

4.7.3 Model of vibrations

These vibrations affecting in a car can be modelled as an uniformly distributed random variables for each axis. The maximum amplitude of these is of the order of 0,8 m/s^2. [35]

So the equations modelling the vibrations of each axis of the car are the following ones:

$$vibrax = \phi_1$$

$$vibray = \phi_2$$

$$vibraz = \phi_3$$

Where Φ1, Φ2 and Φ3 are three uniformly distributed random variables [-0,8,0,8].

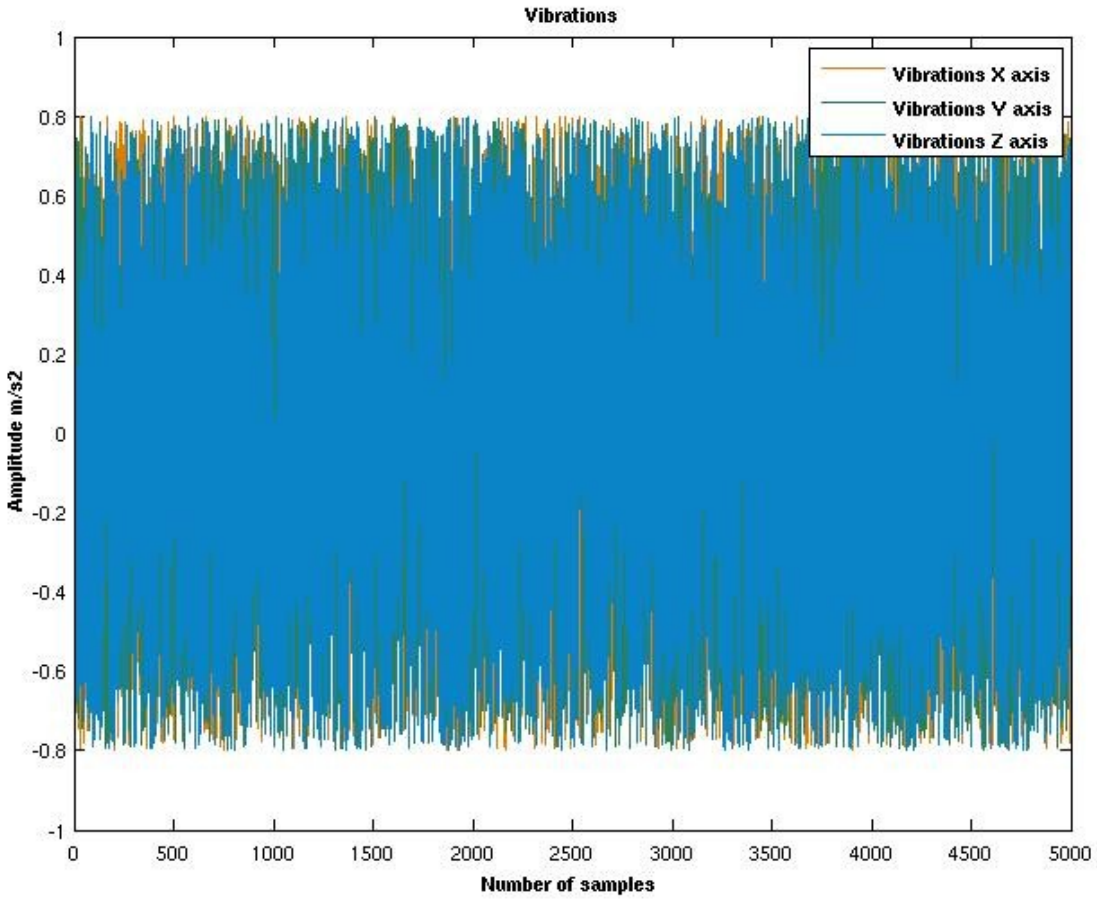

Figure 62: Spectrum of the vibrations

4.7.4 Influence of the vibrations detecting the accidents

The probabilities of detection have been recalculated for observing the influence of the vibrations at the moment of detecting accidents. In the next table there are the comparisons between the probabilities, in one hand taking into account the vibrations, and in the other without.

PROBABILITY OF DETECTION ACCIDENT 2		
Threshold	**With vibrations**	**Without vibrations**
5,5	93,75	93,75
6	93,75	93,75
6,5	93,75	93,75
7	93,75	93,75
7,5	93,75	93,75
8	90,62	90,62
8,5	90,62	90,62
9	87,5	87,5
9,5	87,5	87,5
10	87,5	87,5

Table 17: Influence of the vibrations in the Probability of detection in the case of Accident 2

PROBABILITY OF DETECTION ACCIDENT 107		
Threshold	**With vibrations**	**Without vibrations**
5,5	93,62	93,62
6	93,62	93,62
6,5	93,62	93,62
7	93,62	93,62
7,5	93,62	93,62
8	93,62	93,62
8,5	93,62	93,62
9	90,62	90,62
9,5	90,62	90,62
10	87,5	87,5

Table 18: Influence of the vibrations in the Probability of Detection in the case of Accident 107

PROBABILITY OF DETECTION ACCIDENT 400		
Threshold	**With vibrations**	**Without vibrations**
5,5	98,36	96,88
6	98,36	96,88
6,5	98,36	96,88
7	98,36	96,88
7,5	98,36	93,65
8	97,54	93,65
8,5	97,54	93,65
9	97,54	93,65
9,5	97,54	93,65
10	97,54	93,65

Table 19: Influence of the vibrations in the Probability of Detection in the case of Accident 400

The influence of the vibrations is not very high, in the only accident that they have changed the probabilities of detection is in the accident 400. But they are going also to influence in the probability of false alarm, so it has to be recalculated.

Taking the same threshold T'=7, the maximum value in the acceleration of a normal driving has increased, μ' =3.6. So the new value of A (see Section *4.3.2 Election of the threshold*) is:

$$A'' = \frac{(T' - \mu')}{(\sigma * \sqrt{2})} = 2{,}4$$

$$erfc(A'') = P_{fa}(x) * 2$$

$$P_{fa}(x) = 0{,}00034425$$

$$P_{fa}(X) = \binom{3}{2} * (P_{fa}(x))^2 * (1 - P_{fa}(x)) = 3{,}5528 * 10^{-7}$$

So the probability of false alarm has increased considerably.

In the other hand there is the possibility of changing the threshold, in this case the value of the new threshold would be:

$$A' = 3$$

$$T' = \sqrt{2} * A' + \mu'$$

$$T' = \sqrt{2} * 3 + 3{,}6 = 7{,}8$$

So in this case, the probabilities of detection would be decreased, but the probability of false alarm is maintained.

So finally the threshold that must been used for obtaining the desired probability of false alarm is eight. With this threshold the probabilities obtained for the data of a normal conduction followed by the three accidents which during this report have been worked with and with vibrations are:

- *Accident 2*

  Probability of detection 90,62%

  Probability of false alarm 10^{-7}%

- *Accident 107*

  Probability of detection 93,62%
  Probability of false alarm 10^{-7} %

- *Accident 400*

  Probability of detection 97,54%

  Probability of false alarm 10^{-7}%

4.8 Free fall

Until now the system has compared the value of the acceleration and the formed angle with the calculated gravity, for deducing if an accident was happening or not. But in case of falling the device a false alarm would occur.

When something is falling without rotation, the detection of the fall is easily detectable, due to the measurements of the accelerometers. In this case, as the accelerometers measures the acceleration it experiences relative to free fall, the measurements will be zero.

The problem happens, when during the falling occurs a rotation, in this case, the measurements will not be null, due to the centripetal and the centrifugal accelerations. If the fall is not detected when the device arrives to the floor will suffer great accelerations, causing a false alarm.

Following there are the graphics representing the reading of a conventional accelerometer as a function of time of an object initially being held, and then being dropped until after the object comes to rest on the floor. The first image is representing a fallen without spin, and the second one with spin.

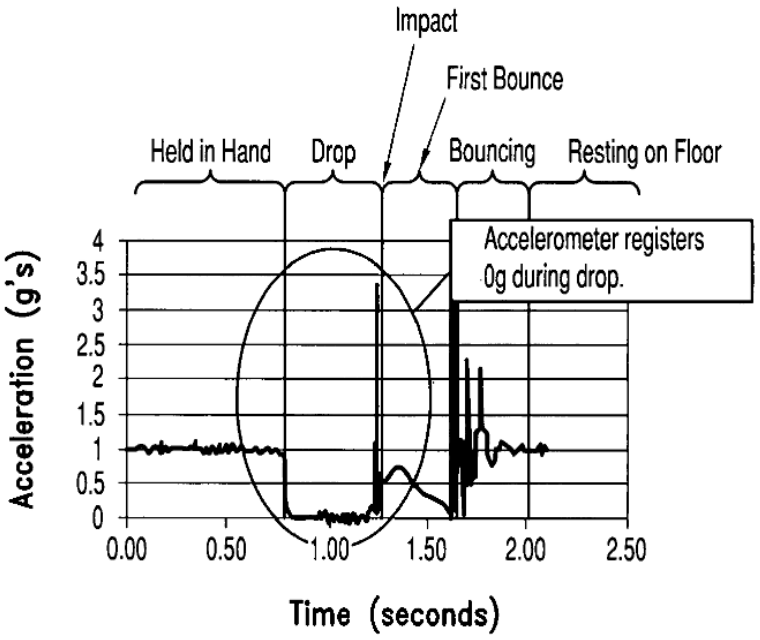

Figure 63: Acceleration while falling without spin

In the image all the process can be seen. During the first 750 milliseconds, the object is being held, and consequently the acceleration measured is 1 g. Then during the free fall the acceleration is 0 g, till 1,25 millisecond. In that moment the impact is happening, achieving accelerations of 3 gs. Then some bounces happen, generating peak of less intensity. Finally the device rests on the floor.

This case is easy to detect, a verification of the non null acceleration is the only premise that it has to be checked.

The following image represents a fallen, but in this case with spin.

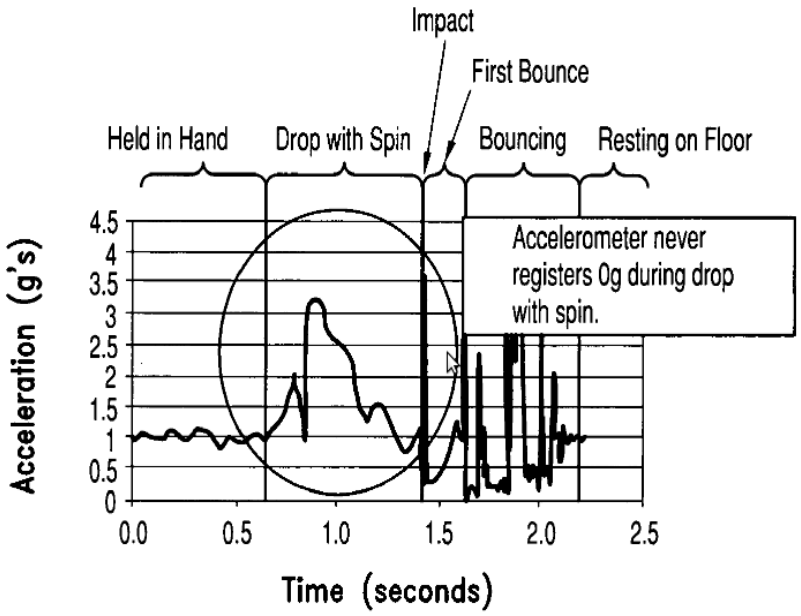

Figure 64: Acceleration while falling with spin

This sequence is very similar to the previous one, but in this case the acceleration during the falling is not null, due to the centripetal accelerations.

This second case is more difficult to detect than the previous one, because the accelerometers would never measure 0 g. Due to this difficulty two different algorithms have been analysed.

4.8.1 Detection of the floor

The first idea for discarding the falls, and for not generating false alarms, was to estimate the direction of the floor all the time. This means having a vector pointing to the floor, and in case of having a great acceleration in that direction not treating it as an accident.

When a rigid body is falling with rotation the acceleration measure by the devices is:

$$\overline{a}_i = \overline{a}_p + \overline{\alpha} x \overline{d}_i + \overline{\omega} x (\overline{\omega} x \overline{d}_i)$$

Where a_i is the total acceleration of a point "i", a_p is the linear acceleration, α is the angular acceleration ω is the angular velocity d_i is the distance from the point "i" to the centre of rotation and x is vectorial multiplication.

When only translation occurs, the angular acceleration and velocity are null.

$$\overline{v}_p \neq 0 \rightarrow \overline{a}_p \neq 0$$

but

$$\overline{\omega} = 0 \quad \& \quad \overline{\alpha} = 0$$

So the measured acceleration is the following one:

$$\overline{a}_i = \overline{a}_p$$

In the other hand when only rotation happens, the linear velocity and acceleration are zero.

$$\overline{\omega} \neq 0 \rightarrow \overline{\alpha} \neq 0$$

but

$$\overline{v}_p = 0 \quad \& \quad \overline{a}_p = 0$$

So the acceleration is:

$$\overline{a}_i = \overline{\alpha} x \overline{d}_i + \overline{\omega} x (\overline{\omega} x \overline{d}_i)$$

So having two accelerometers, if the subtraction from the data of the first accelerometer from the second one (projected) is made the result is twice the rotational acceleration *(See annex IV with the demonstration)*

A little explanation of how to use two accelerometers for measuring rotational accelerations is going to be introduced, first of all using two-axis accelerometers, for making more comprehensible [36].

The device has two accelerometers rigidly mounted at distances d_1 and d_2 from the centre of rotation as shown in *Figure 65.*

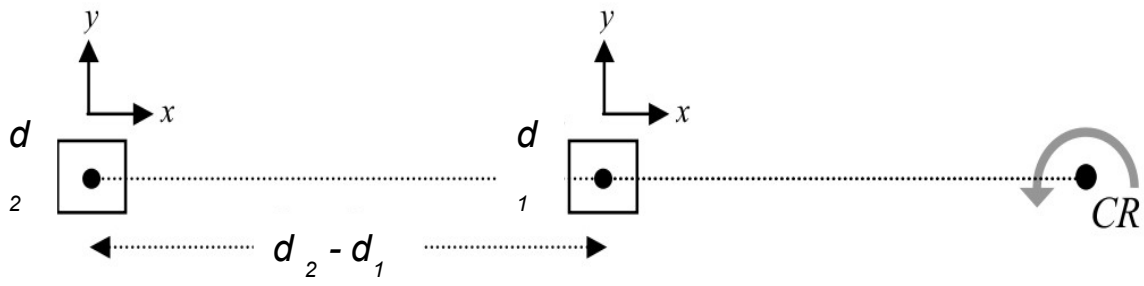

Figure 65: Locations of two accelerometers on a rotating object

The radial acceleration measured by accelerometer 1 is:

$$a_{x1}=|\omega|^2|d_1|$$

Where ω is the angular velocity, which is the same in all the points of the rigid body.

The radial acceleration measured by accelerometer 2 is:

$$a_{x2}=|\omega|^2|d_2|$$

Taking the difference between the two measurements:

$$a_{x2}-a_{x1}=|\omega|^2(|d_2|-|d_1|)=|\omega||D|$$

where D = r2 – r1 is the fixed separation between the two accelerometers. From this equation the magnitude of the angular velocity can be determined:

$$|\omega|=\sqrt{(\frac{(a_{x2}-a_{x1})}{|D|})}$$

The tangential acceleration measured at accelerometer 1 is:

$$a_{y1}=\overline{\alpha}\,\overline{d}_1$$

Where α is the angular acceleration.

The tangential acceleration measured at accelerometer 2 is:

$$a_{y2}=\overline{\alpha}\,\overline{d}_2$$

Taking the difference between the two measurements:

$$a_{y2} - a_{y1} = \overline{\alpha}(\overline{d}_2 - \overline{d}_1) = \overline{\alpha}\,\overline{D}$$

Re-arranging the terms to determine the angular acceleration:

$$|\alpha| = \frac{(a_{y2} - a_{y1})}{|D|}$$

Looking at the equations of the angular acceleration and velocity, a couple of observations can be made. First, it is not necessary to know where the centre of rotation is to determine the angular velocity or angular acceleration. The separation between the accelerometers, is the only parameter needed. Second, this separation and the resolution of the accelerometers determines the resolution that can be obtained in the angular measurements.

Now considering two tri-axis accelerometers separated by distance D with Y-axes aligned as shown in Figure . The radial and tangential accelerations should be able to determine angular velocity around the X-axis and the Z-axis ., but not around the Y-axis.

Figure 66: Locations of the accelerometers on the rotating Neo FreeRunner

The radial acceleration measured, will be the same that in the case of bi-axis accelerometers. In this case the total rotation rate is know, but the direction and the rotation rate about the Y axis and the Z axis are unknown. The angular accelerations about the Z axis and X axis are calculated as it is shown in the following equations.

$$\alpha_z = \frac{(a_{x2} - a_{x1})}{|D|}$$

$$\alpha_x = \frac{(a_{z2} - a_{z1})}{|D|}$$

Integrating α_x and α_z when ω is nonzero allows to determine ω_y and ω_z. Thus, the relative magnitude and direction of rotation are calculated from the integrals of the tangential accelerations.

$$\omega_z = \int \alpha_z dt$$

$$\omega_x = \int \alpha_x dt$$

The vector sum of ω_y and ω_z from is equal to the magnitude of the total angular rotation rate, ω_{total}.

$$\omega_{total} = \sqrt{(\omega_x{}^2 + \omega_z{}^2)}$$

Using the total rotation rate magnitude calculate in the equations before and the relative magnitude and direction of rotation obtained before the final rotation velocity can be determined

$$\omega_{zfinal} = |\omega| \left(\frac{\omega_z}{\omega_{total}} \right)$$

$$\omega_{xfinal} = |\omega| \left(\frac{\omega_x}{\omega_{total}} \right)$$

So as it has been commented previously, the rotation magnitudes can be obtained, but only from the two axes, where the accelerometers are not collocated. In other words, there is always going to be a direction where the rotation magnitudes can not be measured, the direction which joins the two accelerometers.

For detecting the floor, the rotation of the device in the three axes have to be measure. When the accelerometers measure the acceleration, they measure the translational and the rotational accelerations. For detecting where the floor is, the one that is interesting is the rotational one.

4.8.2 Detection of free-fall with rotation

Ruling out the possibility of detecting every-time the position of the floor,another way for using an algorithm for detecting freefall with spin has been used. Once having detected the fall, the program will not have into account the next acceleration.

If the object is falling with spin, then it rotates around a certain axis while falling. The 2 centrifugal accelerations will lie on a certain plane, because the 2 accelerometers are attached physically to the rigid body. As the object is falling and spinning ,and the gravity is not measured the only measures in the accelerometers will be the centrifugal force. Due to this acceleration, the two vectors will lie on the same plane, this mean, there will be either parallel or they will intersect at some point [37].

Otherwise, during normal usage, or during an accident the gravity is always involved in the measurement, so the measurement vectors cannot intersect, because the gravity skews the two vectors in 3-dimensional space.

So the base of the algorithm is to check whether the two acceleration vectors are lie on the same plane, which means that the two accelerations will be parallel or will intersect in any point.

The condition that must satisfy the vectors for being parallel is that their cross product have to be zero. This means that they are lied on the same plane and that they not intersect.

$$A1xA2=0 \qquad \textit{(Condition 1)}$$

Where A1 and A2 are the measurements of the first and the second accelerometer.

Once having checked if they are parallel, the verification of if the two measurements lie on a plane through intersection have to be done. In order to check it, the result of the cross product, have to be scalarly multiplied by the vector , which joins the two accelerometers. If the vector resultant of the cross product is perpendicular to the vector that joins the two accelerometers(R), then the vector R should be on a plane made by two measurement vectors. This means that A1 and A2 meets in a certain point. So in case of been null the result, this will mean that the two measurements are lie on the same plane, and that they intersect in a certain point.

$$R\cdot(A1xA2)=0 \qquad (\textit{Condition 2})$$

Where A1 and A2 are the measurements of the first and the second accelerometer, and R is the vector that joins the two accelerometers.

Although in most of the cases with this two verifications the free-fall with spin can be detected, there are three cases in which it is impossible. If the accelerations of the two accelerometers (A1 and A2) are equals, it is impossible to detect spin. Gravity affects both accelerometers equally, and they would be parallel even though the object is under gravity. This case can rarely happen.

There is another case in which the free fall is impossible to detect. If at least one of the

measurements is parallel to the the gravity ($A1xG=0 \vee A2xG=0$), then it cannot be detected.

The last exception case is when the rotation axis is the same as the direction of gravity ($G \cdot (A1xA2)$)

In the next diagram there is the step by step flow of the method is illustrated.

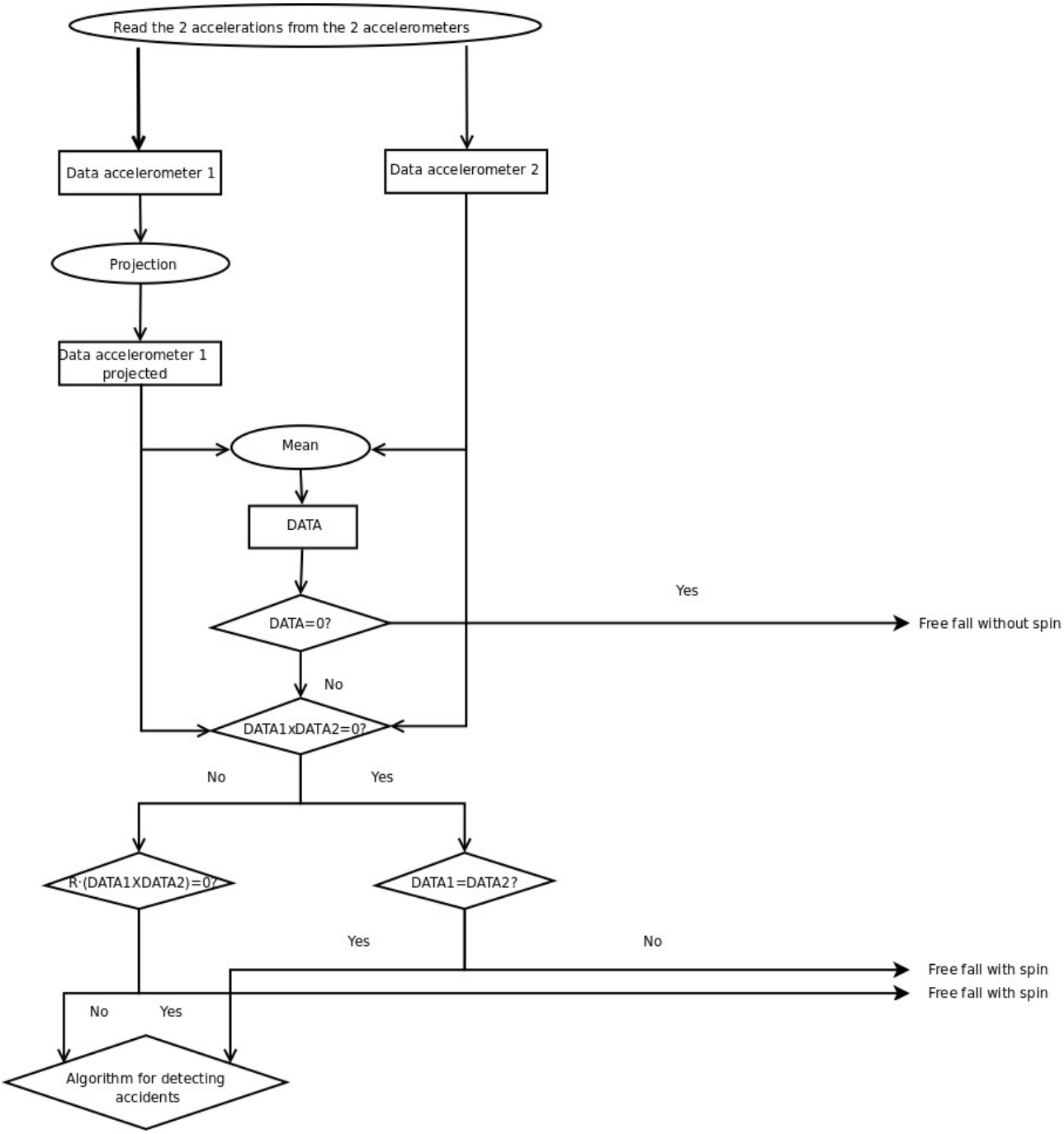

Diagram 8: Flowchart of the algorithm for detecting free fall

First the acceleration signals generated by each accelerometer are read for a later analysis. In the next step the data of the first accelerometer is projected, due to the different orientation of the accelerometers. Once the data is conditioned the next step is to calculate the mean for reducing the noise. This result is used for verifying if there is happening a free fall without spin, checking if it is null. Then the cross product of the two vectors is calculated. If this is zero, then the vectors cannot intersect and will, in fact, be parallel assuming the vectors are not the same as one another. The latter condition is checked in the next step, if the vectors are the same, then it is concluded that the detected movement is not free fall with spin and the data is send for a later analysis with the algorithm for detecting accidents. On the other hand if the two vectors are different, the algorithm determines that the object is undergoing free fall with spin.

The next step is to check for intersection of the two vectors which also indicates that they lie on the same plane. It is determine whether the $R \cdot (A1xA2) = 0$ .If so, free fall with spin is detected. If not, the data is transmitted to the accident detection algorithm for studying it.

5 CONCLUSIONS AND FUTURE RESEARCH

5.1 Conclusions

During this project, the possibility of implementing an ACNS has been studied. The European Commission has taken the track of implementing it in the car, during this project instead, the possibility of implementing it in a mobile have been explained.

The correct functionality of the application for sending a SMS with the GPS position have been developed, as well as corroborated, sending and receiving in another mobile phone the SMS.

Another important point in the development of the project, is what it refers to the device. In one hand the quality of the accelerometers is acceptable, it is remarkable that most of the mobile phones in the market (Iphone, Blackberry Storm, Palm Pre, Nokia N95, Nokia N96, HTC Touch Diamond and all the Sony Ericsson) use the same ones. In the other one, most programs available for Openmoko smart-phones are Free Software, thus they are always being modified,and redesigned, what means that the software used would be not the best one.

The problem with the packet losses is probably caused by the software of the device. This could give the priority to other processes, and as consequence some packets from the accelerometer would be lost.

The other obstacle found during the development of the project has been the noise in the accelerometer data. The possible cause of this problem is a hardware failure, which makes that different signals of different frequencies were strained, affecting the study of the noise.

As far as accident detection concerns, the possibility of the implementation in the mobile phones, has been demonstrated. The probabilities of detection which have been worked with are of the order of 93 %. This probability although not been a legislation which regulates this nowadays, it is considered reasonable.

What it concerns to the implementation in the mobile phone, in one hand it is the possibility of implementing it as a process activated only during a car trip. This means, the user would have to attach the device to the car and activate the program manually before a car trip. In this way, the detection of free fall would not be necessary.

In the other hand, there is the possibility of implementing it as a process executed continuously in background, this is a daemon. In this implementation the detection of free fall is very important due to the avoidance of false alarms. The problem with this implementation is that the algorithm for detecting the free fall is not reliable at 100 %, because it has some cases in which would not be detected.

To sum all the conclusions up, comment that the implementation of an ACNS it is a real possibility, with some restrictions. This track has some advantages in comparison to the implementation of the black box in the car. The most important one is the economical theme. With this implementation the expenses of all the devices would be cut out, because everything will be in the user's mobile phone.

5.2 Future research

Following the steps that follow the project will be commented.

The first step would be the design of a simulator. Its main characteristic should be the clarity and visual. It should be very visual, what means that everybody could understand it. Showing the internal functionalism should not be it main function. Instead of it, it should show the main function. How the car is driving normally and the algorithm do not detect, and as it has a crash, the algorithm throws an advice.

The next step should be the implementation of the algorithm in the "*Neo FreeRunner"*. The functions developed in Matlab®, should be changed for being capable to work in C.

Following the work should be focused on the integration of the algorithm with the function of sending the SMS with the position, obtaining a process able of detecting accidents and sending the position through a SMS to an established telephone number.

The final step should be the checked of the algorithm in a real situation. This is the most difficult stage, due to the necessity of a special laboratory prepared for the study of the car crashes.

Finally the development of a legislation telling the main characteristics of the application and the necessities of the device, could be a huge step for a possible commercialization of the application.

5.3 Recommendations for a future work

As it has been previously commented the correct functionality of the system is assured. For continuing with the work some suggestions and advice are going to be given:

- *The threshold*. As it has been commented in the section 4.7, taking into account the different vibrations affecting to the accelerometer the suggested threshold is of the order of 8.

- *The decision of accident.* As it has been proofed in section 4.6 taking 2 of 3 samples of accident for decide if it has been accident or not is the best solution.

- *The mixed up in the packets*. This problem has to be taken into account. It is very important to corroborate if the packet are mixed up or not and in case of being, these should be rejected.

- The possibility of implementing it in *another mobile phone.* In my opinion it would be interesting to implement the application in another mobile phone with the same accelerometer as the Iphone for example, for corroborating the absence of the great noise.

6 REFERENCES

[1]World Health Organization ,Regional Office for Europe, Department of Violence & Injury prevention & Dissability,*Global status report on road safety*, 2009.

[2]RACC Automovil Club, Fundacion*, Siniestralidad en las carreteras españolas, Balance 2008*, 2009.

[3]RACC Automobil Club, Fundacion*, Memoria 2007,* 2008.

[4]André Malm, Berg Insight's LBS Research Series,*GPS and Mobile Handsets.*

[5]iSuppli, *One Third of Mobile Phones to Use Accelerometers by 2010*, 2009.

[6]Openmoko main page http://wiki.openmoko.org/wiki/Main_Page

[7]Openmoko page http://www.openmoko.com/

[8]European Commision*, European emergency number 112 now works in all the EU Member States*, Brussels, December 2008,[IP/08/1968,].

[9]European Commision *, eCall – saving lives through in-vehicle communication technology* ,Brussels, August 2009 [factsheet 49].

[10]European Commission*, 112: Commission says EU single emergency number must get multilingual* , , Brussels, February 2009,[IP/09/240]

[11]Europa Information Society Portal: eSafety Home page:http://ec.europa.eu/esafety

[12] eSafety support: http://www.esafetysupport.org

[13]Europe's Information Society Thematic Portal: http://ec.europa.eu/information_society/

[14]Mayday information website http://www.enterprise.prog.org/mayday.htm

[15] ATX Technologies main page: http://www.atxg.com/

[16]TechMarcom for Motorola,Marcom, *Telematics is Driving Automotive Communications into the 21st Century* Fall 1999.

[17]Onstar's website: http://www.onstar.com/us_english/jsp/vzw_discontinue.jsp

[18]Toyota and helpnet website : http://www2.toyota.co.jp/en/news/05/0414.html

[19] BMW website, BMW Assist Introduction : http://www.bmw.com/com/en/owners/navigation/assist_1.html

[20] Teleaid website : http://www.teleaid.com/

[21] Volvo website, Volvo On Call information: http://www.volvocars.com/intl/corporation/NewsEvents/News/Pages/default.aspx?item=30

[22] Datasheet and information of the Ublox Antaris 4: http://www.u-blox.com/en/gps-modules/pvt-modules/antaris-4.html

[23] Sensr, *Practical guide to Accelerometers*, , www.sensr.com

[24]Datasheet of the LIS302DL: http://www.st.com/stonline/products/literature/ds/12726/lis302dl.htm

[25]Wright, J.F, *Monte Carlo Simulation in Scientific & Engineered Systems,* October 2002.

[26]André M. *Real-world driving cycles for measuring cars pollutant emissions – Part A: The Artemis European driving cycles,* 2004.

[27]P.N. Pathirana, A.V. Savkin and S. Jha, "*Location estimation and trajectory prediction for cellular networks with mobile base stations"*, IEEE Transactions on Vehicular Technology, 2004, pp. 1903–1913.

[28]Accident database of NHTSA: http://www.nrd.nhtsa.dot.gov/database/aspx/vehdb/querytesttable.aspx .

[29]NHTSA , *Test Reference Guide, Version 5, Volume I:Vehicle Tests,* Revision March 2006.

[30]NHTSA, *Data Reference Guide, Version 4, Volume I:Vehicle Tests,* April 1997.

[31]A. Jerri, *The Shannon Sampling Theorem—Its Various Extensions and Applications: A Tutorial Review*, Proceedings of the IEEE, 65:1565–1595, Nov. 1977.

[32]Matlab®'s fdatool website: http://www.mathworks.com/access/helpdesk/help/toolbox/signal/index.html?/access/helpdesk/help/toolbox/signal/fdatool.html&http://www.google.com/cse?cx=014345598409501589908%3Amplknj4r1bu&ie=UTF-8&q=fdatool&sa=Search

[33]Morrison, Ann Michelle. 2005. *Receiver Operating Characteristic (ROC) Curve Preparation - A Tutorial. Boston:* Massachusetts Water Resources Authority. Report ENQUAD 2005-20. 5 p.

[34 Grimpampi, E. *An integrated approach to whole-body vibration,* 2008.

[35]Meirovitch, L. *Fundamentals of Vibrations*. McGraw-Hill International Edition, 2001.

[36]Mansfield NJ, Griffin MJ (2000) *Difference thresholds for automobile seat vibration*. Applied Ergonomics 31, 255–61.

[37]KIONIX, *Using two tri-axis accelerometers for rotational measurements,* January 2008 [AN 019]

[38] Kim, D.Y, Miller, S.A., *System and method for detection of freefall with spin using two tri-axis accelerometers*, November 2008.

Index of Figures

Index of Diagrams

Index of Tables

ANNEX I

Characteristics of the NeoFreeRunner

Specifications of the Neo FreeRunner

Physical Dimensions

- 120.7 x 62.0 x 18.5 mm (4.752 x 2.441 x 0.728 inch)
- 110 +/- 5 g (4 ounces) without battery

Hardware

- High resolution touch screen 2.84" (43mm x 58mm) 480x640 pixels
- 128MB SDRAM memory
- 256 MB integrated flash memory (expandable with microSD or microSDHC card)
- microSD slot supporting up to 16GB SDHC (Secure Digital High Capacity) cards
- Internal GPS module: u-blox ANTARIS 4 chip
    - Connected to: S3C2442 UART2, /dev/ttySAC1 in userspace
    - Driver: none needed, talks standard NMEA
    - u-blox Antaris 4 Protocol Protocol download page
    - ATR0635 Datasheet: u-blox ATR0635
- Bluetooth
- 802.11 b/g WiFi
- 400Mhz ARM processor
- 2 3D accelerometers : ST LIS302DL
    - Homepage:http://www.st.com/stonline/products/literature/ds/12726/lis302dl.htm
    - Datasheet: http://www.st.com/stonline/products/literature/ds/12726.pdf
    - Connected to: S3C2442 via SPI interface
    - S3C2442 SPI EINT interrupt inputs
- 2 LEDs illuminating the two buttons on the rim of the case (one bicolor [blue|orange] behind the power button, 1 unicolor [red] behind the aux button)
- Tri-band GSM and GPRS :The GSM (including GPRS) modem is Texas Instruments Calypso based.
    - Connected to: S3C2442 UART1 (full-uart, RxD, TxD, CTS, RTS), /dev/ttySAC0 in userspace
    - PM Driver: https://svn.openmoko.org/trunk/src/target/kernel/patches/gta01-power_control.patch
    - Accessible GSM/GPRS antenna jack (if battery cover is removed)
- USB Host function with 500mA power, allowing you to power USB devices for short periods

Versions: The Neo FreeRunner is available in two versions, one for the GSM bands of North America (850/1800/1900 Mhz), and one for the GSM bands in the rest of the world (900/1800/1900 Mhz).

ANNEX II

Process of the generation of the noise

In the next graphics, all the process for characterizing the noise introduced by the first accelerometer is shown. After, the results obtained with the second accelerometer are plotted.

First Accelerometer

In this first step, the white noise is generated, the figures belongs to the spectrum of each axis.

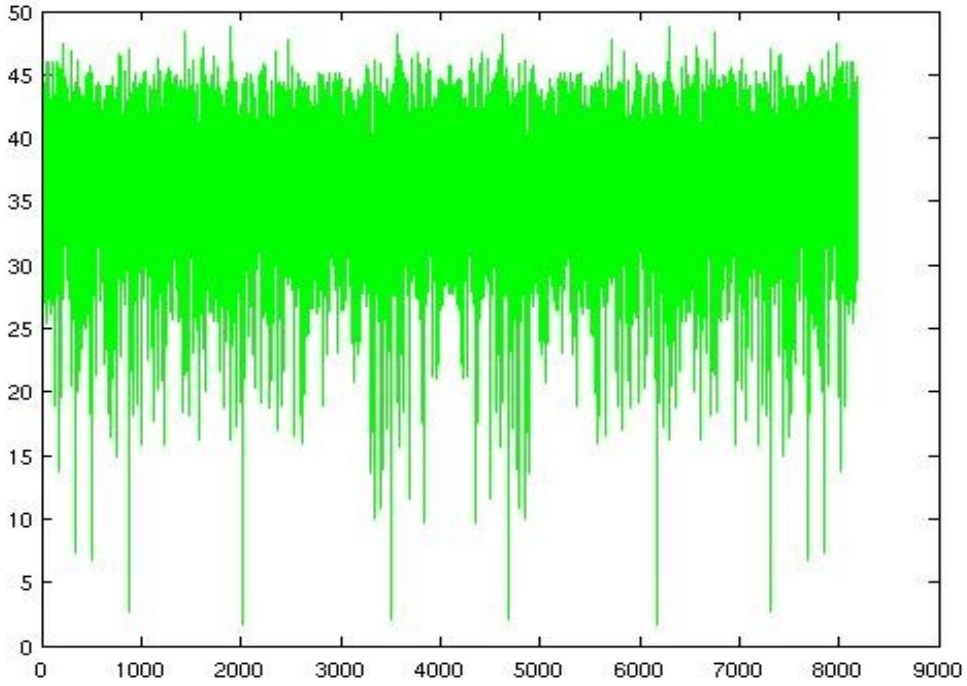

Spectrum of the X axis's white noise

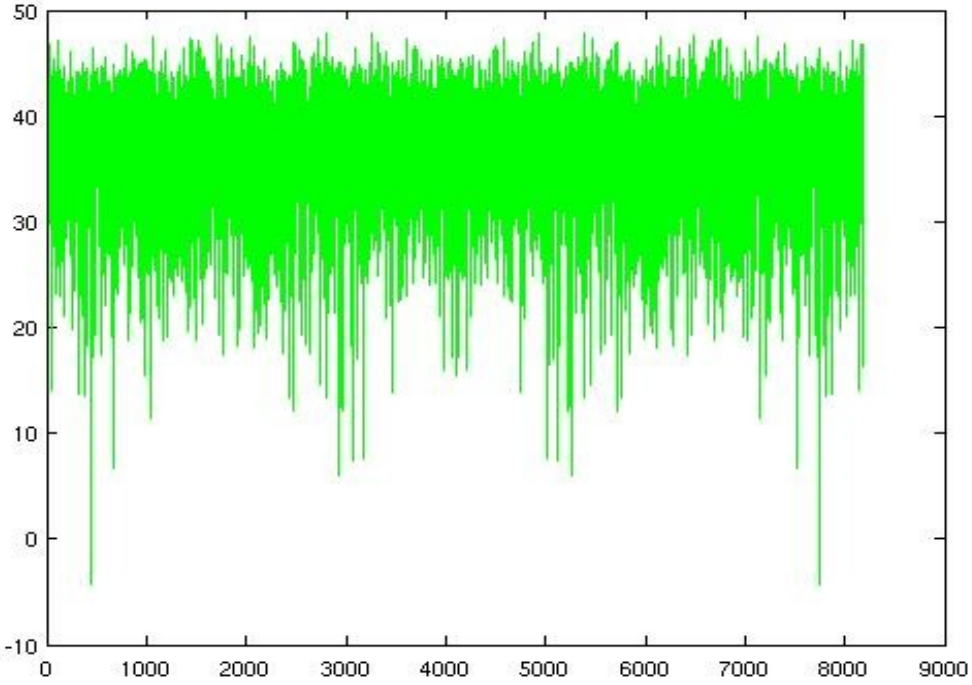

Spectrum of the Y axis's white noise

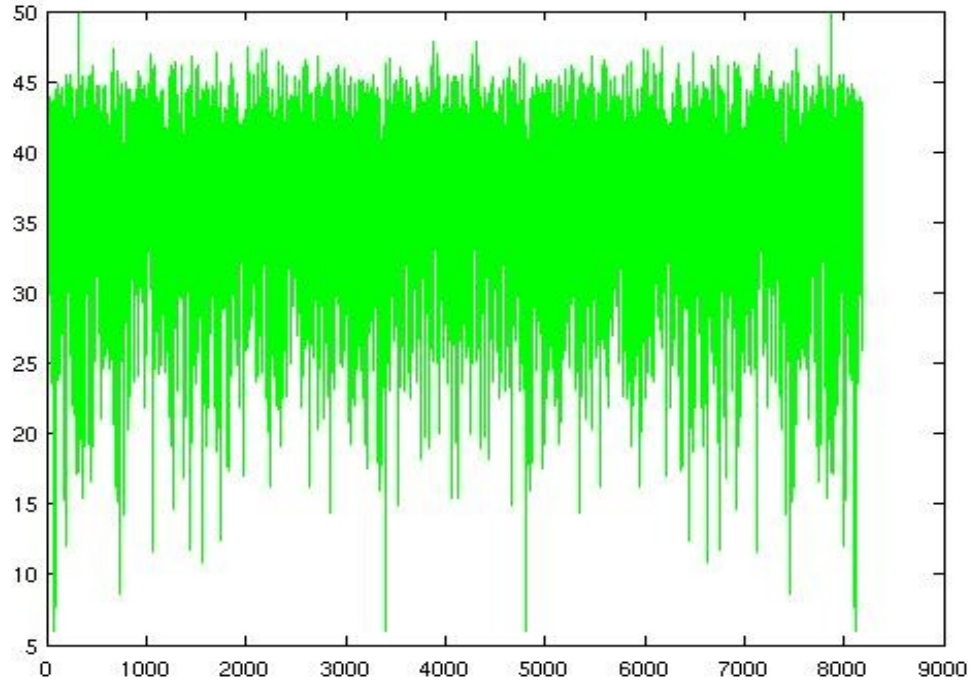

Spectrum of the Z axis's white noise

In the second step, the multiplication by the *"Cholesky"* matrix is made. Next there are the graphics comparing the spectrum of the initial white noise, and the spectrum of the vector achieved after the multiplication.

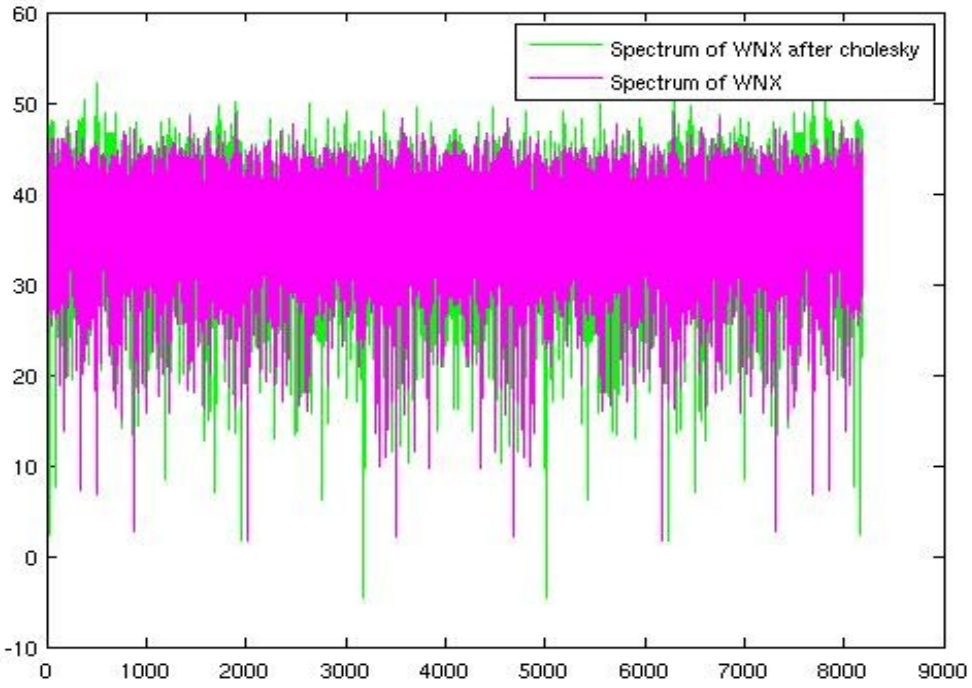

Comparison of the X axis spectrum before and after "Cholesky"

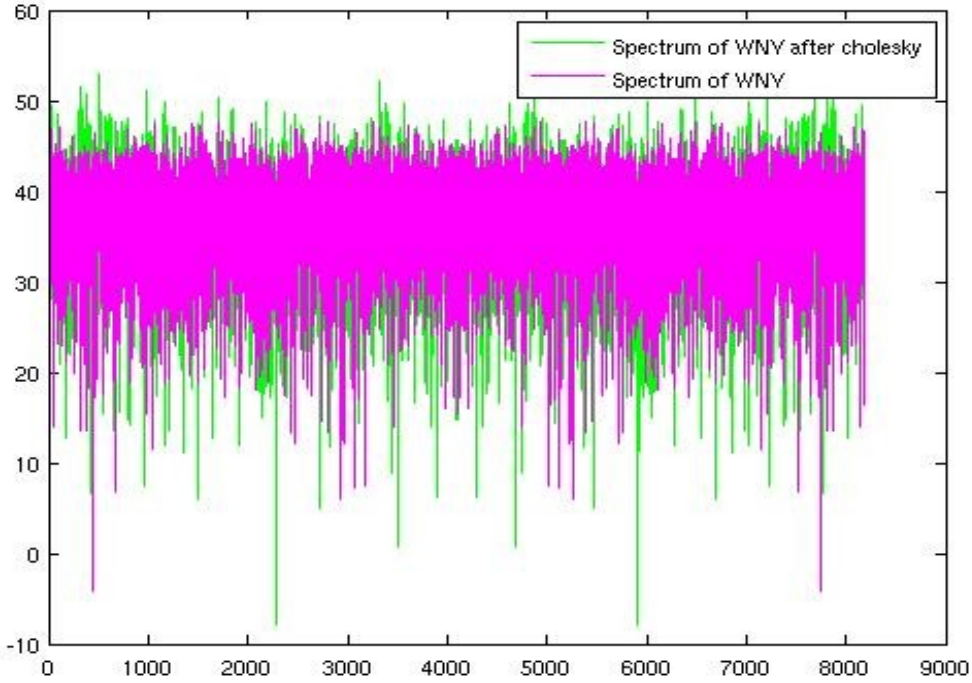

Comparison of the Y axis spectrum before and after "Cholesky"

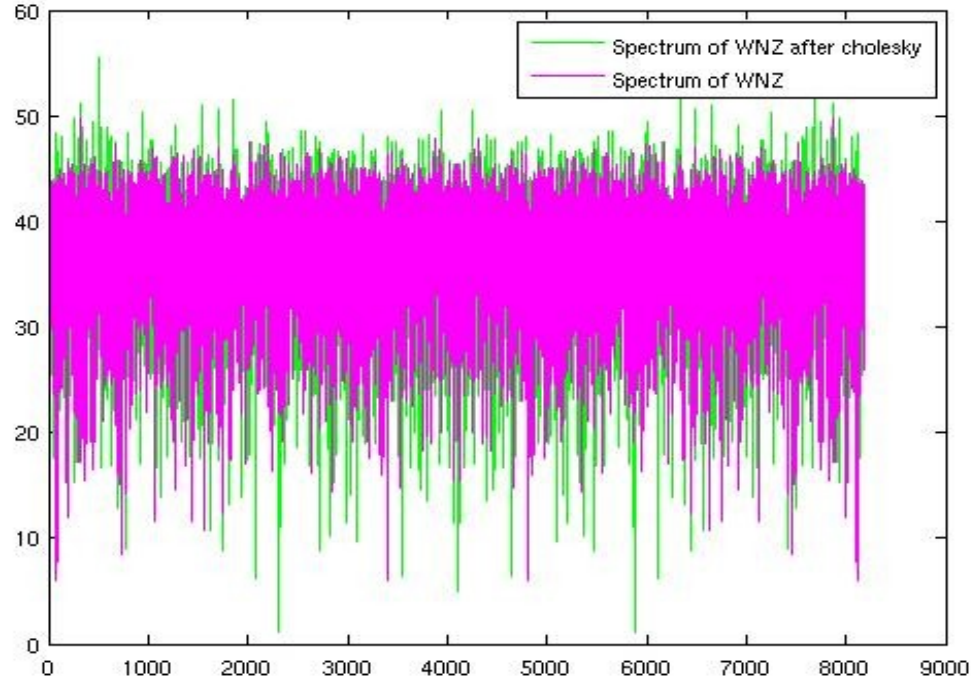

Comparison of the Z axis spectrum before and after "Cholesky"

In this second step, the spectrum seems more to the desired one, due to the introduction of some peaks.

In the third step, the gain has been added, obtaining the same spectrum but elevated. Finally we have added the bias. Next there are the comparison between the spectrum of the obtained result, and of the first one.

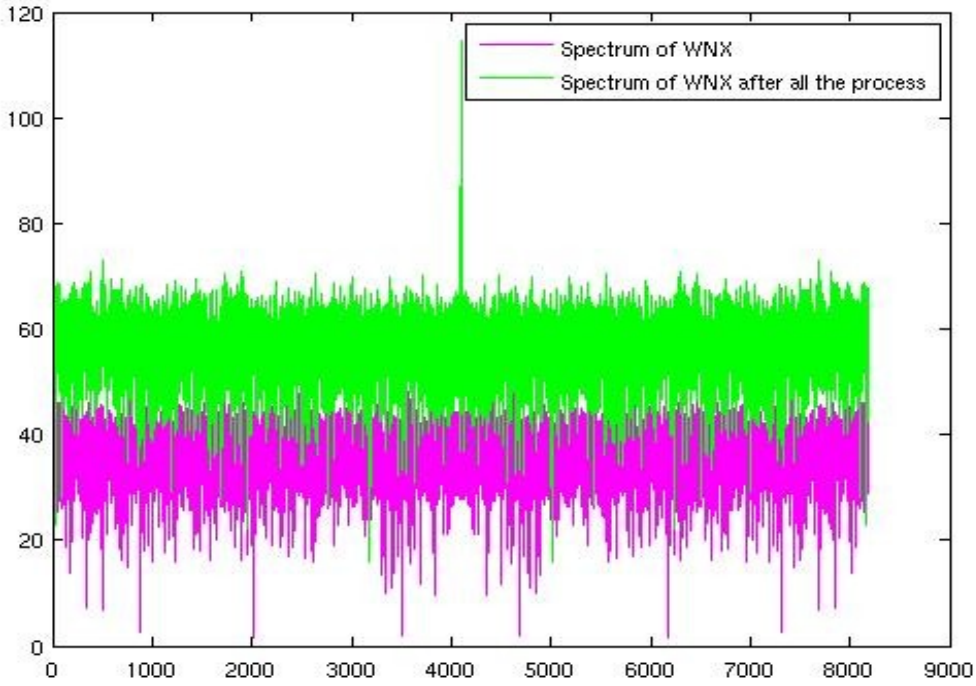

Comparison between the X axis spectrum before and after all the process

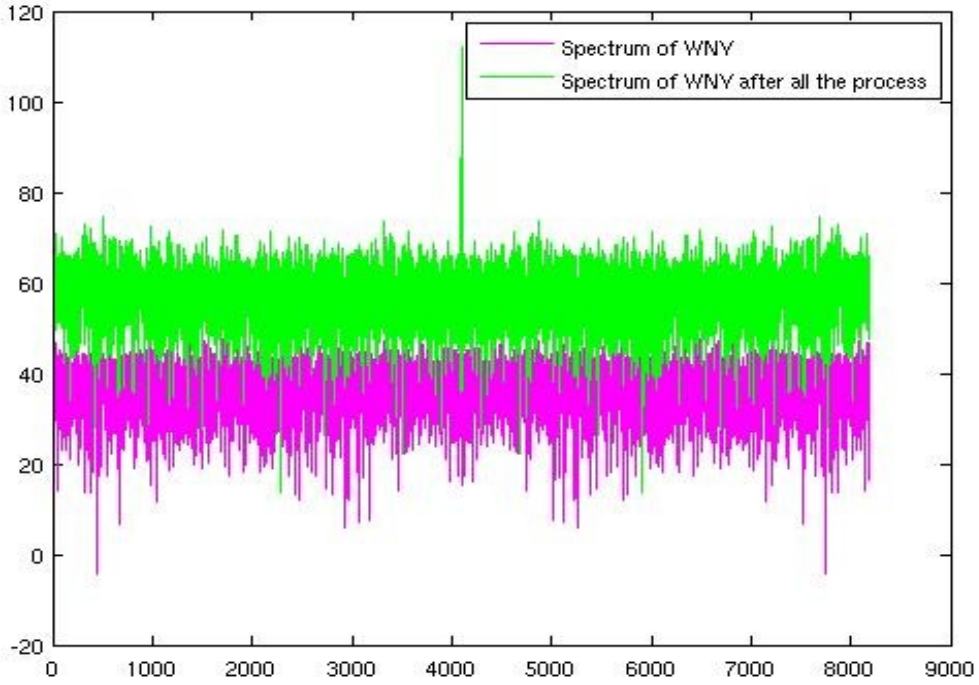

Comparison between the Y axis spectrum before and after all the process

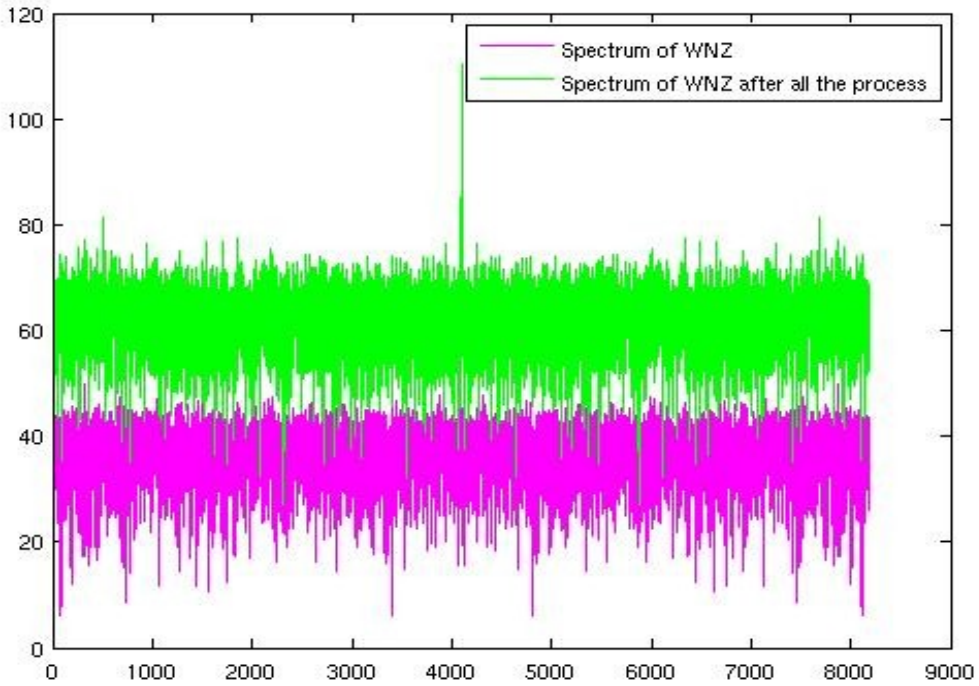

Comparison between the Z axis spectrum before and after all the process

In the following figures, the obtained spectrum with the real one is compared:

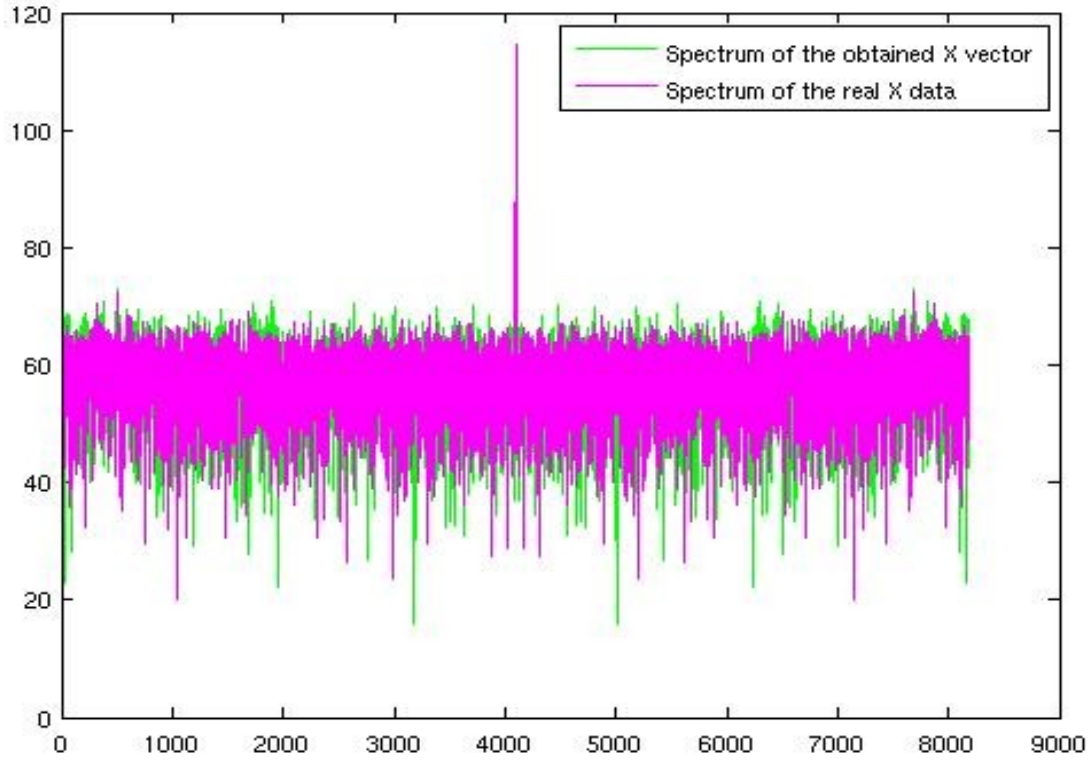

Comparison between the obtained X axis spectrum and the real one

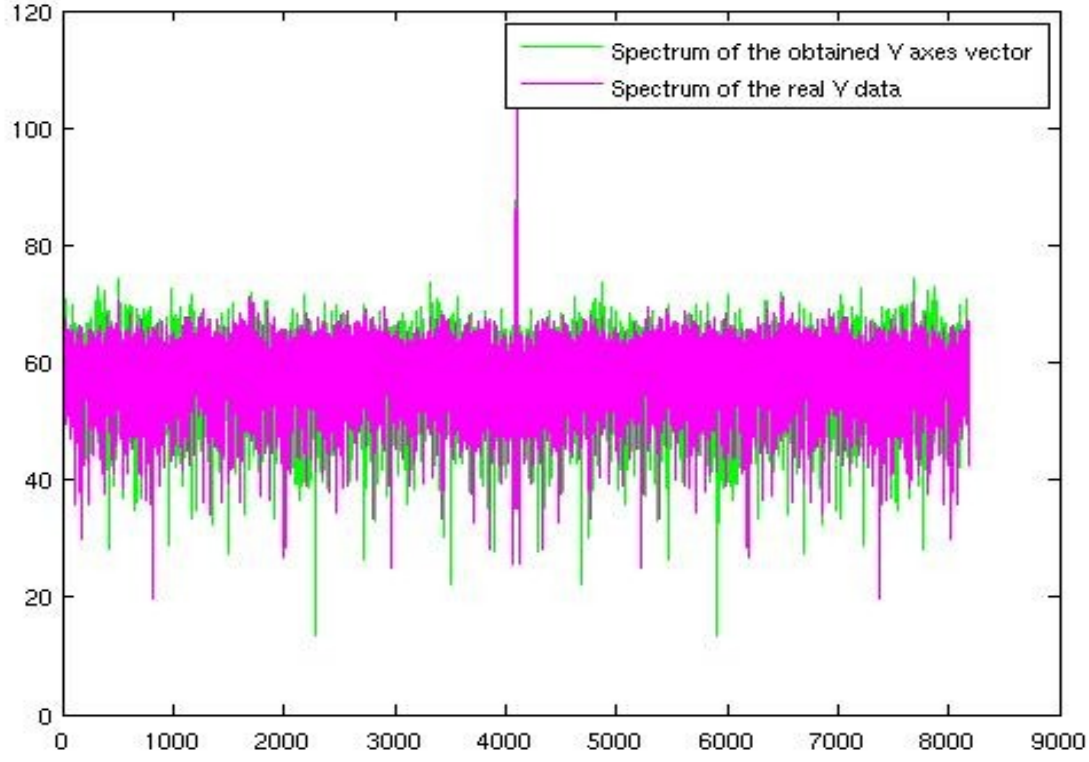

Comparison between the obtained Y axis spectrum and the real one

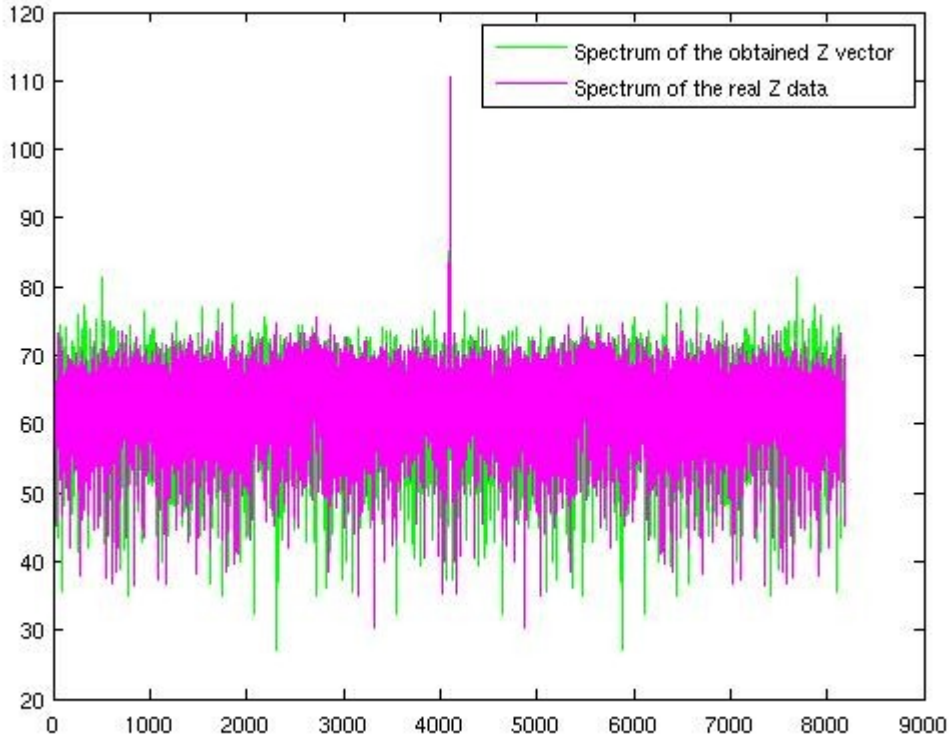

Comparison between the obtained Z axis spectrum and the real one

Second Accelerometer

The spectrum of the generated white noise, for each axis:

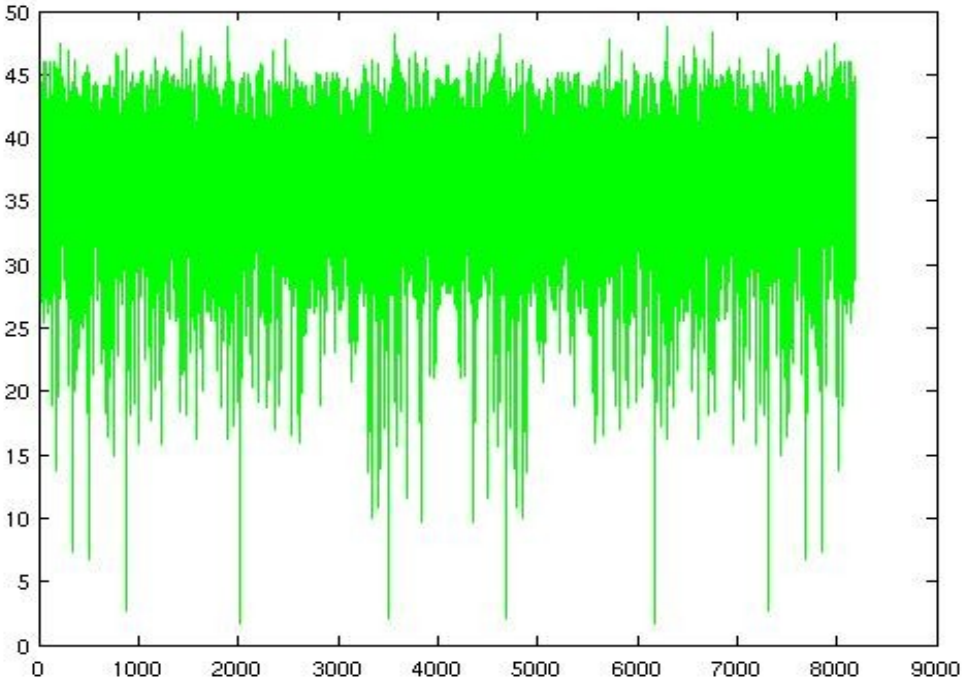

Spectrum of second accelerometer's X axis white noise of the second accelerometer

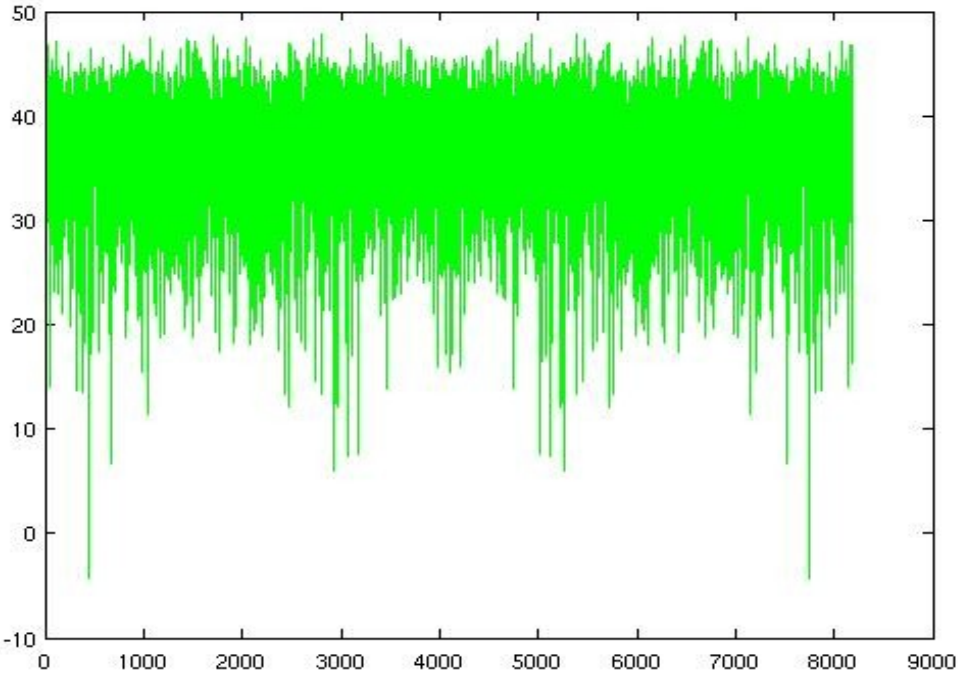

Spectrum of second accelerometer's Y axis white noise of the second accelerometer

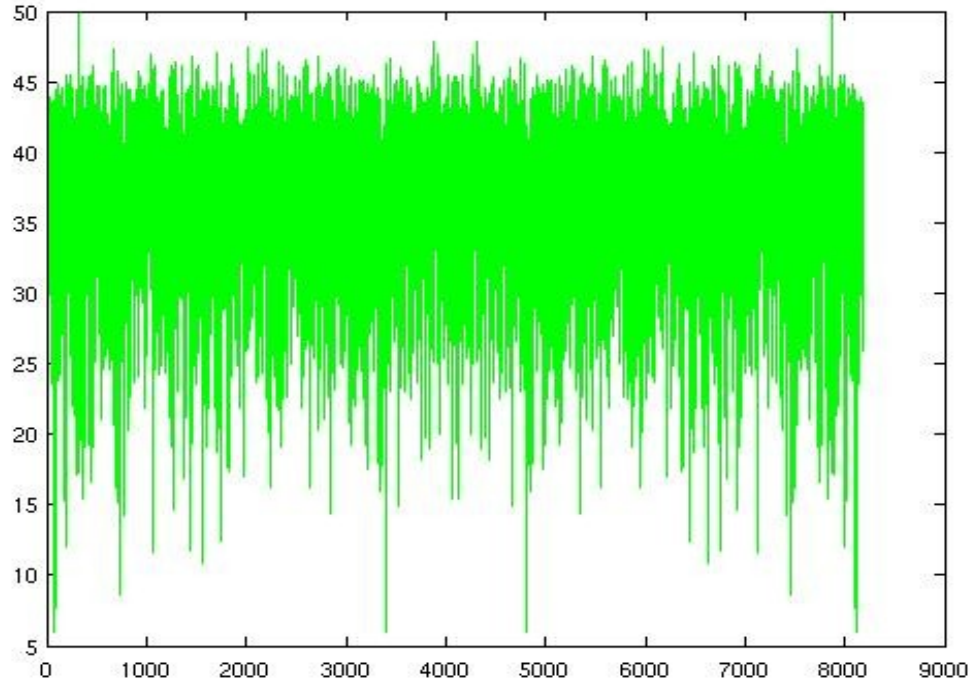

Spectrum of second accelerometer's Z axis white noise of the second accelerometer of the second accelerometer

The comparison of the spectrum of the white noise and the resulting vector multiplying this white noise by the "*Cholesky* matrix".

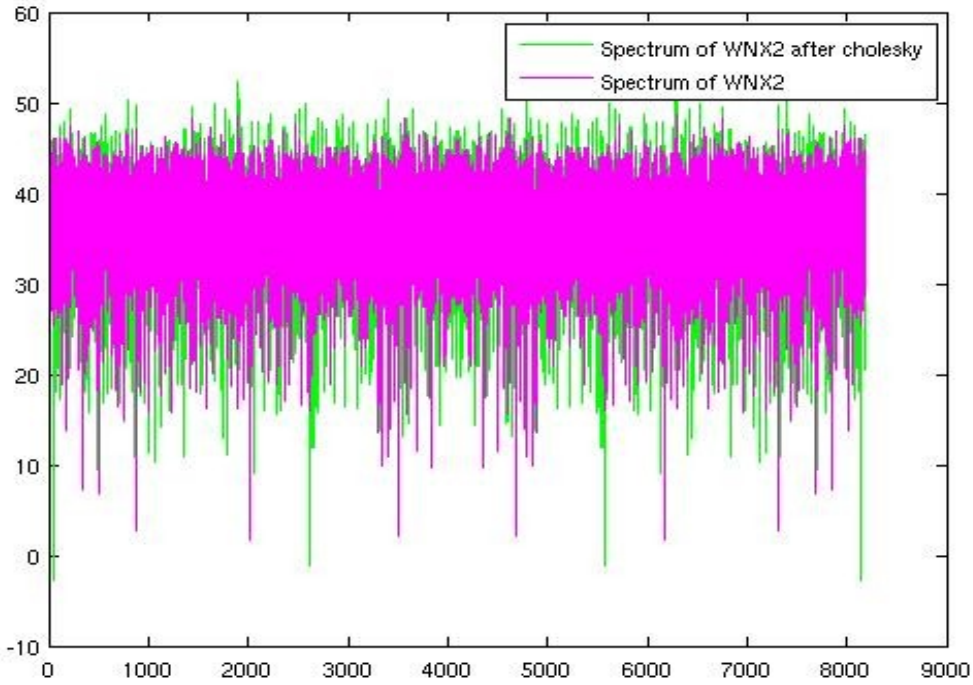

Comparison of the second accelerometer's X axis spectrum before and after "Cholesky"of the second accelerometer

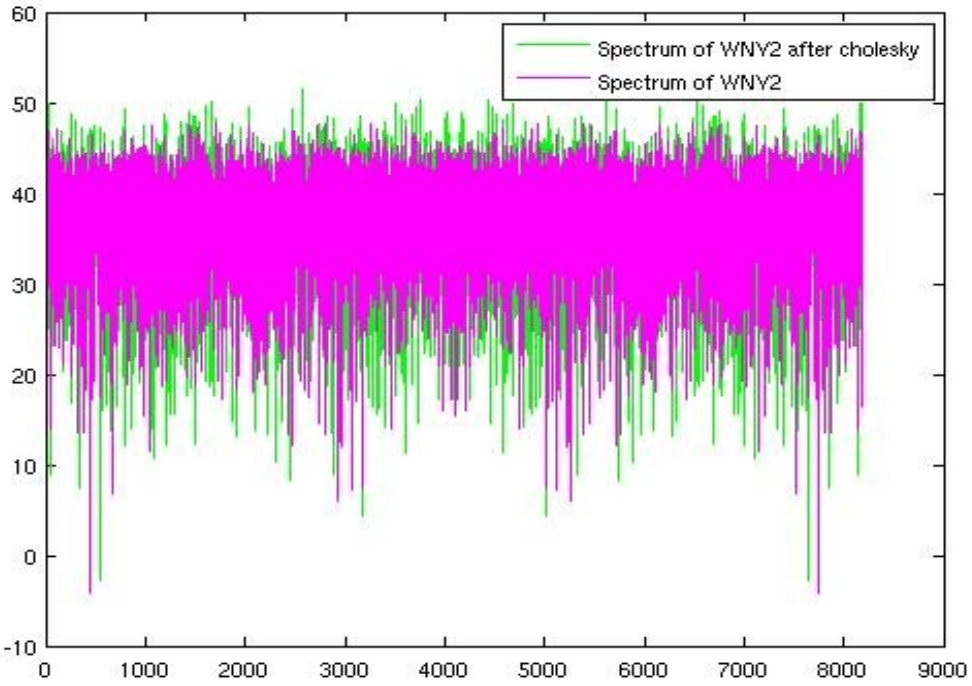

Comparison of the second accelerometer's Y axis spectrum before and after "Cholesky"of the second accelerometer

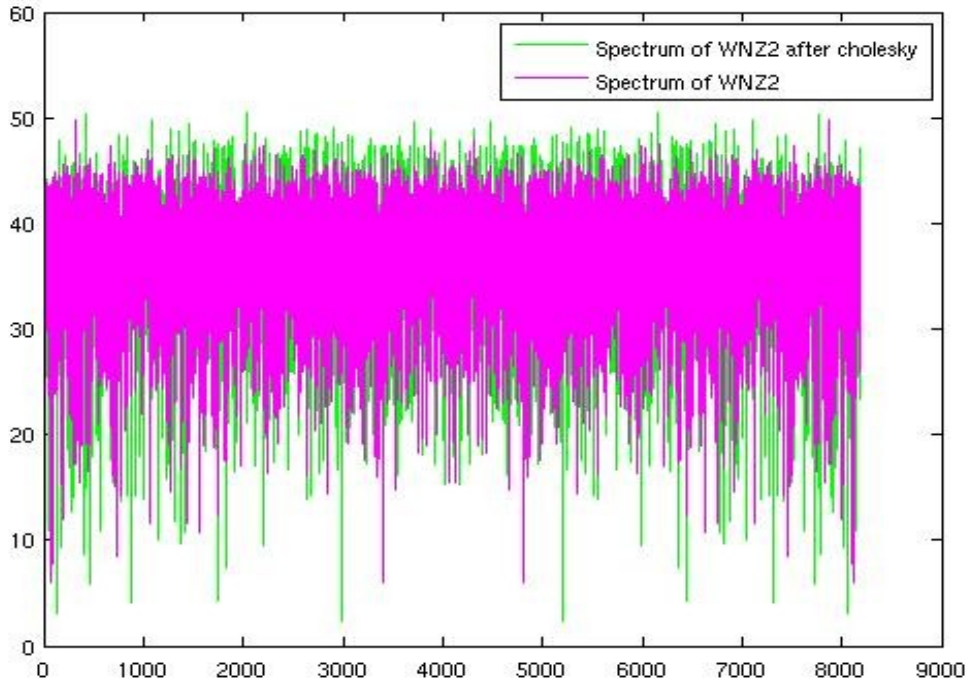

Comparison of the second accelerometer's Z axis spectrum before and after "Cholesky"of the second accelerometer

The third step is the multiplication by the gain, which generates the same effect as in the first accelerometer, the elevation of the spectrum. Finally the addition of the bias. Following there are the comparisons of the spectrum of the obtained final result and the spectrum of the white noise.

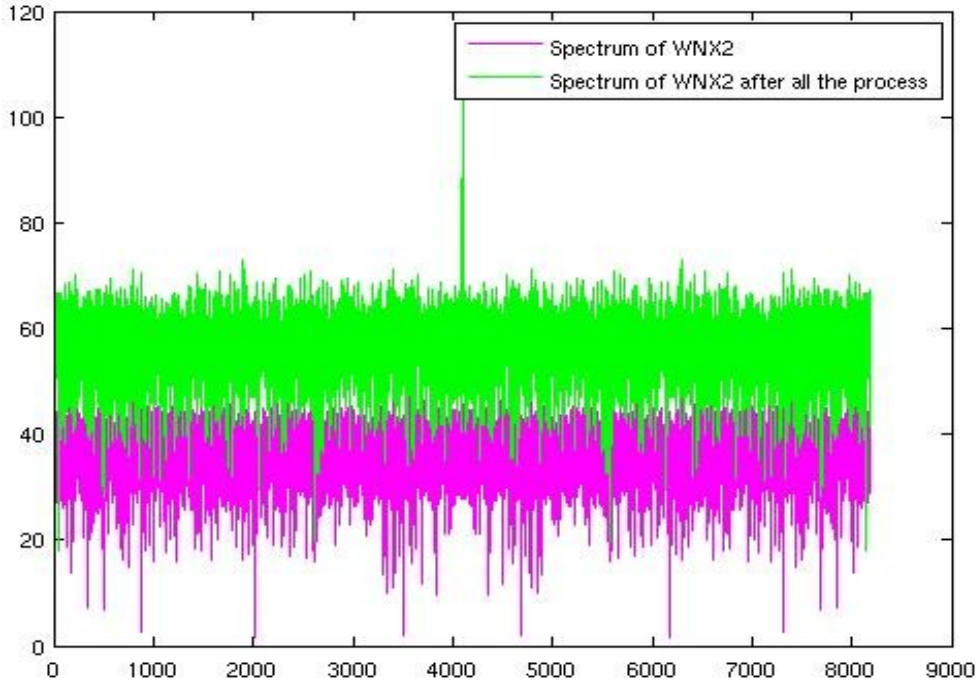

Comparison between the second accelerometer's X axis spectrum before and after all the process of the second accelerometer

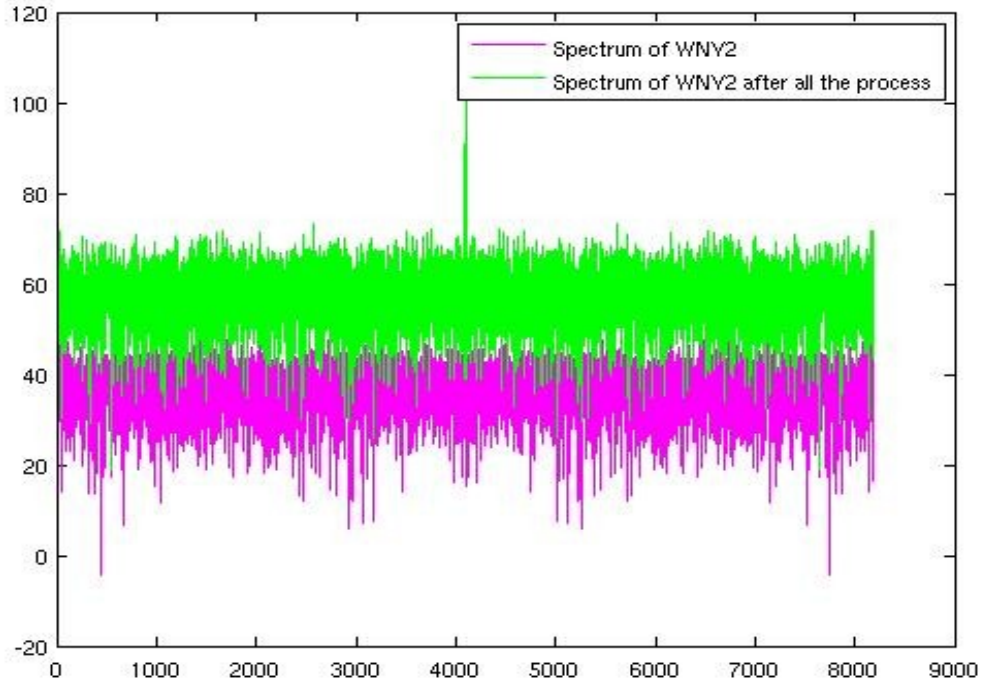

Comparison between the second accelerometer's Y axis spectrum before and after all the process of the second accelerometer

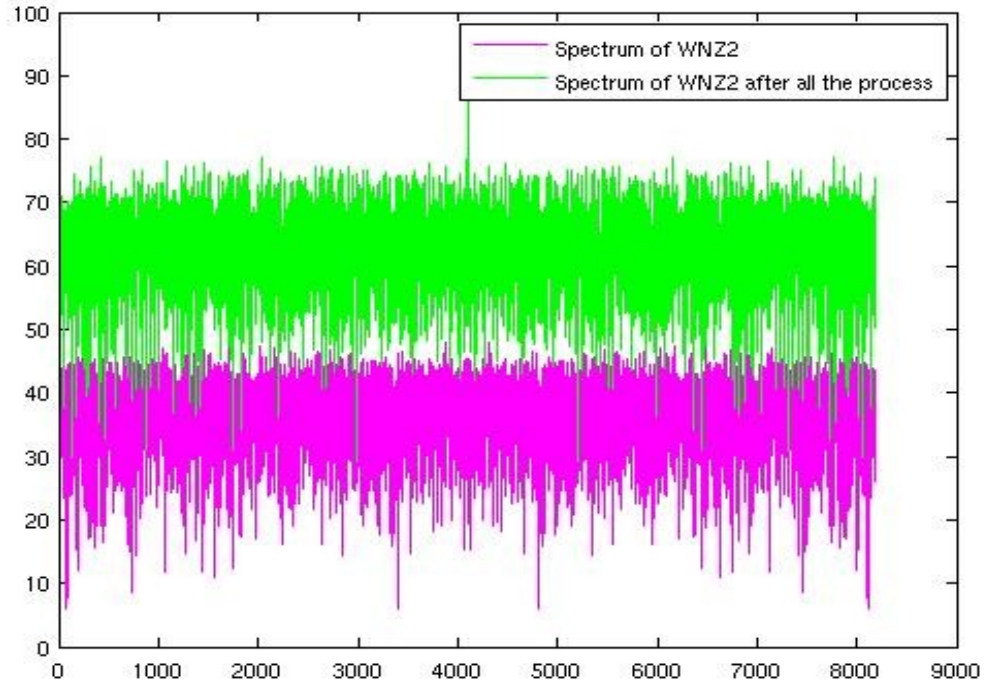

Comparison between the second accelerometer's Z axis spectrum before and after all the process of the second accelerometer

In the following figures, we compare the obtained spectrum with the real one:

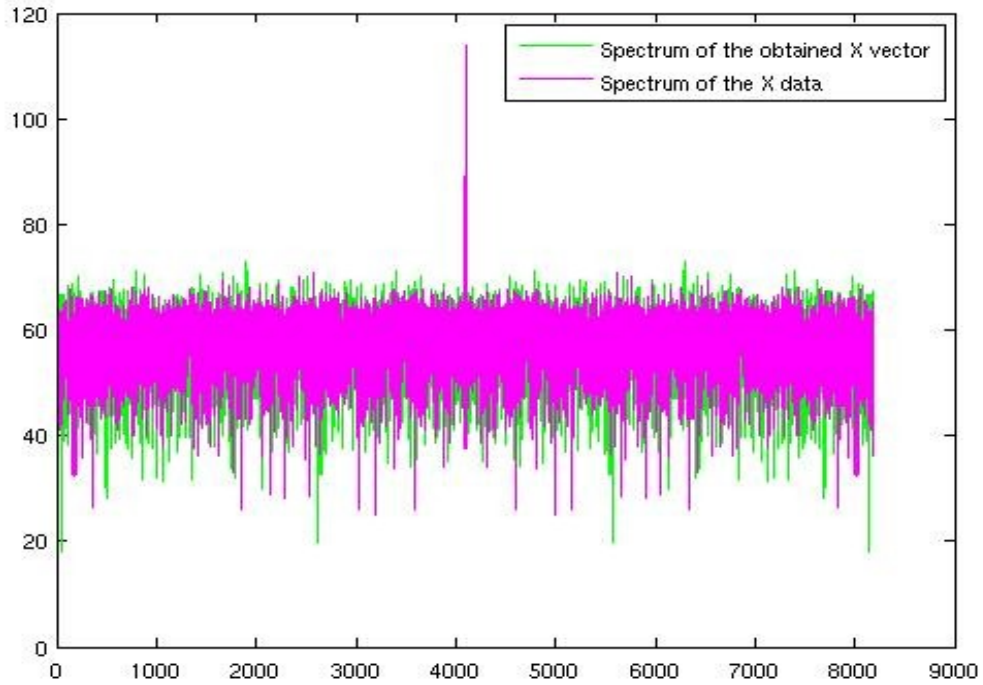

Comparison between the obtained second accelerometer's X axis spectrum and the real one of the second accelerometer

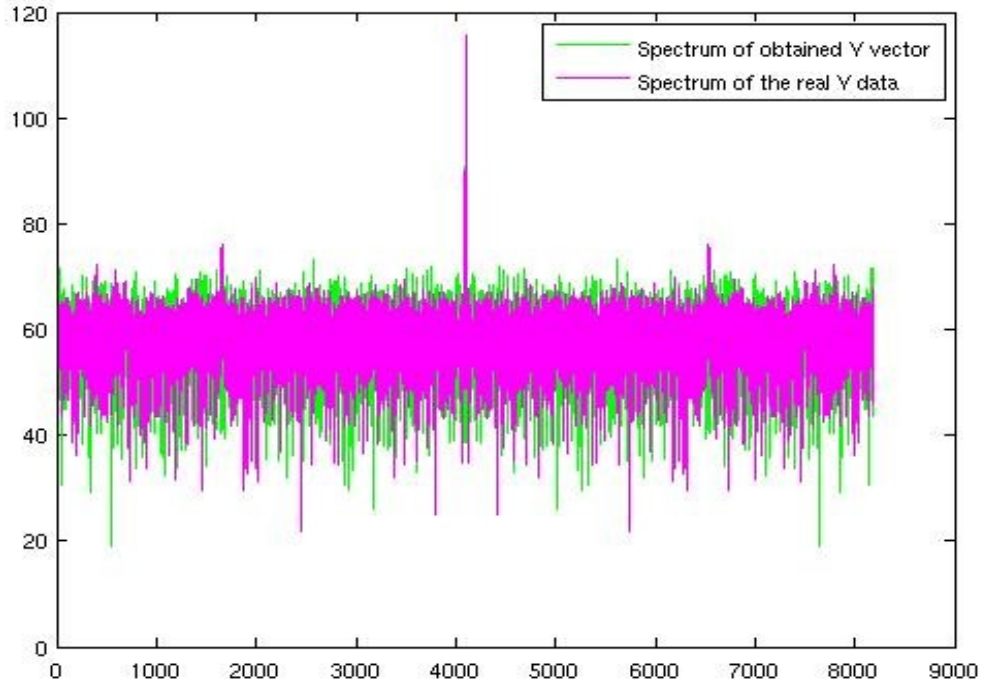

Comparison between the obtained second accelerometer's Y axis spectrum and the real one of the second accelerometer

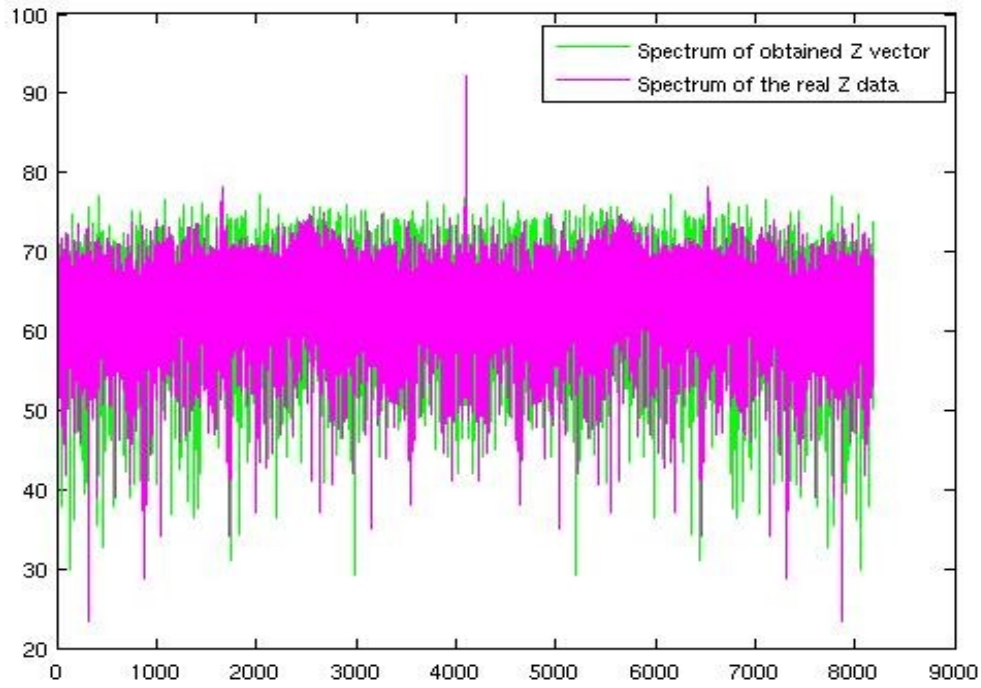

Comparison between the obtained second accelerometer's Z axis spectrum and the real one of the second accelerometer

ANNEX III

Data of different Accidents

In the next graphics, different accidents are going to be plotted.

Test Number	***Type of Accident***	***Impact Angle (degrees)***	***Closing speed (kph)***
Accident 3	Vehicle into vehicle	300	48,4
Accident 88	Vehicle into vehicle	300	48,3
Accident 91	Vehicle into vehicle	300	33,5
Accident 196	Vehicle into vehicle	60	47,3
Accident 208	Vehicle into vehicle	60	56,2
Accident 281	Vehicle into vehicle	60	47,6

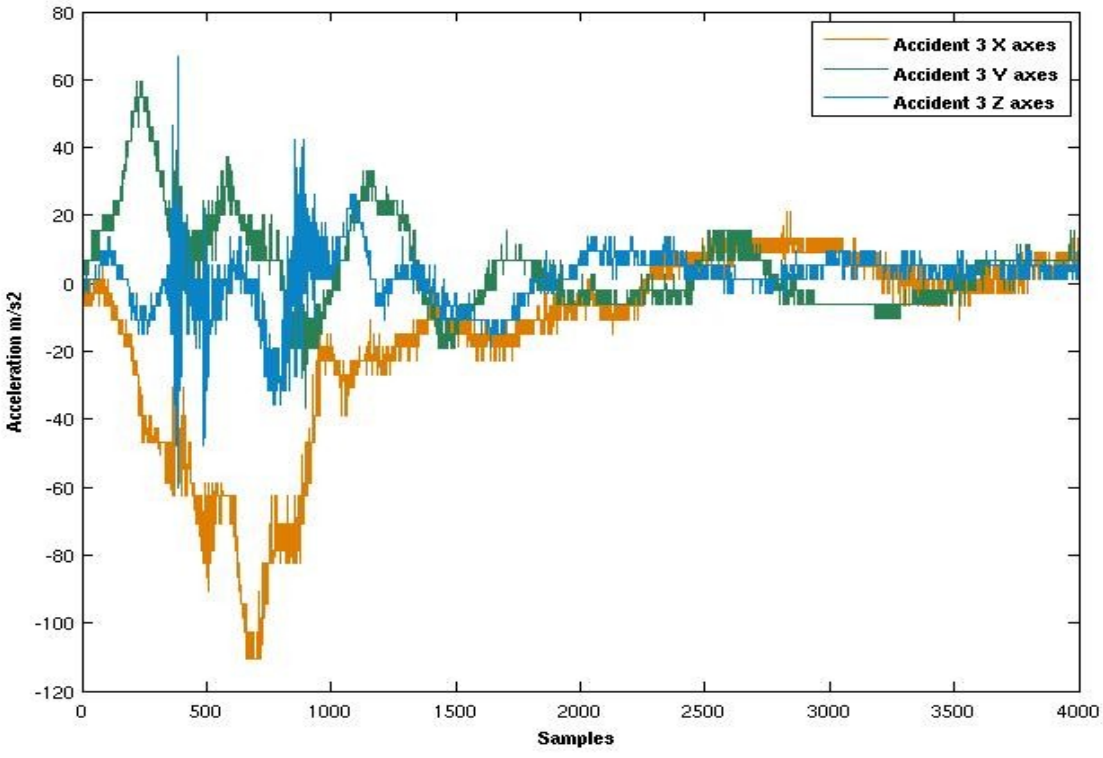

Data of Accident 3

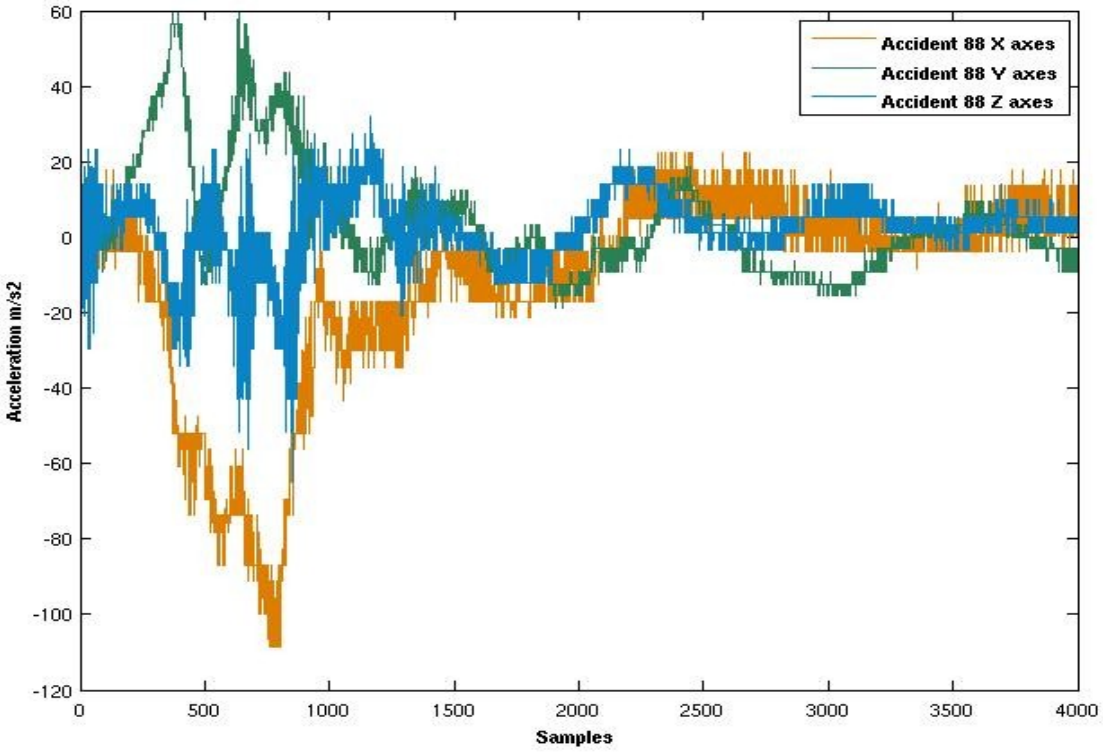

Data of Accident 88

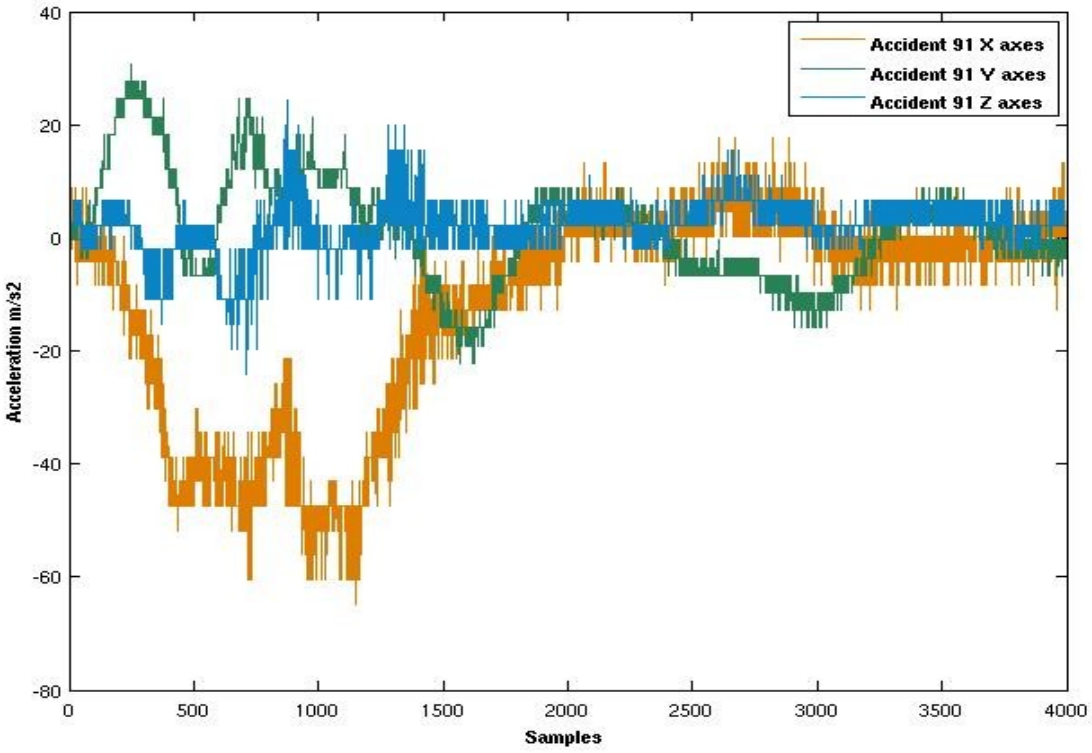

Data of accident 91

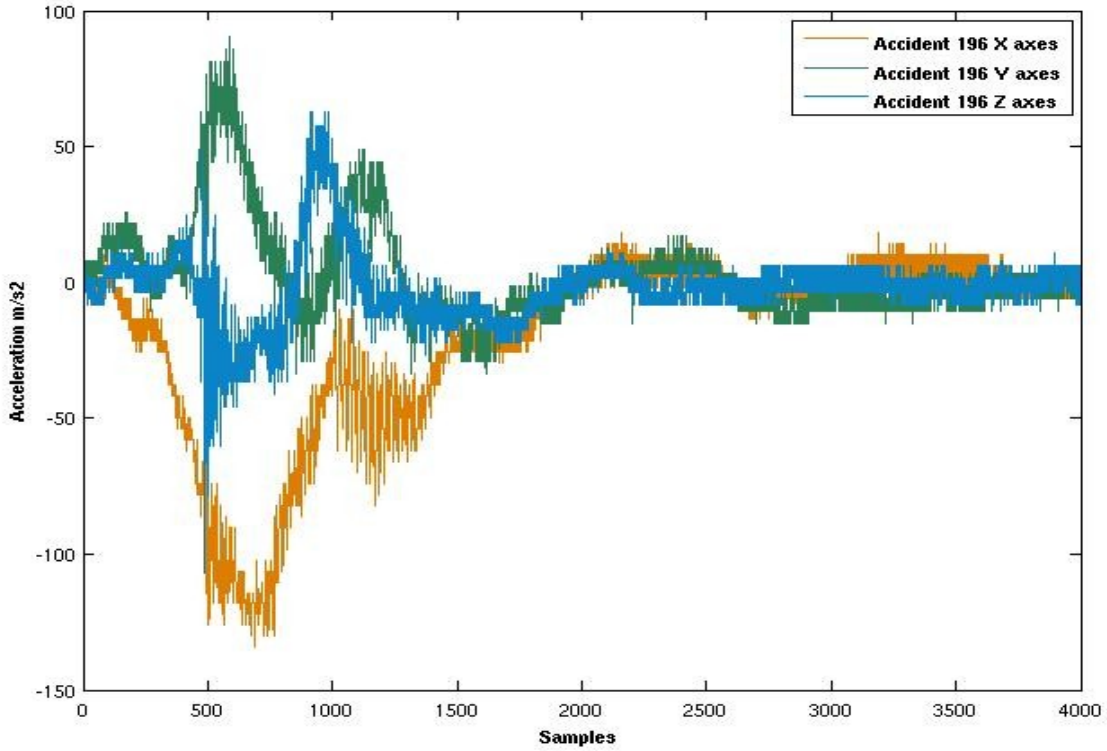

Data of Accident 196

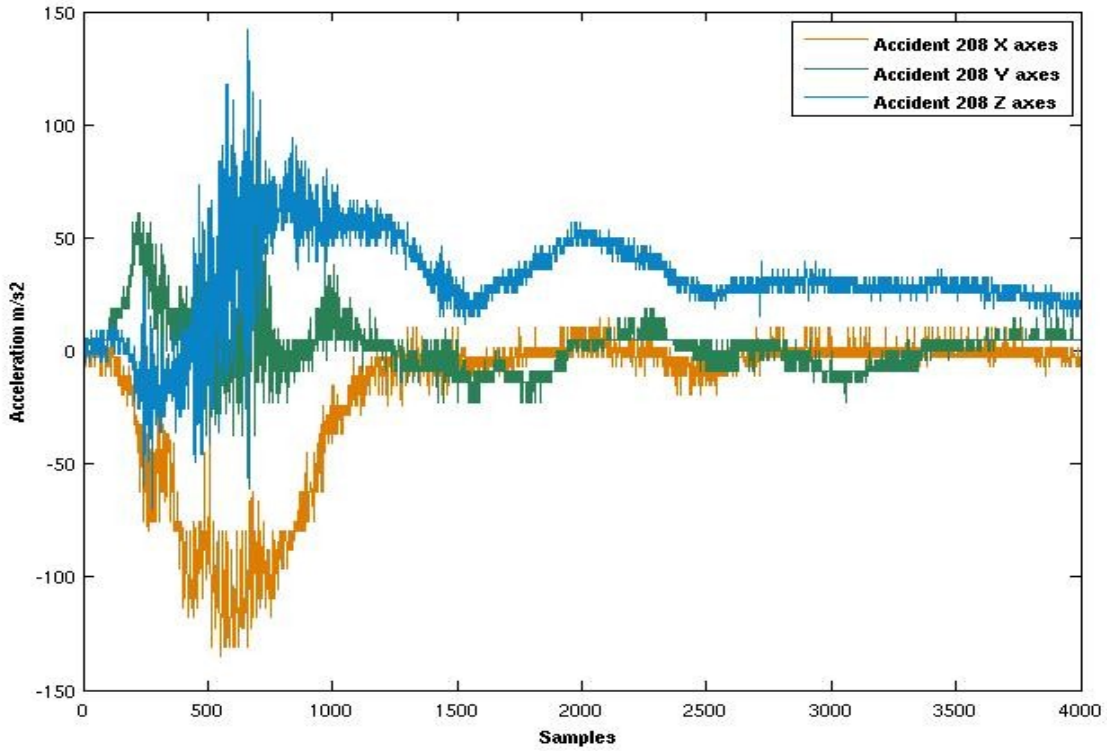

Data of Accident 208

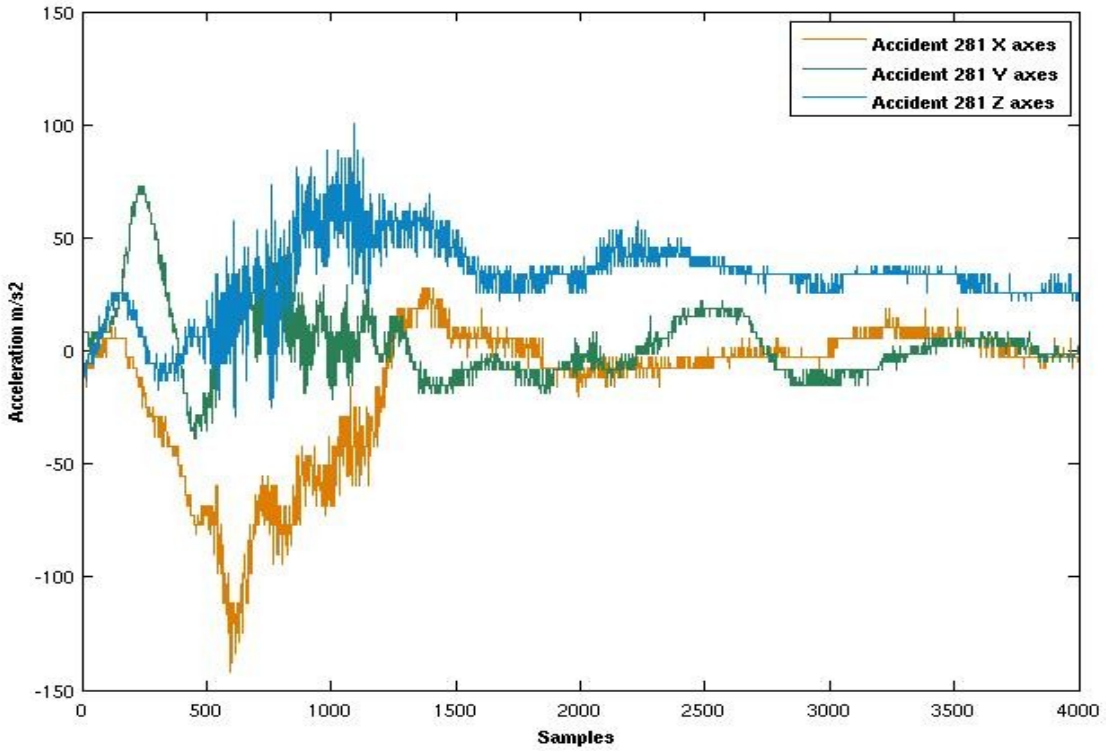

Data of Accident 281

ANNEX IV

Demostration of Rotational Acceleration

Demonstration that in a solid object the subtraction of the accelerations measures by two accelerometers gives twice the acceleration of one of the accelerometers.

The acceleration measured by the two accelerometers are the following ones,
The linear acceleration in all the points of the body is the same.

$$\overline{a}_i = \overline{a}_p + \overline{\alpha} x \overline{d}_i + \overline{\omega} x (\overline{\omega} x \overline{d}_i)$$

$$\overline{a}_q = \overline{a}_p + \overline{\alpha} x \overline{d}_q + \overline{\omega} x (\overline{\omega} x \overline{d}_q)$$

The linear acceleration in all the points of the body is the same so subtracting the measured acceleration of one accelerometer, from the measured in the other one: the linear acceleration disappear from the equation:

$$\overline{a} = \overline{a}_i - \overline{a}_q = (\overline{a}_p - \overline{a}_p) + (\overline{\alpha} x \overline{d}_q) - (\overline{\alpha} x \overline{d}_i) + \overline{\omega} x (\overline{\omega} x \overline{d}_i) - \overline{\omega} x (\overline{\omega} x \overline{d}_q)$$

Where:

$\overline{d}_i = (0, -\frac{d}{2}, 0)$, $\overline{d}_q = (0, \frac{d}{2}, 0)$, $\overline{\omega} = (\omega \hat{x}, \omega \hat{y}, \omega \hat{z})$, $\overline{\alpha} = (\alpha \hat{x}, \alpha \hat{y}, \alpha \hat{z})$ and x is the vectorial product.

Following there are the results of the vectorial products.

$$(\overline{\alpha} x \overline{d}_i) = \begin{pmatrix} \hat{x} & \hat{y} & \hat{z} \\ \alpha_x & \alpha_y & \alpha_z \\ 0 & \frac{-d}{2} & 0 \end{pmatrix} = -\left(\frac{d}{2}\right)\alpha_x \hat{z} + \frac{d}{2}\alpha_z \hat{x}$$

$$(\overline{\alpha} x \overline{d}_q) = \begin{pmatrix} \hat{x} & \hat{y} & \hat{z} \\ \alpha_x & \alpha_y & \alpha_z \\ 0 & \frac{d}{2} & 0 \end{pmatrix} = \frac{d}{2}\alpha_x \hat{z} - \frac{d}{2}\alpha_z \hat{x}$$

$$(\overline{\omega} x \overline{d}_i) = \begin{pmatrix} \hat{x} & \hat{y} & \hat{z} \\ \omega_x & \omega_y & \omega_z \\ 0 & \frac{-d}{2} & 0 \end{pmatrix} = -\left(\frac{d}{2}\right)\omega_x \hat{z} + \frac{d}{2}\omega_z \hat{x}$$

$$(\overline{\omega} x \overline{d}_q) = \begin{pmatrix} \hat{x} & \hat{y} & \hat{z} \\ \omega_x & \omega_y & \omega_z \\ 0 & \frac{d}{2} & 0 \end{pmatrix} = \frac{d}{2}\omega_x \hat{z} - \frac{d}{2}\omega_z \hat{x}$$

$$\overline{\omega} x (\overline{\omega} x \overline{d}_i) = \begin{vmatrix} \hat{x} & \hat{y} & \hat{z} \\ \omega_x & \omega_y & \omega_z \\ \left(\frac{d}{2}\right) w_z & 0 & -\left(\frac{d}{2}\right) w_x \end{vmatrix} = -\left(\frac{d}{2}\right) \omega_y \omega_x \hat{x} + \left(\frac{d}{2} \omega_z{}^2 + \frac{d}{2} \omega_x{}^2\right) \hat{y} - \left(\frac{d}{2}\right) \omega_z \omega_y \hat{z}$$

$$\overline{\omega} x (\overline{\omega} x \overline{d}_q) = \begin{vmatrix} \hat{x} & \hat{y} & \hat{z} \\ \omega_x & \omega_y & \omega_z \\ -\left(\frac{d}{2}\right) w_z & 0 & \frac{d}{2} w_x \end{vmatrix} = \frac{d}{2} \omega_y \omega_x \hat{x} - \left(\frac{d}{2} \omega_z{}^2 + \frac{d}{2} \omega_x{}^2\right) \hat{y} + \frac{d}{2} \omega_z \omega_y \hat{z}$$

Going back to the first equation, the result of the subtraction is the following one:

$$\overline{a} = (\overline{a}_i - \overline{a}_q) = \overline{a}_p + \overline{\alpha} \overline{d}_i + \overline{\omega} x (\overline{\omega} x \overline{d}_i) - \overline{a}_p + \overline{\alpha} \overline{d}_q + \overline{\omega} x (\overline{\omega} x \overline{d}_q) =$$
$$-(\frac{d}{2}) \alpha_x \hat{z} + \frac{d}{2} \alpha_z \hat{x} - \frac{d}{2} \alpha_x \hat{z} + \frac{d}{2} \alpha_z \hat{x} - (\frac{d}{2}) \omega_y \omega_x \hat{x} - (\frac{d}{2}) \omega_y \omega_x \hat{x}$$
$$+(\frac{d}{2} \omega_z{}^2 + \frac{d}{2} \omega_x{}^2) \hat{y} + (\frac{d}{2} \omega_z^2 + \frac{d}{2} \omega_x^2) \hat{y}$$
$$-(\frac{d}{2}) \omega_z \omega_y \hat{z} - (\frac{d}{2}) \omega_z \omega_y \hat{z} =$$
$$-d\, \alpha_x \hat{z} + d\, \alpha_z \hat{x} - d\, \omega_y \omega_x \hat{x} + (d\, \omega_z{}^2 + d\, \omega_x^2) \hat{y} - d\, \omega_z \omega_y \hat{z}$$

As the acceleration due to the rotation is the following one:

$$\overline{a}_i = \overline{\alpha} x \overline{d}_i + \overline{\omega} x (\overline{\omega} x \overline{d}_i) = \frac{-d}{2} \alpha_x \hat{z} + \frac{d}{2} \alpha_z \hat{x} - \frac{d}{2} \omega_y \omega_x \hat{x} + (\frac{d}{2} \omega_z{}^2 + \frac{d}{2} \omega_x{}^2) \hat{y} - \frac{d}{2} \omega_z \omega_y \hat{z}$$

So the result of the subtraction of the acceleration measured in the two accelerometers is twice the acceleration of one of the points, when there is only rotation.